

Reviewer #1

Formatted

We would like to thank the Reviewer for his/her thorough report that helped us improving the quality of our study. Through his/her constructive comments and suggestions the submitted manuscript has been updated significantly. Below are given point-by-point replies (regular font) to the comments (bold font) raised by the Reviewer.

This study describes a new dust optical depth (DOD) data set, MIDAS, which is derived by taking MODIS (Aqua only) satellite-based aerosol optical depth (AOD) and the aerosol speciation from the MERRA2 reanalysis. CALIOP and AERONET are used for evaluation.

The manuscript is in scope for the journal, though would be a closer fit to the other Copernicus journal ESSD because it is mostly a data set description paper. The material is important because speciated AOD is one of the next frontiers for better climate and air quality applications of data sets. The quality of language and visuals is satisfactory overall, though some edits are needed, and figures 5, 7, 9 would benefit from labels being increased in font size (hard to read without zooming in). Some of the content in the Supplement should be in the main paper. Overall, I recommend major revisions and would like to review the revision.

We agree with the Reviewer that our study fits well also with the scope of ESSD. Actually, the manuscript had been submitted to ESSD. The problem with ESSD was the long delay (3 months +) finding an editor. For this reason, we took the decision to withdraw the paper and resubmit it to AMT. Regarding the quality of the figures, we have reproduced all of them and their illustration has been improved.

General comments:

The main technical weak point of this study is that all the observational data sets used are out of date: MODIS Collection 6 instead of 6.1; CALIOP version 3 instead of version 4; AERONET version 2 instead of version 3. So this affects the AOD source used (MODIS), the optical properties used for matching (AERONET), and the data sets used for evaluation (AERONET, CALIOP). Some of the differences between old and new versions are systematic. So it is not clear to me how different the derived data set, or the evaluation results, would be if the newest data versions were used. To my best knowledge all of these latest data versions have been available for 1.5 years or so (i.e. they are not that new), so it is unfortunate that outdated versions were used when this analysis was done. It sounds like the authors are using a post-processed CALIOP product from another group (LIVAS?) rather than the official NASA CALIOP data products, so maybe that can't be changed. But, if the authors intend for others to use MIDAS for scientific analyses, it would really be best to use the most up to date inputs. I know that this means more work downloading files and rerunning code but this should mostly be computer time if the analysis code has already been written. So my main recommendation is to do that. I guess it is up to the authors and editor to decide what is most reasonable here. The 2007-2016 time period could also possibly be extended, I see no reason why it couldn't cover more of the Aqua record. Longer time series are of course more beneficial for things like trend analyses.

We decided to follow the reviewer's suggestion and in the revised manuscript we have used the MODIS-Aqua C061 data as well as the AERONET Version 3 retrievals. Moreover, the temporal availability of the MIDAS dataset has been extended from 10 (2007-2016) to 15 years (2003-2017). Therefore, the major comment raised by the Reviewer has been addressed adequately to our opinion. For the evaluation of the MDF we have used the CALIOP data which have been post-processed from our group and are provided via the LIVAS database ([Amiridis et al., 2015](#)). In the submitted manuscript, we stated (Lines 248 – 250) the published works describing the methodology for the derivation of the pure dust product (accounting for dust plus its portion from dust mixtures; [Amiridis et al., 2013](#)) as well as the series of filters applied in order to analyze only the quality assured CALIOP profiles ([Marinou et al., 2017](#)). The aforementioned techniques are also briefly discussed in our manuscript (Section 2.3). The in-house developed LIVAS database has been built using

CALIOP V3 data and its temporal availability spans from 2007 to 2015. Currently, the group responsible for the ESA-LIVAS database is working on the development of an updated version, covering the entire CALIPSO CALIOP observational period, in which the CALIOP V4.2 profiles are used. We acknowledge that there is a confusion to the reader regarding the terms "CALIOP" and "LIVAS" which has been addressed in the revised document following the recommendation made also by the Reviewer 2.

Numbers are often given to too many significant digits. One example I'll mention again later includes referring to an offset as 4.264%. Including all these digits gives an unrealistic impression of the precision of these estimates: can you really say that the true population offset is 4.264% and not 4.265%? Is it important that it is 4.264% and not 4.265%? If the answer to either of these is no, this is an indication that there are too many significant digits being reported. The authors should consider all numbers presented in this manuscript. For this case, for example, I'd probably just say 4.3%. This will also make the paper more readable.

We agree with Reviewer. We have kept only one digit in all numbers mentioned in the text.

I downloaded some MIDAS data from the link in the paper to have a look. The contents of those files seemed as described. I have four suggestions based on looking at these files:

1. I didn't see a MIDAS file version identifier, but the Readme file notes that some things are in testing or will be added in a future version. So it would be good to add a MIDAS version number somewhere in the filenames so the user can be sure which version of MIDAS they have (and which version of MIDAS technical documents such as this refer to). It may be unclear for the data user otherwise.

We agree with the Reviewer that it was an omission from our side not including a file version identifier. We have changed the filenames by adding the MIDAS Version (V1) while the necessary notification is given in the new README file.

2. One issue with is that the files contain some negative AOD values, which are unphysical. This is a result of the Dark Target land AOD algorithm which allows small negative retrievals. However since this is unphysical I recommend that in the next version, the authors set these values to 0. This is one issue with the source data which is easily fixed.

We prefer to keep the negative values and give the option to the user to decide how he/she will treat them. For example, the inclusion of negative AOD values (reducing the positive biases in low-AOD conditions according to previous evaluation studies) in the calculation of long-term averages will give more "accurate" results. On the other hand, for the calculation of temporal or spatial, median or geometrical mean values the negative AODs can be replaced with very small positive values as it has been done in [Sayer and Knobelspiesse \(2019\)](#).

3. It would also be useful to add an uncertainty estimate to each pixel. There is extensive discussion in the middle of the paper about uncertainty estimates, but these don't appear to have made it through to the data set itself, based on the files I looked at.

The pixel-level DOD uncertainty has been added in the netcdf files.

4. Finally, the files seem to contain some data fields inherited directly from the MODIS aerosol product, e.g. Angstrom exponents. As these are for total AOD and not dust AOD, I wonder if it would be better to remove these. Or, combine the Deep Blue land Angstrom exponent with one of the Dark Target ocean ones. There's also solar and sensor zenith angles, but I'm not sure what these are in there for. This would decrease the size of the archive to be downloaded somewhat.

As correctly stated by the Reviewer, the Ångström exponents are related to AOD and not to DOD. We are storing them in the MIDAS netcdf files in case where a user would like to work only with AODs (also available in the netcdf files) and use these size parameters in parallel for a discrimination between coarse- or fine-particles dominant conditions. We think that it is better not to merge ocean and land Ångström exponents because they are provided at different wavelength pairs and this might confuse the users. The solar and sensor zenith angles are required for the estimation of the air mass factor (AMF, Eq. 6) according to [Sayer et al. \(2013\)](#) as clearly stated in the manuscript. Each MIDAS daily file has a size of ~10MB which is not “prohibitive” for a fast downloading.

My more specific comments are as follows:

Line 133: should the word “conclusions” be added before “are drawn”?

The missing word has been added.

Lines 143-147: I suggest rewording this sentence. The Dark Target algorithms are really two different approaches as they have different bands used and completely different assumptions between them. Also, Deep Blue is over all snow-free land, not just bright deserts. So really it is one water algorithm (Dark Target ocean) and two land algorithms (Dark Target land, and Deep Blue). It is probably worth acknowledging that there are other MODIS aerosol algorithms too (e.g. MAIAC), they are just not included in those files.

The sentence mentioned by the Reviewer has been rewritten in the revised manuscript as follows:

“The derivation of AOD is achieved through the implementation of two retrieval algorithms based on the Dark Target (DT) approach, valid over oceans (Remer et al., 2002; 2005; 2008) and vegetated continental areas (Levy et al., 2007a; 2007b; 2010) but relying on different assumptions and bands, or the Deep Blue (DB) approach (Hsu et al., 2004; Sayer et al., 2013) over arid and semi-arid surfaces.”

We don't see the point of mentioning other MODIS aerosol algorithms in Section 2.1 since it is discussed only the standard product which has been processed in our analysis.

Line 153: I think the authors mean either “increasing pixel size” or “decreasing pixel resolution” here. Not “increasing pixel resolution”, which is the opposite.

We have corrected the sentence as suggested.

“Each swath is composed by 203 x 135 retrievals, of increasing pixel size from the nadir view (10 km x 10 km) towards the edge of the satellite scan (48 km x 20 km), in which a Quality Assurance (QA) flag is assigned (Hubanks, 2018).”

Line 206 and 212-215: note that the MODIS aerosol product is not assimilated. Rather, it is a neural network retrieval based on MODIS radiances that is assimilated. Not a neural network bias correction based on the MODIS retrieval. So the MODIS information going into MERRA2 is not the same as is being used as the main AOD data set here.

We have modified the relevant part of the text. Below is given the paragraph in the revised document.

“For aerosol data assimilation, the core of the utilized satellite data is coming from the MODIS instrument multichannel radiances in addition to observational geometry parameters, cloud fraction and ancillary wind data. Over oceans, AVHRR radiances are used as well, from January 1980 to August 2002, and over bright surfaces (albedo > 0.15) the non-bias-corrected AOD (February 2000 – June 2014) retrieved for the Multiangle Imaging SpectroRadiometer (MISR; Kahn et al., 2005) is assimilated. Apart from spaceborne radiances and retrievals, the Level 2 (L2) quality-assured AERONET retrievals (1999 – October 2014; Holben et al., 1998) are integrated in the MERRA-2 assimilation system (Goddard Aerosol Assimilation System,

GAAS) which is presented in Randles et al. (2017; Section 3). The cloud-free MODIS (above dark target continental and maritime areas, Collection 5) and AVHRR (above oceanic regions) radiances are used for the derivation of bias-corrected AODs, via a neural net retrieval (NNR), adjusted to the log-transformed AERONET AODs.”

Line 333: note that Levy reference is only for Dark Target over land. For discussion of Deep Blue Angstrom exponent over land, see the Sayer et al (2013) paper that is cited later in the manuscript.

The sentence has been rephrased to:

“Previous evaluation studies (Levy et al., 2013; Sayer et al., 2013) have shown that size parameters acquired by MODIS are highly uncertain, particularly over land and at low AOD conditions.”

Line 357: I am not sure it makes to take the quadrature sum of DT and DB uncertainties when they are merged. This means the overall uncertainty is worse than either DT or DB. If you think the uncertainties on these algorithms are independent, then you are effectively averaging two observations which means the uncertainty in the sum should be divided by sqrt(2). Since the retrieval is the average of two algorithms then the uncertainty should represent the uncertainty on that average.

The merged AOD uncertainty in the revised document is calculated based on the following formula:

$$\Delta(AOD_{DTDB-Land}) = \pm \frac{\sqrt{[\Delta(AOD_{DT-Land})]^2 + [\Delta(AOD_{DB-Land})]^2}}{2}$$

which is the uncertainty of the mean of DT and DB using the quadrature.

Line 386-389: If the output is at 0.1 degrees, then there should only be 1 retrieval in each (as the MODIS product is 10x10 km at nadir), so I don't understand this part about decreasing uncertainties when you have multiple retrievals. Or is this about when there are overlapping retrievals at the edge of swath from consecutive orbits? If so, that should be stated. If this is about averaging to a coarser space/time scale, then I don't think it makes sense to use the root n factor here because we know there is high spatial correlation in the errors because the errors are mostly not noise.

In this sentence we are describing the calculation of the DOD uncertainty at each pixel and at various temporal scales (i.e., monthly, seasonally, annually). Therefore, we are dealing with a time-series in which the applied algorithm (when possible) over land through time (i.e., from day-to-day) can switch from DT to DB depending on the NDVI threshold (see [Sayer et al., 2014](#)) while over oceans the AODs are retrieved always via the DT-Ocean algorithm.

Section 4.1: I am not sure that it is useful to compare total MERRA2 and MODIS AOD in this way. Or at least, the framing of the purpose here is not right. If there is a systematic disagreement, then that tells you that there might be an error in the derived MERRA2 dust fraction as well. Would it not be more meaningful for the present analysis to compare MERRA2 and MODIS dust AOD rather than total? Or to report summary results of the evaluation of MODIS AOD against AERONET (from DT/DB team studies)? As written, section 4.1 doesn't fit well with the rest of the paper.

We agree with the Reviewer and we have removed Section 4.1 from the revised manuscript. A similar comment regarding the usefulness of comparing MERRA-2 AOD versus MODIS in the current study has been raised also by the Reviewer 2. The intercomparison between MERRA-2 and MIDAS (MODIS) DODs, along with LIVAS (CALIOP), is already presented in Section 4.4.

Section 4.3: The authors here frame the differences as if MIDAS is in error. However, unlike the direct-Sun AERONET AOD data, the AERONET almucantar scan retrievals used here have non-negligible uncertainties

(which are not necessarily random). So some of the discrepancies and biases might in fact come from uncertainties in the AERONET DOD estimates. This was not directly discussed beyond a mention that the AERONET DOD estimates made here neglect fine-mode dust, although I think with the AE filtering this is likely to be a negligible effect in most cases.

The comparison here includes two aspects. The use of the direct sun AERONET retrievals for AOD and the coincident inversions (using the SSA). Regarding AOD, the uncertainty is reported to be between 0.01 and 0.02, [Eck et al. \(1999\)](#). For the SSA, based on the results of [Sinyuk et al. \(2020\)](#) for the Mezairah site (i.e., predominance of dust aerosols), its uncertainty (being lower than 0.06) decreases significantly for increasing AODs. Since the $\text{SSA}_{675} - \text{SSA}_{440}$ difference (i.e. positive values) is used as a criterion for the discrimination of dust from sea-salt particles, the obtained SSA uncertainties, particularly those at 440nm, can affect the spectral signature of SSA and subsequently dust identification. Therefore, in some cases the AERONET DODs can be misclassified.

So to summarize, still AERONET AODs have lower uncertainty than the MODIS retrievals. For the case of the use of AERONET inversions, spectral SSA related uncertainties can lead to a misclassification of such cases.

Lines 666, 667: here the authors say that MERRA2 has “biases” and “overestimates” compared to CALIOP. It would be better to refer to positive and negative “offsets” or “differences” instead, because “bias” and “overestimate” imply a problem and that CALIOP is the truth. Really none of the data sets are the truth and we are only making comparisons and not diagnosing errors. So more neutral language like “offsets” should be used here (and throughout), and terms like “bias” and “overestimate” should be avoided unless it involves a comparison with something that can be considered a reference truth. I mentioned only these examples although there are others in this section and through the paper where these or similar terms are used (and there are places where the wording is ok as well).

We agree with the Reviewer’s comment and we have made the appropriate modifications throughout the paper.

Line 716: authors should check and clarify which of the data sets corresponds to which number here. For example the wording implies that 4.264% is more than 9.405% which is obviously backwards.

Thanks for the correction!

Sections 4.2 to 4.5 were honestly a little hard to read because it’s a large amount of text which is basically describing several figures and providing references. This also comprises about 11 of 28 pages of body text in the paper. I wonder if this can be streamlined a bit. The authors write that there will be a follow up paper looking at this same material in more detail as well. So I wonder if here it is best to just show figures and highlight where the data sets do not agree well (and maybe try to figure out why), as these are areas to focus future study on. That type of approach (figure out where and why there are differences) would also make the paper fit better in AMT.

We have made an effort to reduce the length of the text. As it concerns the interpretation of our findings we believe that we are providing all the necessary explanations without just describing plots. For example, there are statements about issues that can affect CALIOP (e.g., lidar ratio, total attenuation of the laser beam, cloud screening) and MODIS (e.g. surface reflectance) performance as well as MERRA-2 reliability (e.g., consideration only natural dust sources).

Table 1: This is a bit of a sea of numbers. It is difficult to easily pull out the main message here. What is the main message here? Or is this just for reference? Given it relies on regional acronyms, it would be better to present the map defining the regions in the main paper rather than in the supplement.

We are providing the long-term annual averages as well as their margins during the study period in order to have an overall view among the three DOD products at planetary scale, for the northern and southern hemisphere as well as for each sub-region. Figure S7 has been moved to the main text in order to help the reader. We think that it is useful for a scientist wanting to use such an information for a particular area or globally to have an easy and direct way of using these numbers.

Figures 2,3: most of the world here is in the 0-0.2 range in Figure 2, which is very hard to distinguish visually because it is different tones of blue. Figure 3 solves this but as it's a separate figure, it is hard to glance back and forward. Also, I am not sure how helpful it is to show an annual map here because dust seasonality is strong. So I suggest making seasonal maps instead of annual to replace these figures, this would give more insights. I am also not sure whether the maps of FB and FGE are needed for this panel. Maybe just replace this with an 8-panel figure: left column is seasonal MDF, right column is seasonal MDF minus CALIOP dust fraction (i.e. mean bias)? Then Figure 3 could be 4 panels showing seasonal correlation coefficients? I think they are the most crucial metrics to show here because they show the level of consistency in typical dust fraction and the variation captured by MERRA2, which are what inform the DOD uncertainty here. The other panels could maybe move to the Supplement if the authors think they are useful. I know there are a few seasonal maps in the Supplement but think the maps discussed above should be in the main paper.

Following the suggestion made by the Reviewer, we have added in the Supplement a panel of figures presenting the biases and the correlation coefficients obtained on a seasonal basis. Also, the most important findings are briefly discussed in the main text. The FB and FGE metrics are less affected by outliers with respect to bias and serve as a complementary diagnostic tool.

Figure 4 (and text discussion): I don't think the linear regression is appropriate here, so it should be removed. Since the uncertainty on DOD is proportional to total AOD, it is likely that the assumptions of regression are violated. Also I don't think a global regression is useful because it is likely there are regional differences in the errors, meaning that the global regression line is not informative. Same comments apply to Figure S5 in the Supplement.

The way we define the uncertainty here is exactly the one that MODIS is using for AOD. It is a common practice to compare ground-based and spaceborne AODs (DODs in our case) through scatterplots. Figure 4 shows the overall comparison of MIDAS and AERONET DODs at global scale. Of course there are regional differences which are presented in the calculated metrics at station level in Figure 5. Therefore, all the necessary information is included. Figure S5 has been removed from the revised supplementary material.

Figure 5: the circles are all too small to see.

We have increased the size of the circles.

Figure 8 (iii): this is the mean of the DOD uncertainties, right? Or is it the uncertainty on the mean DOD? This needs to be stated more clearly.

We acknowledge that the description in the submitted document was not clear to the reader and for this reason we have modified accordingly the revised text. Figure 8-iii in the submitted document shows the uncertainty of the DOD average while in the revised text depicts the mean of the DOD uncertainties over the study period. Below is given the relevant part of the revised text.

“Depending on the selected MODIS algorithm, the appropriate combination between AOD (Eqs. 4, 5, 6 and 7) and MDF (Eq. 8) uncertainties is applied to calculate the $\Delta(\text{DOD})$ (Eq. 3) on each measurement (i.e., DOD) and at each grid cell. These pixel-level DOD uncertainties are averaged over the entire study period as well as for each season and the obtained findings will be discussed along with the global spatial patterns (Section 4.5) of dust optical depth in order to provide a measure of the reliability of the derived MIDAS DOD product.”

Figure S4: this illustrates a problem I have with the validation methodology. A 4-hour averaging window is pretty huge! And the time variation of AERONET DOD in that window can be much bigger than the AERONET uncertainty. So some of the disagreement seen in Figure 4 is due to this time mismatch. For this example, the range of DOD in this window is about 0.09, or 40% of the average. This makes it hard to assess the performance of MIDAS. This is something that shouldn't be buried in the Supplement; I didn't see the mention of a 4-hour window in the main paper (if it is there, it is not clear) so the reader may not realise how big it is. Probably a smaller window is needed, and some filter based on AERONET time homogeneity. I know this will decrease the data volume, maybe a lot, but with such a big time variation in DOD within the window it makes the AERONET comparison a lot less useful for MIDAS evaluation.

It is true that the 4-hour time window is not the optimum and it would be better to be reduced down to ± 30 minutes (a temporal margin applied in many evaluation studies). However, there are reasonable arguments which can support our approach. Please note that we are using the almucantar retrievals which have substantial less amount of data with respect to O'Neill retrievals or to sun-direct measurements. This volume of ground-based data is further suppressed when we are applying the criteria for the "determination" of AERONET DOD. By adding a time homogeneity criterion (which probably would be arbitrary), as suggested by the Reviewer, then more data are masked out from our sample. In our case, we had identified the MODIS-AERONET common pairs based on the ± 30 min and ± 1 hour time-window frames but the number of coincident observations, derived mainly at desert stations, was very small.

We believe that the Figure S4 should remain in the supplement rather than move it to the main text because it is just an illustration of the collocation method. Likewise, we would like to clarify that the MODIS map and the AERONET timeseries both refer to AOD and not DOD. The treatment of both datasets for the derivation of DOD is described sufficiently in the relevant sections of the paper.

On a non-scientific note, I thought the use of MIDAS as an acronym was amusing and a good choice.

Thank you!

Reviewer #2

We would like to thank the Reviewer for his/her constructive comments that helped us to improve the quality of our work as well as to clarify misleading points. Our replies (regular font) for each comment (bold font) are provided below.

This manuscript describes the methodology to obtain a dust aerosol optical depth data set from MODIS total AOD combined with the use of MERRA-2 to determine the dust fraction in the AOD. This opens nice perspectives, offering specificity to the aerosols retrievals and this with global coverage once per day, nice horizontal resolution and a long time series.

Although the concepts at the basis of this work, the goal and the obtained data set are scientifically very good, the manuscript itself needs major revision (and I am willing to review the revised version if the Editor finds it needed). The manuscript is very long and some parts are pretty difficult to read, being very descriptive with many numbers. Some parts do not bring a lot to the manuscript, while being quite long. Also, there is a lack of consistency in terms used to refer to the products (see below), which renders the reading a bit difficult. Ideas to improve this can be found in the different comments.

We would like to thank the Reviewer for his/her positive opinion about the scientific contribution and the importance of our study. Regarding the issues raised here, we would like to inform that we have made a major effort to reduce the length of the manuscript and shrink parts of the text in which many numbers are given. Moreover, a better clarification of the used/obtained datasets has been made thus addressing inconsistencies mentioned by the Reviewer. Our detailed replies are given in the relevant comments listed below.

I have some major general comments then addition specific major comments, then some minor comments (editing / suggestions).

Major general comments:

- 1. There is no mention of the thermal infrared (TIR) based DOD data (SEVIRI and IASI - for IASI data is available in the climate data store). These are very interesting as the TIR is only sensitive to dust, but gives DOD at TIR wavelength which needs to be converted to visible (step that includes some assumptions on particle size and properties, but also a bunch of assumptions are needed in this work). I am not saying the study should be redone with a full comparison with TIR dust data (although that would be pretty interesting, see also a further comment on the comparisons undertaken in this work), but that when trying to obtain pure dust AOD one should at least mention the TIR DOD. For example, after lines 110-113 it would be nice to have some sentences describing what MIDAS data brings in addition to the TIR-based DOD (for example IASI is also long-term, global twice per day instead of once, and 12km ground resolution at nadir). To be perfectly clear, this is not me being skeptical about the scientific interest of this work, but I think that some information on other methods to obtain DOD from satellites should be added to the manuscript.**

We have added in the revised manuscript the missing information about DOD retrievals operating at TIR wavelengths, as correctly pointed out by the Reviewer. We find very interesting the idea of comparing MIDAS DOD against those provided by IASI and SEVIRI. Actually, it is a very nice perspective for a further exploitation of the MIDAS dataset!

- 2. Data from CALIOP and MODIS are used, but there is a confusion as to which data exactly. Indeed, the authors use for CALIOP either the “official” CALIOP product from NASA, or the LIVAS product that some of the authors have previously developed, but both are referred to as “CALIOP”, making it pretty difficult to keep track of things. It is a little bit the same for the MODIS “official” AOD product and the MIDAS here developed product, it needs thinking to be sure which one is referred**

to in the manuscript. I recommend to use the product names everywhere in the manuscript, to avoid any confusion: wherever referring to the “non-official” product, please use consistently LIVAS and MIDAS, while keep the instrument name for the “official” products. This also includes the plot titles, legends and caption.

All the necessary replacements, as suggested by the Reviewer, have been made throughout the revised manuscript (text, plots and captions).

3. For the MERRA-2 dust fraction, please always use the acronym defined (MDF) or at least the same words, avoid using dust "portion" or other terms, for consistency and clarity.

We think that it is pretty clear to the reader that MDF and MERRA-2 dust portion (or fraction) have the same meaning and there are not consistency or definition issues. However, in the revised manuscript the number of MDF “instances” has been increased at the expense of those of “dust portion (fraction)” trying at the same time to avoid the usage of this term very frequently which makes difficult, to our opinion, the readability of the text.

4. Why do you use only the MODIS data from Aqua (and not Terra)?

The obvious reason is that Aqua and CALIPSO are flying in the A-Train constellation which means that MODIS and CALIOP retrievals are almost coincident in temporal terms. This ensures that time departures between these two spaceborne sensors are not affecting our results in contrast to Terra which flies three hours earlier than Aqua. Nevertheless, the MODIS-Terra L2 data currently are processed and the derived MIDAS netcdf files will be uploaded as soon as possible in the same repository.

5. Why old versions are used both for CALIOP and AERONET while the new versions exist for some time now?

A same (similar) comment has been raised by the Reviewer 1. We are copying our reply below.

In the revised manuscript we have used the MODIS-Aqua C061 data as well as the AERONET Version 3 retrievals. Moreover, the temporal availability of the MIDAS dataset has been extended from 2007-2016 (10 years) to 2003-2017 (15 years). Therefore, the major comment raised by both Reviewers has been addressed adequately to our opinion. For the evaluation of the MDF we have used the CALIOP data which have been post-processed from our group and are provided via the LIVAS database ([Amiridis et al., 2015](#)). In the submitted manuscript, they are stated (Lines 248 – 250) the published works describing the methodology for the derivation of the pure dust product (accounting for dust plus its portion from dust mixtures; [Amiridis et al., 2013](#)) as well as the series of filters applied in order to analyze only the quality assured CALIOP profiles ([Marinou et al., 2017](#)). The aforementioned techniques are also briefly discussed in our manuscript (Section 2.3). The in-house developed LIVAS database has been built using CALIOP V3 data and its temporal availability spans from 2007 to 2015. Currently, we are working on the development of the updated LIVAS database, spanning from 2006 to 2020, in which the CALIOP V4 profiles are used.

6. I think that there are too many descriptions of different data sets and of different comparisons, each time with a long description of the geographical features. This makes the paper a bit difficult to read.

In the revised manuscript, better clarifications are given in order to avoid any confusion to the reader. In our study we have used four datasets (MODIS-Aqua, CALIOP, MERRA-2 and AERONET) which are utilized as follows. MODIS-Aqua AOD and MDF (i.e., MERRA-2) are combined in order to obtain MIDAS DOD. The evaluation of MDF is made against LIVAS, which has been developed based on the CALIOP profiles. MIDAS

DOD is compared versus MERRA-2 and LIVAS DODs while it has been evaluated against AERONET DODs, extracted according to the methodology described in Section 2.4.

7. Many numbers are given with too many digits. Please try to only provide significant digits.

We have reduced the number of decimal digits.

Major specific comments:

1. **Line 33: “ground-truth AERONET-derived DODs” -> There is no “truth”, any measurement has uncertainties and biases. In particular, here the DOD derived from AERONET is a complex product with a number of assumptions and no-one should see it as “the truth”.**

We agree that the word “truth” is not appropriate and we have removed it.

2. **Section 2.3 on CALIOP: It is a bit unclear to me how the CALIOP subtypes are used in LIVAS. I have the feeling that LIVAS is a different retrieval, not using the CALIOP “official” features/retrievals and therefore I would recommend to only mention here what is really needed to understand LIVAS. Otherwise it is a bit confusing.**

Section 2.3 consists of two paragraphs where in the first one, a brief discussion about CALIOP retrievals and products is given while in the second one the main steps for the derivation of the post-processed CALIOP-related pure dust product, available from the ESA-LIVAS database, maintained and hosted at the National Observatory of Athens (NOA), are intentionally briefly described because all the relevant publications ([Amiridis et al., 2013](#); [2015](#); [Marinou et al., 2017](#); [Proestakis et al., 2018](#)) are already provided. A short comment that may help in the clarification of any misleading points. LIVAS is the outcome of the post-processing of CALIOP profiles by applying: (i) “corrections” on dust lidar ratio ([Amiridis et al., 2013](#)), (ii) a discrimination technique for “extracting” dust aerosols from dusty mixtures, (iii) a series of quality control filters ([Marinou et al., 2017](#)) and (iv) aggregation into Level 3 outputs ([Tackett et al., 2018](#)).

3. **Section 3.1 on the methodology: Do you see a discontinuity in the MODIS DOD linked to changing of MERRA-2 grid cell?**

The spatial variations found in MIDAS DOD are attributed to those of MODIS AOD since the MERRA-2 grid cell has not been changed for the derivation of the fine resolution dataset. For the intercomparison among MIDAS, LIVAS and MERRA-2, all datasets have been regressed to $1^\circ \times 1^\circ$ pixels for consistency reasons without noticing pronounced features, discontinuities and abrupt changes in the DOD geographical patterns.

4. **Lines 330 to 332: “Our approach avoids on purpose the inclusion of additional optical properties providing information on aerosol size (alpha) available from MODIS and absorptivity (Aerosol Index) from OMI that are characterized by inherent limitations”. -> This is probably very unclear for the non-specialist reader and comes a bit out of the blue. If OMI is mentioned, the authors should at least explicit why using OMI would make sense when looking for dust aerosols and what are the potential drawbacks with it, other than data availability.**

We have added a reference ([Torres et al., 1998](#)) describing the theoretical background. We think that this clarifies the published approach that positive AI values are associated with the presence of absorbing mineral particles. Even higher AI levels are found when biomass particles are probed. There are numerous studies which have been relied on AI thresholds (usually above 1) for the monitoring and tracking loads of absorbing particles. The theoretical background of the UV retrievals is given in [Torres et](#)

al. (1998) while updates of the applied OMI algorithm are described in [Torres et al. \(2013\)](#). Likewise, a nice overview of the OMI products can be found in [Torres et al. \(2007\)](#).

5. Lines 359-361: "Here, we are using the same equations replacing AERONET AODs with those given by MODIS. This relies on the fact (results not shown here) that their averages are almost unbiased." -> A bit unclear. Average of MODIS AODs unbiased wrt AERONET? If yes, this feels a bit short and at least a reference to the MODIS validation should be given and this should be discussed. A quick search (<https://doi.org/10.1016/j.atmosenv.2018.12.004>) showed me that indeed on average along many years and globally the MODIS mean bias wrt AERONET is particularly low. However, at regional scale this is not always true. In particular, over the dustiest regions (N Africa and Middle East) it seems that there are more outliers in the comparisons linked to a more difficult AOD retrieval from MODIS. I am not saying that the MODIS AOD should not be used to estimate the uncertainty on the AOD, but that it should be discussed a bit more.

We have rephrased this sentence as follows.

"This relies on the fact (results not shown here) that their averages from a global perspective are almost unbiased; however, at regional level, small negative or positive offsets (lower than 0.05 in absolute terms) are recorded in the vast majority of AERONET sites, thus supporting our argument."

6. Equations 4 and 5: Those do confirm my thoughts in the previous comment. Levy et al (2013) write that (for DT land) "69.4% of MODIS AOD fall within expected uncertainty of $\pm(0.05 + 15\%)$." This is, I guess, the origin of equation 5 here (and something similar can be found for equation 4). This means, to me, that DT land has a mean bias of 0.05 wrt AERONET, in contradiction with the sentence above saying that there is no bias.

Please see our previous reply.

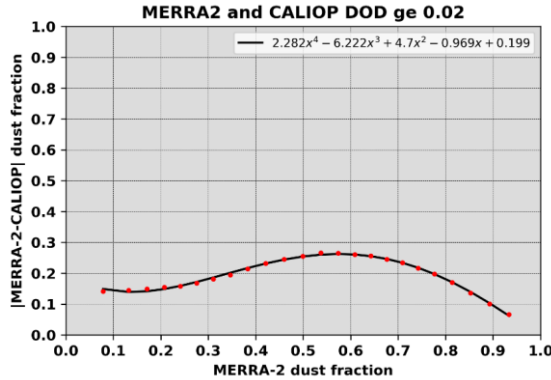
7. Equation 8: I would appreciate a plot here (of the data that lead to this equation), both to show how good the fit is (does it really need such a complex polynomial curve?) and show some values. I computed them myself from the equation to have a feeling. [MDF uncertainty]: [0 0,2]; [0,1 0,14]; [0,2 0,15]; [0,3 0,18]; [0,4 0,22]; [0,5 0,25]; [0,6 0,26]; [0,7 0,24]; [0,8 0,18]; [0,9 0,1]; [1 -0,01]; Those uncertainties are not negligible (especially at low MDF), however they are not discussed at all.

The requested plot along with the relevant text (copied from the submitted manuscript) are provided below.

"The CALIOP DOD-to-AOD ratio is our reference for estimating the uncertainty limits of the MERRA-2 dust fraction (MDF). The analysis is performed at $1^\circ \times 1^\circ$ spatial resolution considering only grid cells in which both MERRA-2 and CALIOP DODs are higher to or equal than 0.02. According to this criterion, more than 450000 CALIOP-MERRA2 collocated pairs have been found which are sorted (ascending order) based on MERRA-2 MDF (ranging from 0 to 1) and then are grouped in equal size bins containing 20000 data each sub-sample. For every group, we computed the median MDF (x axis) as well as the 68th percentile of the absolute MERRA-2 – CALIOP dust fraction (y axis) and then we found the best polynomial fit (Eq. 8)."

The geographical distributions illustrated in Figs. 1 and 2, along with the plot given here, indicate that the MDF uncertainties are not negligible and at the same time reveal that they are higher over areas where the dust loads do not dominate in the total burden. Based on the uncertainty analysis, it is apparent that the relative error gradually decreases from ~50% to ~10%, for increasing dust fraction, when MDF values higher than 0.5 (or 50%) are considered. For lower MDF levels (<0.5), the performance of MERRA-2 in reproducing dust fraction downgrades which makes sense since the dust "signal" is weak

over far distant areas or regions that do not affected by dust transport. The relevant discussion about the performance of MDF is thoroughly discussed in Section 4.2 of the submitted text.



8. Section 4.1 (and also in the conclusion): I do not at all understand this section. Why should the MODIS and MERRA-2 AODs be different? That would underline problems in one of the data sets (at least). And why do they need to be different for this analysis to work? I would say the opposite, that MODIS and MERRA-2 AODs should be similar enough to allow for this work to be relevant. Overall, I find this section 4.1 quite confusing, I am unsure what the authors are trying to show and how it fits in the rest of the paper. I would better see here a short summary of the MERRA-2 AOD validation (with references). And then a short discussion how this will impact the MIDAS data set. Also, this section contains discussions linked to the MDF (dust emission in GOCART for example), which should be moved to the next section.

As suggested by the Reviewer, we have totally removed Section 4.1 from the revised manuscript and we have kept only parts which fit to the revised text.

9. Lines 455 to 457: Is the MIDAS DOD expected to be overestimated because the GOCART model overestimates dust emissions?

In theory yes but that is why we decided to use also LIVAS. In addition, it is not easy to give a sufficient answer because the number of AERONET stations in dust emission areas are limited. For example, in N. Africa, we found slight positive bias [0.0, 0.02] in the Tamanrasset site. Regarding dust transport, there are several factors (e.g., size distribution, winds, identification and activation of the sources, etc.) that can affect the representation of dust burdens by MERRA-2. According to the global DOD maps (Figs. 5 and S6 in the revised manuscript), the agreement of MERRA-2 with respect to LIVAS and MIDAS is good both on annual and seasonal scales. We would like to point out again that from MERRA-2 we are using the dust fraction which is determined by the ability of the model to reproduce accurately both dust and non-dust aerosol species.

10. Figure 3: High resolution figures are needed. Here if I zoom in (to see details discussed) it becomes blurry

The quality of the produced png files might have been affected by the conversion of the word file to pdf. However, in order to improve the illustration, we have increased the dpi from 300 to 600.

11. Lines 485 to 490: I don't understand. If there is a bias of about 10% but other metrics show the algorithm performs well, then why is there a bias? This should be explained also in the manuscript.

By default, mean bias is affected by outliers in contrast to FB and FGE which are more “smoothed”. Some short clarifications along with a reference of the evaluation metrics have been added in the revised manuscript.

12. Lines 493-494: the correlation between MERRA-2 and CALIOP (LIVAS??) is less good over dust source regions due to the high variability. This is linked by the authors to a poor behaviour of the model in these cases. Can't we also imagine that CALIOP is not perfect there, as the very thin ground coverage makes it miss many events? This is discussed a bit further (lines 521 onwards), but I think it would be good to also mention around lines 493-494 that CALIOP (LIVAS?) is also not perfect.

We don't think that the narrow footprint of CALIOP at the ground plays such an important role since dust plumes are in general spatially wide (i.e., covering a whole 1-degree grid cell). Definitely CALIOP does not provide the “perfect retrievals” and the main reasons causing a departure from the “ideal scenario” are mentioned mainly in Section 4.2 as well as in relevant parts of the text.

13. Lines 533-534: the underestimation of CALIOP with respect to AERONET, is it the official product or LIVAS? Here, in this section, it is very confusing. I think most of the section refers to LIVAS but this specific sentence to the official product. If this is indeed the case, then I do not see how this information (and the discussion following) is useful here in the paper, where LIVAS and MERRA-2 are compared. That discussion is already in section 2.3 in a different formulation.

Between lines 533 and 542 are mentioned two important factors which can hamper CALIOP's performance in reproducing columnar DOD. The first one is related to the dust lidar ratio (LR), which has to be used for the derivation of the extinction profiles (resulted from the multiplication of backscatter coefficients with lidar ratio) and subsequently are vertically integrated in order to get the columnar DOD. This is what actually has been proposed in [Amiridis et al. \(2013\)](#) while in the global map of Figure S1 are depicted the most “representative” lidar ratios applied in our study. The second factor is related to the total attenuation of the laser beam by mineral particles accumulated at very high concentrations and this means that the columnar DOD will be underestimated under these cases since there are not available retrievals throughout and beneath the very thick dust layer ([Konsta et al., 2018](#)). Summarizing, the impact of the first factor has been mitigated in the LIVAS database (i.e., selection of more realistic LR than the universal values used in the raw CALIOP data) while for the second one cannot be done nothing.

14. Lines 558-560: Does this mean that overall, only 10 to 20 CALIOP measurements per grid cell were averaged along 9 years? If yes, this is very low and I don't think it can be considered representative.

The number of CALIOP L2 profiles (5km resolution) aggregated for the derivation of each LIVAS $1^\circ \times 1^\circ$ grid cell varies from 1 to 24. Overall, we have ~ 3.4 million of MERRA2-LIVAS pairs (i.e., total number of collocated $1^\circ \times 1^\circ$ grid cells) and we show how these are distributed among classes defined based on the number of CALIOP L2 profiles falling within the $1^\circ \times 1^\circ$ grid cell. A short clarification has been added in the revised manuscript and it is given below.

“Figure S3-ii displays the long-term averaged geographical distribution of the number of CALIOP L2 profiles (up to 24) aggregated for the derivation of the LIVAS $1^\circ \times 1^\circ$ grid-cell.”

15. General on section 4.2: this section is quite long, it contains the description of the differences and some discussion about the origin of those differences, but no discussion on the implications of underlined shortcomings on the MIDAS data set? In particular, the underestimation of MERRA-2 over dust sources should be discussed in terms of “how will it affect the MIDAS DOD”.

As we wrote in our introductory response, we have made an effort to reduce the manuscript, shortening also Section 4.2. Regarding MERRA-2 underestimations over dust sources, we think that our reply in a

similar comment mentioned above is valid also here. Focusing only over sources, the underestimation of dust emission by MERRA-2 most probably has minor impact on our results since the amount of mineral particles will be lower but their portion (i.e., MDF) to the total load (in optical terms) will be rather stable and above ~90% considering that the contribution from other aerosol species is very small or even zero. As it concerns dust transport, the situation becomes more complex because an accurate representation of the MDF is determined both from dust and non-dust AODs. Actually, our findings (Section 4.1) can be the starting point of a dedicated assessment analysis in which all the factors that affect MERRA-2 dust fraction will be investigated in-depth. Finally, we would like to express our disagreement with the comment "..., but no discussion on the implications of underlined shortcomings on the MIDAS data set?". There are several "links" in Sections 4.2 and 4.3 with the obtained findings from Section 4.1 facilitating the interpretation of the deviations found between MIDAS and AERONET (Section 4.2) as well as the disagreements among MIDAS, LIVAS and MERRA-2 DODs (Section 4.3).

16. Section 4.3: Why redo a MODIS validation against AERONET (not bringing anything new)? I think there are enough papers on that to just refer to one and remove this part, making the paper a bit shorter and less confusing.

We have removed the relevant part in the revised manuscript.

17. Figure 5: please change the colour scale for the correlation coefficient as it is now very difficult to see

Done.

18. Section 4.4: I think that somehow this section should show what the new MIDAS product brings. The comparisons are currently done in a way that gives the impression it's just another product but not really improved or different from MERRA-2 or the LIVAS climatology. This is linked to the fact that averages over long periods are analysed, so at the end we are just comparing (validating?) climatologies from different products. As MIDAS is not meant to be a climatology, I would not do this kind of comparisons a big point in the paper, but I would instead emphasize what MIDAS gives that those other products can't give. And validate the product at its resolution - but this is done in the comparison with AERONET.

The powerful elements of the MIDAS dataset, as already have been mentioned in the submitted text, are the almost global coverage, the long-term availability as well as the fine spatial resolution. These features are demonstrated in Section 4.4 where a short discussion about the annual and seasonal global DOD patterns is given. A more detailed climatological analysis is under preparation whereas other studies, relying on the MIDAS dataset, are ongoing and they have already mentioned in the abstract (Lines 35-37), in the introduction (Lines 129-132) and in the last paragraph of the summary.

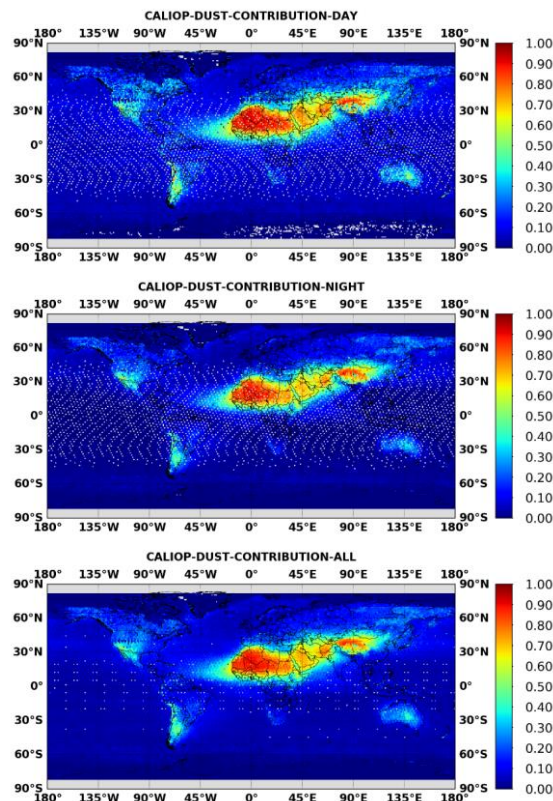
In Section 4.3, our intention is to make an intercomparison among MERRA-2, LIVAS and MIDAS DODs aiming at assessing the consistency of our product with respect to those provided by simulations and active remote sensing techniques. To our opinion this a very important aspect in our study taken into account the advantages/disadvantages of each dataset. Based on this analysis, we highlighted differences found at specific regions of the planet while through the intra-annual plots for each subdomain the obtained deviations among the three datasets are illustrated and interpreted. Finally, the length of the section has been reduced after refining the submitted document.

19. Line 648-649: "the study period extends from 2007 to 2015, driven again from CALIOP's temporal availability" -> this is very confusing. . . CALIOP is still running. . . so the authors probably mean LIVAS availability. This is only one of the many examples where it is not clear which data is referred to, leaving the reader in possible misunderstanding.

We agree with the Reviewer and the appropriate corrections have been made.

20. Figure 6: Why do we see orbit-like features on a 9 years average?

Please note that CALIOP revisiting time is 16 days and it has a narrow footprint at the ground. In addition, a series of quality checks is applied on the raw vertical profiles. Therefore, it makes sense that orbit-like features are evident on the long-term averaged global distributions even though these are representative for a 9-year period. In the following figure, the patterns of the dust fraction at daytime (first) and nighttime (second) conditions as well as throughout the day (third), are given. It is clarified that the same CALIOP data have been used for the reproduction of Figure 6 (in the submitted manuscript) but here a different parameter is processed. It is clear that the orbit-like features are evident when only daytime or nighttime patterns are studied in contrast to the “full-day” distribution.



21. Line 673: “CALIOP underestimates AOD over the Sahara” -> again, I think this is the official CALIOP product, right? So how is it relevant here where comparing LIVAS? Same comment/question further, line 677: how does the CALIOP misclassification of clouds impact the LIVAS product? Overall in this section I have a feeling that there is discussion of both CALIOP and LIVAS but I can't see which is which and I am very confused as to what is really important for the work presented here.

We agree with this comment and we have clarified all the misleading statements in the text. Most of the cases in which very intense dust layers are misclassified as clouds are encountered over/nearby the sources. Under these conditions, the CALIOP profiles are discarded since they are eliminated by the quality assurance filters. This can be one of the reasons where LIVAS DODs are substantially lower than those of MIDAS and MERRA-2 over Bodele, as already discussed in the document, which consists the most active/intense dust source of the planet. Moreover, the underestimations over the major dust sources as observed in the LIVAS database are directly related to the official CALIPSO product and the undetected dust layers therein, as presented and extensively discussed by [Winker et al. \(2013\)](#). These two artifacts are expected to cause an underestimation of the climatological values (see for example the BOD annual values provided in Table 1) keeping always in mind that the appropriate selection of dust lidar ratios (which is highly variable!) plays a very important (or even dominant) role in potential LIVAS DODs deviations from other relevant products.

22. Lines 686-688: I don't see the point of this sentence

A better clarification is given in the revised manuscript.

"Wei et al. (2019b) showed that MODIS underestimates AOD with respect to AERONET while the maximum MIDAS-AERONET negative DOD differences are found at Ilorin and Djougou sites (Figure 4-iv)."

23. Line 732: any explanation for the local minimum of MIDAS in May? This is very surprising.

Based on the updated analysis (i.e., consideration of MODIS-Aqua C061 data) the local minimum has disappeared.

24. Figure 8: Why is the uncertainty higher off the west coast of N Africa than inland?

The uncertainty of the MIDAS DOD results from the combination of the respective uncertainties of MODIS AOD and MDF. Moving westwards from the Sahara, the MDF uncertainty increases due to the reduction of dust contribution while the oceanic AODs are very reliable (i.e., aerosols are suspended over low-albedo surface). Along the coasts of the Gulf of Guinea, MODIS AODs are very high (probably very overestimated) while the performance of MERRA-2 downgrades. This means that both factors converge towards maximizing the uncertainty of the derived DOD over the area. However, we would like to clarify that in the revised manuscript instead of presenting the uncertainties of the average we are providing the average of the uncertainties and their geographical patterns resemble those of DODs.

Minor comments / suggestions:

1. Line 55: "Gobbi" -> Gobi

Corrected.

2. Reference list lines 87-88 -> This list is clearly not aiming at being exhaustive (which is understandable) but here about half the references (and the newest) are work from the (co-) authors of this paper, while overall I don't think they really do represent half the work on dust aerosols from space, and certainly not recently. Maybe it would be best to cite a review paper?

We prefer to keep the existing references.

3. Line 100 correct reference is Di Tomaso... She is one of the co-authors...

Thanks for correction!

4. Line 133: "Finally, the main findings are summarized and are drawn" -> I think this needs rephrasing

We have changed the sentence.

5. Line 142: "MODIS is mounted on the NASA's twin polar satellites Terra and Aqua acquiring high-quality aerosol data since 2000 and 2002, respectively, while thanks to its wide swath (~2330 km) provides near-global observations, almost on a daily basis" -> I think there's something wrong in the tenses

We have modified slightly the sentence.

6. Line 207: "Over oceans, are also used AVHRR radiances" -> This reads weird, I suggest avoiding the passive formulation

It is true that the sentence was not written appropriately. We have improved it in the revised manuscript.

7. Line 289: "requires the of SSA" -> I think a word is missing

The missing word has been added!

8. Line 347: "in which ~68% of the MODIS-AERONET AOD differences fall within" -> I think it needs rephrasing

We think that it is correct.

9. Line 375: "higher or equal than" -> higher to or equal than?

Done.

10. Line 391: "These two uncertainty quantities" -> values?

We are referring to the measurement and standard errors.

11. Line 398: "On the following sections," -> In?

We think that both are correct.

12. Line 405: "since a climatological study it is the scientific topic of the companion paper" -> reads weird. Rephrase? Or at least remove "it".

We have removed "it".

13. Lines 460: by "enormous number of pairs" do you mean that the histogram contains all the single comparisons and not just the time average comparison? This is unclear in the text.

The histogram contains all the MODIS-MERRA2 pairs found over the period 2007-2016. This part of the text has been removed.

14. Lines 471-472: "showing the ability of MERRA-2 in reproducing the integrated aerosol fields." -> This belongs to Section 4.1 on AOD, not 4.2 on dust fraction

We think that it is stated very clear the separation between existing evaluation studies of MERRA-2 AOD and our assessment analysis of the MDF.

15. Line 480: the terms fractional bias (FB) and fractional gross error (FGE) should be a bit explained, those are not so standard statistics I think

The FB and FGE evaluation metrics have been used in many model assessment studies (i.e., [Binietoglou et al. 2015](#)) while they are implemented in the [forecast evaluation](#) of SDS-WAS. However, we are providing a relevant paper ([Yu et al., 2006](#)) providing the formulas of the aforementioned metrics.

16. Line 580: "discussed" -> described?

Done.

17. Line 582: "while for the derived DOD to check the validity of our approach" -> needs rephrasing

Done.

18. Line 583-584: "At first, a short discussion is made on the" -> I think "made" can't be used in that sense

We think that it can be used in that sense.

19. Lines 592-593 "and the consideration of AERONET data." -> please rephrase

Done.

20. Line 600: "slight" -> slightly?

Done.

21. Line 600 (end) to 604: I think these sentences belong more to the methods section

We think that it is well placed there because we are recalling to the reader which is the applied Angstrom threshold and then we are mentioning the applied sensitivity test.

22. Line 624: "fine DOD on AERONET" -> in?

Done.

23. Line 625-626: " but its contribution to the total dust AOD it is difficult and probably impossible to be quantified" -> remove "it"?

Done.

24. Lines 662-663: "it is apparent a very good agreement" -> A very good agreement is observed?

We think that it is better to keep the sentence as is.

25. Line 671: "relied" -> relying?

Done.

26. Line 675: "works" -> work?

The correct is "works" because we are referring to the studies mentioned in the previous sentence.

27. Line 679: "All these aspects, most likely met over dust sources" -> Please rephrase

We think that we don't have to rephrase this part.

28. Line 682-683: "Across the Sahel, CALIOP provides higher DODs (mainly up to 0.2) both against simulated and satellite products" -> confusing, CALIOP is a satellite, so maybe use here MODIS or MIDAS?

We have replaced CALIOP with LIVAS.

29. Line 792: "since it is not expected the accumulation of dust" -> since the accumulation of dust is not expected

Thanks for the correction!

30. Line 909: "AEROENT" (typo)

Thanks!

31. Line 910: "assuming that dust loads are mainly consist of" -> please rephrase

Done.

32. Line 912: remove "resides"?

Done.

ModIs Dust AeroSol (MIDAS): A global fine resolution dust optical depth dataset

Antonis Gkikas¹, Emmanouil Proestakis¹, Vassilis Amiridis¹, Stelios Kazadzis^{2,3}, Enza Di Tomaso⁴, Alexandra Tsekeli¹, Eleni Marinou⁵, Nikos Hatzianastassiou⁶ and Carlos Pérez García-Pando^{4,7}

¹Institute for Astronomy, Astrophysics, Space Applications and Remote Sensing, National Observatory of Athens, Athens, 15236, Greece

²Physikalisch-Meteorologisches Observatorium Davos, World Radiation Center, Switzerland

³Institute of Environmental Research and Sustainable Development, National Observatory of Athens, Greece

⁴Barcelona Supercomputing Center, Barcelona, Spain

⁵Deutsches Zentrum für Luft- und Raumfahrt (DLR), Institut für Physik der Atmosphäre, Oberpfaffenhofen, Germany

⁶Laboratory of Meteorology, Department of Physics, University of Ioannina, Ioannina, Greece

⁷ICREA, [Catalan Institution for Research and Advanced Studies](#), Barcelona, Spain

Corresponding author: Antonis Gkikas (agkikas@noa.gr)

Abstract

Monitoring and describing the spatiotemporal variability of dust aerosols is crucial to understand their multiple effects, related feedbacks and impacts within the Earth system. This study describes the development of the MIDAS (ModIs Dust AeroSol) dataset. MIDAS provides columnar daily dust optical depth (DOD) at 550 nm at global scale and fine spatial resolution ($0.1^\circ \times 0.1^\circ$) over a 15-year period (2003-2017). This new dataset combines quality filtered satellite aerosol optical depth (AOD) retrievals from MODIS-Aqua at swath level (Collection 6.1, Level 2), along with DOD-to-AOD ratios provided by MERRA-2 reanalysis to derive DOD on the MODIS native grid. The uncertainties of MODIS AOD and MERRA-2 dust fraction with respect to AERONET and LIVAS, respectively, are taken into account for the estimation of the total DOD uncertainty. MERRA-2 dust fractions are in very good agreement with those of LIVAS across the “dust belt”, in the Tropical Atlantic Ocean and the Arabian Sea; the agreement degrades in North America and the Southern Hemisphere where dust sources are smaller. MIDAS, MERRA-2 and LIVAS DODs strongly agree when it comes to annual and seasonal spatial patterns, with collocated global DOD averages of 0.033, 0.031 and 0.029, respectively; however, deviations in dust loading are evident and regionally dependent. Overall, MIDAS is well correlated with AERONET-derived DODs ($R=0.89$), only showing a small positive bias (0.004 or 2.7%). Among the major dust areas of the planet, the highest R values (>0.9) are found at sites of N. Africa, Middle East and Asia. MIDAS expands, complements and upgrades existing

Deleted: Earth Sciences Department.

Deleted: Passeig Lluís Companys 23, 0801

Deleted: 0

Field Code Changed

Formatted: English (United States)

Deleted:)

Deleted: decade

Deleted: 7

Deleted: 6

Deleted: CALIOP

Deleted: (including measurement and sampling uncertainties)

Deleted: CALIOP

Deleted: column-integrated dust fractions

Deleted: CALIOP

Deleted: of

Deleted: s'

Deleted: intensity

Deleted: ground-truth

Deleted: =

Deleted: 882

Deleted: negative

Deleted: -

Deleted: 9

Deleted: -5.307

Deleted: up to

Deleted: 77

observational capabilities of dust aerosols and it is suitable for dust climatological studies, model evaluation and data assimilation.

Formatted: English (United States)

1. Introduction

Among tropospheric and stratospheric aerosol species, dust aerosol is the most abundant component in terms of mass, contributing more than half ~~of~~ the global aerosol amount (Textor et al., 2006; Zender et al., 2011). Preferential sources of dust aerosols ~~s~~ are located in areas where precipitation is low, thus favoring aridity, whereas a significant contributing factor is the accumulation of alluvial sediments. Such regions comprise deserts, dry lake beds and ephemeral channels (e.g., Middleton and Goudie, 2001; Prospero et al., 2002; Ginoux et al., 2012). Previous studies (Prospero et al., 2002; Ginoux et al., 2012), have shown that the major portion of the global dust burden originates from the Sahara Desert, which hosts the most intense dust source of the planet, the Bodélé Depression located in the northern Lake Chad Basin. In North Africa, large amounts of mineral particles are also emitted in the Western Sahara while other noticeable sources of smaller spatial extension are located in the eastern Libyan Desert, in the Nubian Desert (Egypt) and Sudan (Engelstaedter et al., 2006).

Deleted: to

One of the major dust sources of the planet, following N. Africa, is the Middle East with several active regions (Pease et al., 1998; Hamidi et al., 2013; Yu et al., 2013) in which wind-blown dust is emitted from alluvial plains (Tigris-Euphrates River) and sandy deserts (Rub al Khali Desert). Important dust sources are also recorded in the Asian continent, particularly in the Taklamakan Desert (Ge et al., 2014), in the Gobi Desert (Chen et al., 2017), in its central parts (Karakum Desert; Li and Sokolik, 2018), in the Sistan Basin (Alizadeh Choobari et al., 2013) and in ~~the~~ Thar Desert, ~~(Hussain et al., 2005)~~. In North America, mineral particles emitted from the Mojave and Sonoran deserts (Hand et al., 2017) have mainly natural origin while in the Chihuahuan Desert as well as in the Southern Great Plains the anthropogenic interference on soil can favor emission of dust particles and subsequently their entrainment in the atmosphere (Hand et al., 2016). Overall, the major portion of the global dust budget arises from the deserts of the N. Hemisphere (Ginoux et al., 2012) while mineral aerosols are also emitted in Australia (Ekström et al., 2004), South Africa (Bryant et al., 2007; Vickery et al., 2013) and South America (Gassó and Torres, 2019), but to a lesser extent. At global scale, most of the entrained dust loads in the atmosphere originate from tropical and sub-tropical arid regions; however, about 5% of the global dust budget consists of particles emitted from high-latitude sources (Bullard et al., 2016).

Formatted: English (United States)

Deleted: b

Deleted: desert areas (e.g.

Deleted:) situated in the Indus valley plains of Pakistan (

Dust plays a key role in several aspects of the Earth system such as climate (e.g. Lambert et al., 2013; Nabat et al., 2015) and weather (Pérez et al., 2006; Gkikas et al., 2018; Gkikas et al., 2019), attributed to the perturbation of the Earth-Atmosphere system radiation budget (Sokolik and Toon, 1996; Haywood and Bucher, 2000) by mineral particles, the productivity of oceanic waters (Jickells et al., 2005) and terrestrial ecosystems (Okin et al., 2004), and effects on humans' health (Kanatani et al., 2010; Kanakidou et al., 2011; Pérez García-Pando et al., 2014; Du et al., 2016; Querol et al., 2019). Dust is characterized by a pronounced temporal and spatial variability due to the heterogeneity of the emission, transport and deposition processes governing its life cycle (Schepanski, 2018). A variety of atmospheric circulation mechanisms, spanning from local to planetary scales, are responsible for the uplifting of erodible particles from bare soils (Koch and Renno, 2005; Knippertz et al., 2007; Klose and Shao, 2012; Fiedler et al., 2013) and their subsequent transport (Husar et al., 2001; Prospero and Mayol-Bracero, 2013; Yu et al., 2015; Flaounas et al., 2015; Gkikas et al., 2015), accumulation and removal (Zender et al., 2003; Ginoux et al., 2004) from the atmosphere.

Deleted: the dust

Formatted: English (United States)

Given the scientific importance of dust in the Earth system as well as the numerous socioeconomic impacts (Stefanski and Sivakumar, 2009; Weinzierl et al., 2012; Kosmopoulos et al., 2018), there is a need to monitor and forecast dust loads at different spatiotemporal scales. Contemporary satellite observations, available over long-term periods, have been proven a powerful tool in such efforts as they provide wide spatial coverage, relatively high sampling frequency and considerably high accuracy. Spaceborne retrievals have been widely applied in aerosol research for the description of dust load features and their evolution (e.g., Kaufman et al., 2005; Liu et al., 2008; Peyridieu et al., 2013; Rashki et al., 2015; Gkikas et al., 2013; 2016; Marinou et al., 2017; Proestakis et al., 2018). Even more accurate aerosol observations, but locally restricted, are derived by ground-based platforms consisting of sunphotometers, lidars and in-situ instruments. Based on these measurements, columnar optical and microphysical properties of mineral particles have been analyzed extensively (Giles et al., 2012), altitude-resolved information of optical properties has provided insight about the dust vertical distribution (Mamouri and Ansmann, 2014), and a comprehensive description of dust optical, microphysical and chemical properties has been achieved from surface and aircraft in-situ instruments (Rodríguez et al., 2012; Liu et al., 2018). Finally, through the deployment of atmospheric-dust models (e.g., Pérez et al., 2011; Haustein et al., 2012), global (e.g., Ginoux et al., 2004) and regional (e.g., Basart et al., 2012) displays of dust burden are provided.

Deleted: s'

Deleted: have been realized

Traditionally, observations have been utilized to evaluate and eventually constrain model performance. Observations are increasingly used in data assimilation (DA) schemes for aerosol forecast initialization (Di Tomaso et al., 2017) and development of reanalysis datasets (Benedetti et al., 2009; Lynch et al., 2016; Gelaro et al., 2017). The most exploited reanalysis datasets in dust-

Deleted: s

related studies, are the MERRAero (Modern Era Retrospective analysis for Research and Applications Aerosol Reanalysis; Buchard et al., 2015) and its evolution MERRA-2 (Modern-Era Retrospective analysis for Research and Applications, Version 2; Gelaro et al., 2017) as well as CAMSRA (Copernicus Atmosphere Monitoring Service Reanalysis; Inness et al., 2019) and its predecessor MACC (Monitoring Atmospheric Composition and Climate; Inness et al., 2013). Current reanalysis datasets provide information about dust aerosols at high temporal resolution and decadal time scales. However, even though AOD observations are assimilated, the performance of the simulated outputs is partly model-driven and their resolution is relatively coarse.

The overarching goal of the present study is to describe the development of the MIDAS (ModIs Dust AeroSol) dataset, providing dust optical depth (DOD) over a 15-year period (2003–2017). The powerful element of this product is its availability at fine spatial resolution ($0.1^\circ \times 0.1^\circ$) and on a daily basis as well as the provision of full global coverage (i.e., both over land and ocean). Ginoux et al. (2012) analyzed DOD at the same spatial resolution and for a long-term period but restricted the analysis to continental surfaces as the scientific focus was put on the identification of natural and anthropogenic dust sources. Voss and Evan (2020) combined satellite (MODIS, AVHRR) aerosol retrievals and MERRA-2 winds to analyze DOD at coarse spatial resolution ($1^\circ \times 1^\circ$) for extended time periods. CALIOP-based vertical dust backscatter and extinction profiles along with the respective column integrated DODs at $1^\circ \times 1^\circ$ spatial resolution are distributed via the LIVAS database (Amiridis et al., 2015). Taking advantage of the spectral signature of dust at thermal infrared (TIR) wavelengths, DOD is also provided by IASI (Vandenbussche et al., 2013; Capelle et al., 2018; Clarisse et al., 2019) and SEVIRI (Ackerman, 1997) instruments aboard the polar-orbit METOP satellites and the geostationary MSG satellite, respectively. In this case, the conversion of DOD from TIR to mid-visible spectrum range is subjected to several assumptions related to size and other properties. Dust observations from IASI are provided at global scale twice per day and those of SEVIRI cover the hemisphere centered at the prime meridian over the equator every 15 minutes (Schepanski et al., 2012). Thanks to their high sampling frequency, fine spatial resolution and long-term availability, the aforementioned datasets have been used for the identification of dust sources activation across N. Africa (Schepanski et al., 2007; Vandenbussche et al., 2020). Based on the current status described above, MIDAS dataset expands, complements and upgrades existing observational capabilities of dust aerosols being suitable for research studies related to climatology, model evaluation and data assimilation.

For the development of the fine resolution MIDAS DOD, a synergy of MODIS-Aqua (Section 2.1), MERRA-2 (Section 2.2), LIVAS (Section 2.3) and AERONET (Section 2.4) aerosol products has been deployed by exploiting the strong capabilities of each dataset. Based on the applied

Deleted: aerosol optical depth ()
Deleted: ()

Deleted: , which

Deleted: provides

Deleted: decade

Deleted: 2007

Deleted: 2016

Deleted: ,

Deleted: they

Deleted: only above

Deleted: since their

Deleted: in order

Deleted: , and

Deleted: d

Deleted: ,

Deleted: ,

Deleted: over long-term periods

Deleted: at coarse spatial resolution ($1^\circ \times 1^\circ$)

Deleted: V

Deleted: (and among other aerosol species)

Deleted: AODs

Deleted: through

Deleted: mineral particles'

Deleted: the

Deleted: Nevertheless

Deleted: particles'

Deleted: and

Deleted: while

Deleted: and they are given

Deleted: As described below

Deleted: Therefore, Therefore, considering the advantages and drawbacks of the techniques outline before, it is clear that the developed

Formatted: English (United States)

Deleted: CALIPSO-CALIOP

Deleted: -CALIOP

Deleted: taking advantage of

methodology (Section 3.1), the DOD is calculated by the product of MODIS-Aqua Level 2 AOD and the collocated DOD-to-AOD ratio from MERRA-2. The uncertainty of the DOD is calculated by combining the uncertainties of MODIS AOD and MERRA-2 dust fraction (MDF), using AERONET and LIVAS, respectively, as reference (Section 3.2). We thoroughly compare MDF against the LIVAS dust portion in Section 4.1. The MIDAS DOD is evaluated against AERONET in Section 4.2 and compared with MERRA-2 and LIVAS DODs in Section 4.3. In section 4.4, we provide the annual and seasonal global geographical distributions of the MIDAS DOD as a demonstration of the developed product. Finally, the main findings are summarized and the conclusions are drawn in Section 5.

2. Datasets

2.1. MODIS

The MODerate resolution Imaging Spectroradiometer (MODIS) is a passive sensor measuring the top of atmosphere (TOA) reflectance in order to retrieve aerosol optical depth (AOD), among other aerosol optical properties, at various wavelengths spanning from the visible to the near infrared spectrum range. MODIS, mounted on the NASA's twin polar satellites Terra and Aqua, acquires high-quality aerosol data since 2000 and 2002, respectively, while thanks to its wide swath (~2330 km) provides near-global observations, almost on a daily basis. The derivation of AOD is achieved through the implementation of two retrieval algorithms based on the Dark Target (DT) approach, valid over oceans (Remer et al., 2002; 2005; 2008) and vegetated continental areas (Levy et al., 2007a; 2007b; 2010) but relying on different assumptions and bands, and the Deep Blue (DB) approach (Hsu et al., 2004; Sayer et al., 2013) providing retrievals over all cloud-free and snow-free land surfaces, including arid and semi-arid surfaces. MODIS datasets are organized into various collections depending on the version of the retrieval algorithms, and into a number of levels depending on their spatial and temporal resolution. For our purposes, we are utilizing Collection 6.1 (C061) MODIS-Aqua Level 2 (L2) retrievals over the period 2003-2017, which are reported at 5-min swath granules (Levy et al., 2013) and are accessible from the Level-1 and Atmosphere Archive & Distribution System (LAADS) Distributed Active Archive Center (DAAC) (<https://ladsweb.modaps.eosdis.nasa.gov/>). All the updates applied in the latest version of MODIS DB and DT retrievals with respect to Collection 6, are provided in the relevant technical documents available at the Atmosphere Discipline Team Imager Products webpage (<https://atmosphere-imager.gsfc.nasa.gov/documentation/collection-61>).

Deleted: from the
Deleted: both
Deleted: the
Deleted: CALIOP
Deleted: a
Deleted: the MERRA-2 dust fraction
Deleted: CALIOP
Deleted: 2
Deleted: 3
Deleted: CALIOP
Deleted: 4
Deleted: 5
Formatted: English (United States)

Deleted: is
Deleted: ing
Deleted: ,
Deleted: three
Deleted: or
Deleted: suitable
Deleted: land surfaces characterized by high reflectivity
Deleted: Depending on the version of the retrieval algorithms, the
Deleted: at
Deleted: as well as at
Deleted: various
Deleted: corresponding
Deleted: to
Deleted: the
Deleted: 0
Deleted: ,
Deleted: 7
Deleted: 6
Field Code Changed
Deleted: ,
Deleted: ,
Field Code Changed
Formatted: English (United States)

Each MODIS swath is composed of 203 x 135 retrievals with increasing pixel size from the nadir view (10 km x 10 km) towards the edge of the satellite scan (48 km x 20 km), and to which a Quality Assurance (QA) flag is assigned (Hubanks, 2018). More specifically, these bit values represent the reliability of the algorithm output and are equal to 0 (“No Confidence”), 1 (“Marginal”), 2 (“Good”) and 3 (“Very Good”). MODIS AOD retrievals are acquired based on different algorithms according to the underlying surface type. In order to fill observational gaps, attributed to the assumptions or limitations of the applied MODIS algorithms, the DT-Ocean (QA≥1), DT-Land (QA=3) and DB-Land (QA≥2) AOD retrievals are merged based on the Normalized Difference Vegetation Index (NDVI) and the highest accuracy criterion (Sayer et al., 2014). This “merged” AOD is stored in the scientific data set (SDS) named “AOD_550_Dark_Target_Deep_Blue_Combined”, which is extracted and processed for the needs of the current work. Finally, two quality filtering criteria are applied to the raw MODIS AODs for eliminating observations which may be unreliable. AODs associated with cloud fraction (CF) higher than 0.8 as well as those with no adjacent retrievals are masked out following the recommendations of previous studies (Anderson et al., 2005; Zhang and Reid, 2006; Hyer et al., 2011; Shi et al., 2011). The first criterion is associated with the potential cloud contamination on AODs, while the second one discards “suspicious” retrievals from the dataset.

2.2. MERRA-2

The Modern-Era Retrospective Analysis for Research and Applications, version 2 (MERRA-2), developed by the NASA Global Modeling and Assimilation Office (GMAO), is the first atmospheric reanalysis spanning over the new modern satellite era (1980 onward) in which aerosol-radiation interactions and the two-way feedbacks with atmospheric processes are taken into account (Gelaro et al., 2017). The key components of MERRA-2 (Buchard et al., 2017) are the Goddard Earth Observing System (GEOS-5) (Rienecker et al. 2008; Molod et al. 2015), which is radiatively coupled to the Goddard Chemistry Aerosol Radiation and Transport model (GOCART; Chin et al. 2002; Colarco et al. 2010), and the three-dimensional variational (3DVar) Gridpoint Statistical Interpolation analysis system (GSI) (Wu et al. 2002).

The GOCART aerosol module, simulates emission, sinks, removal mechanisms (dry deposition and gravitational settling, large-scale wet removal and convective scavenging) as well as the chemical processes of five aerosol species: dust, sea-salt, sulfate, and black and organic carbon. Their optical properties are based on the updated Optical Properties of Aerosols and Clouds (OPAC) database (Hess et al. 1998), incorporating dust non-spherical shape (Meng et al. 2010; Colarco et al. 2014), and are calculated according to Colarco et al. (2010). For coarse particles (i.e., dust and sea-salt), five non-interacting size bins are considered whose emissions are driven by the wind speed based on the

Deleted: by

Deleted: , of

Deleted: spatial resolution

Deleted: in

Deleted: As it has been mentioned above, the

Deleted: , as it has been presented by Sayer et al (2014)

Deleted: From the raw MODIS files,

Deleted: t

Deleted: and

Deleted: of

Deleted: , and

Deleted: attempts at removing

Formatted: English (United States)

Deleted: data assimilation

Formatted: English (United States)

Deleted: In t

Deleted: ,

Deleted: (

Deleted:) are simulated

parameterizations of Marticorena and Bergametti (1995) for dust and on the modified version of Gong (2003) for sea-salt. Both hydrophobic and hydrophilic black (BC) and organic (OC) carbon emitted from anthropogenic activities (i.e., fossil fuel combustion) and natural processes (i.e., biomass burning) are considered. Regarding sulfate aerosols (SO_4), these either are primarily emitted or are formed by the chemical oxidation of sulfur dioxide gas (SO_2) and dimethyl sulfide (DMS). Until 2010, daily emissions of eruptive and degassing volcanoes are derived from the AeroCom Phase II project (Diehl et al. 2012; <http://aerocom.met.no/>) and afterwards only a repeating annual cycle of degassing volcanoes is included in MERRA-2. The hygroscopic growth of sea-salt, sulfate and hydrophilic carbonaceous aerosols is determined by the simulated relative humidity (RH) and the subsequent modification of particles' shape and composition is taken into account in computations of particles' fall velocity and optical parameters (Randles et al., 2017). A detailed description of the emission inventories along with the global climatological maps, representative for the period 2000 – 2014, are given in Randles et al. (2017).

MERRA-2 is a multidecadal reanalysis in which a variety of meteorological and aerosol observations are jointly assimilated (Gelaro et al., 2017). The former group of observations consists of ground-based and spaceborne atmospheric measurements/retrievals summarized in Table 1 of Gelaro et al. (2017) while the full description is presented in McCarty et al. (2016). For aerosol data assimilation, the core of the utilized satellite data is coming from the MODIS instrument multichannel radiances, in addition to observational geometry parameters, cloud fraction and ancillary wind data. Over oceans, AVHRR radiances, from January 1980 to August 2002, are used as well and over bright surfaces (albedo > 0.15) the non-bias-corrected AOD, retrieved for the Multiangle Imaging SpectroRadiometer (MISR; Kahn et al., 2005) is assimilated from February 2000 to June 2014. Apart from spaceborne radiances and retrievals, the Level 2 (L2) quality-assured AERONET measurements (1999 – October 2014; Holben et al., 1998) are integrated in the MERRA-2 assimilation system (Goddard Aerosol Assimilation System, GAAS) which is presented in Randles et al. (2017; Section 3). The cloud-free MODIS radiances (DT algorithm, Collection 5) and AVHRR radiances (above oceanic regions) are used for the derivation of bias-corrected AODs, via a neural net retrieval (NNR), adjusted to the log-transformed AERONET AODs. It must be clarified, that only the MERRA-2 AOD is directly constrained by the observations while the model's performance (background forecast) and data assimilation structure (parameterization of error covariances) are “responsible” for the aerosol speciation, among other aerosol diagnostics (Buchard et al., 2017).

In the present study, we use the columnar MERRA-2 total and dust AOD at 550 nm in order to calculate the contribution, in optical terms, of mineral particles to the overall load. The computed dust-to-total AOD ratio (i.e., MDF) is evaluated against LIVAS and then used for the derivation of MIDAS DOD. MERRA-2 products (M2T1NXAER files; V5.12.4; aerosol diagnostics) have been

Deleted: are also used AV

Deleted: (February 2000 – June 2014)

Deleted: from satellite datasets

Deleted: retrievals

Deleted: From

Deleted: from the

Deleted: over land and ocean,

Deleted: above dark target continental and maritime areas,

Deleted:

Deleted: , the AODs are retrieved from the

Deleted: cloud-free

Deleted: radiances

Deleted:

Deleted: and adjusted (bias correction)

Deleted: corresponding

Deleted: , via a neural net retrieval (NNR)

Formatted: English (United States)

Deleted: CALIOP retrievals

Deleted: dust optical depth (DOD) on MODIS-Aqua swaths

downloaded from the GES DISC server (<https://disc.gsfc.nasa.gov/>) and are provided as hourly averages at $0.5^\circ \times 0.625^\circ$ lat-lon spatial resolution.

Deleted: reported

Formatted: English (United States)

2.3. LIVAS

The ESA LIVAS database (Amiridis et al., 2015; <http://lidar.space.noa.gr:8080/livas/>) contains a pure dust satellite-based product spanning from 2007 to 2015, which has been derived from the Cloud Aerosol Lidar with Orthogonal Polarization (CALIOP) sensor, onboard the Cloud-Aerosol Lidar and Infrared Pathfinder Satellite Observation (CALIPSO) satellite. This active sensor acquires altitude resolved observations of aerosols and clouds since mid-June 2006 (Winker et al., 2010). CALIPSO, flying in the A-Train constellation (Stephens et al., 2002), provides almost simultaneous observations with Aqua thus making feasible and powerful their synergistic implementation for aerosol research. CALIOP, an elastic backscatter two-wavelength polarization-sensitive Nd:YAG lidar in a near-nadir-viewing geometry (since 28th November 2007, 3 degrees off-nadir), emits linearly polarized light at 532 and 1064 nm and detects the co-polar components at 532 and 1064 nm and the cross-polar component at 532 nm, relative to the laser polarization plane (Hunt et al., 2009). Based on the attenuated backscatter profiles (Level 1B) and the implementation of retrieval algorithms (Winker et al., 2009), aerosol/cloud profiles as well as layer products are provided at various processing levels (Tackett et al., 2018). CALIOP Level 2 (L2) aerosol and cloud products are provided at a uniform spatial resolution along horizontal (5 km) and vertical (60 m) dimensions. Detectable atmospheric features are first categorized to aerosols or clouds and then are further discriminated into specific subtypes according to Vaughan et al. (2009). For aerosols, in the Version 3 used here, 6 subtypes are considered consisting of clean marine, dust, polluted continental, clean continental, polluted dust and smoke (Omar et al., 2009). Based on the aerosol subtype classification, specific extinction-to-backscatter ratios (Lidar Ratio - LR) are applied for the provision of extinction coefficient profiles along the CALIPSO orbit-track (Young and Vaughan, 2009).

Deleted: - CALIOP

Field Code Changed

Deleted: T

Deleted: ,

Deleted: provides

Deleted: 28,

Deleted: both

Deleted: at

Deleted: at

Formatted: English (United States)

In this study we use the CALIOP pure dust product available in the aforementioned LIVAS database, (hereafter called the LIVAS dataset), which has been developed according to the methodology described in Amiridis et al. (2013) and updated in Marinou et al. (2017). The aforementioned technique relies on the incorporation of aerosol backscatter coefficient profiles and depolarization ratio, providing a strong evidence of dust presence due to mineral particles' irregular shape (Freudenthaler et al., 2009; Burton et al., 2015; Mamouri and Ansmann, 2017), thus allowing the separation of the dust component from aerosol mixtures. The LIVAS dataset is obtained by applying appropriate regionally-dependent LR values (see Figure S1; Marinou et al., 2017; Proestakis et al. 2018 and references within), instead of the raw universal CALIOP dust LR (40 sr; Version 3),

Deleted: developed in the framework of the ESA-

Deleted: (Amiridis et al., 2015)

Deleted: (

Field Code Changed

Deleted: <http://lidar.space.noa.gr:8080/livas/>

Deleted:)

Deleted: ,

Deleted: signal

Deleted: For our purposes, instead of the raw universal CALIOP dust LR (40 sr; Version 3),

Deleted: we are applying

Deleted: s

which are multiplied with the dust backscatter coefficient profiles at 532 nm in order to calculate the corresponding extinction coefficient profiles. After a series of strict quality screening filters (Marinou et al., 2017), the columnar total/dust/non-dust optical depths as well as the DOD-to-AOD ratio over the period 2007–2015 are aggregated at $1^\circ \times 1^\circ$ grid cells covering the whole globe. The performance of the [LIVAS](#) pure DOD product has been assessed against AERONET over N. Africa and Europe (Amiridis et al., 2013) revealing a substantial improvement when the abovementioned methodological steps are applied. [The LIVAS pure DOD product has been utilized in variety of](#) research studies, such as the assessment of dust outbreaks (Kosmopoulos et al., 2017; Solomos et al., 2018) and phytoplankton growth (Li et al., 2018), the 4D description of mineral loads over long-term periods (Marinou et al., 2017; Proestakis et al., 2018), the evaluation of dust models (Tsikerdekis et al., 2017; Georgoulias et al., 2018; Konsta et al., 2018) [as well as](#) the evaluation of new satellite products (Georgoulias et al., 2016).

Deleted: This has led to a broadening of

Deleted: and

Deleted: in which the LIVAS pure DOD product can be utilized

Formatted: English (United States)

2.4. AERONET

Ground-based observations acquired from the AEronet RObotic NETwork (AERONET; Holben et al., 1998) have been used as reference [in this work](#) in order to evaluate the accuracy of the [MIDAS](#) DOD product. The evaluation analysis has been performed by utilizing the almucantar (inversion) retrievals, providing information for the total aerosol amount (AOD) as well as for other microphysical (e.g., volume size distribution) and optical (e.g., single scattering albedo) properties (Dubovik and King, 2000; Dubovik et al., 2006). In the present study, focus is put on the aerosol optical properties retrieved at four wavelengths (440, 675, 870 and 1020 nm) utilizing as inputs spectral AODs and sky (diffuse) radiances. More specifically, we used [Version 3 \(V3\)](#) AERONET data ([Giles et al., 2019; Sinyuk et al., 2020](#)) of AOD (for total and coarse aerosols), Ångström exponent (α) and single scattering albedo (SSA). For the amount (AOD) and size (α) related optical parameters, [only](#) quality assured retrievals (i.e., Level 2; L2) are used, whereas for the SSA, the L2 and Level 1.5 (L1.5) observations are merged in order to ensure maximum availability. Unfavourable atmospheric conditions or restrictions on solar geometry result in a reduced amount of inversion outputs [compared](#) to the [availability of](#) sun-direct measurements or the Spectral Deconvolution Algorithm (SDA; O'Neill et al., 2003) retrievals. Even though [the aforementioned](#) AERONET data provide information about aerosol size (i.e., Ångström exponent) or coarse AOD ([from SDA retrievals](#)), the optimum approach for identifying dust particles and discriminating them from other coarse particles (i.e., sea-salt) requires the [use](#) of SSA [as it will be discussed in the next paragraph.](#)

Deleted: quality assured MODIS AOD as well as of the

Deleted: derived

Deleted: MODIS

Deleted: the

Deleted: 2

Deleted: 2

Deleted: the

Deleted: only

Deleted: with respect

Deleted: both types of

Deleted: .

Deleted: i.e.,

Deleted: , along with size optical properties,

Formatted: English (United States)

Through the combination of the selected optical properties from almucantar retrievals we achieved the spectral matching between ground-based and spaceborne observations as well as the determination of DOD on AERONET retrievals. Regarding the first part, the $\alpha_{440-870\text{nm}}$ and $\text{AOD}_{870\text{nm}}$ values are applied in the Ångström formula in order to interpolate the AERONET AOD at a common wavelength (i.e., 550 nm) with MODIS. For the evaluation of DOD, a special treatment of AERONET retrievals is required in order to identify conditions where dust particles either only exist or clearly dominate over other aerosol species. The vast majority of previous studies (e.g., Fotiadi et al., 2006; Toledano et al., 2007; Basart et al., 2009) have relied on the combination of AOD and α for aerosol characterization, associating the presence of mineral particles with low α levels and considerable AODs. Here, we are keeping records where the $\alpha_{440-870\text{nm}} \leq 0.75$ and $\text{SSA}_{675\text{nm}} - \text{SSA}_{440\text{nm}} > 0$, without taking into account the aerosol optical depth. The first criterion ensures the predominance of coarse aerosols, while the second one serves as an additional filter for discriminating dust from sea-salt particles, taking advantage of the specific spectral signature of SSA (i.e., decreasing absorptivity for increasing wavelengths in the visible spectrum) in pure or rich dust environments (Giles et al., 2012).

Then, from the coarse AODs at 440, 675 and 870 nm we calculate the corresponding α , which is applied in order to obtain the AERONET coarse AOD at 550 nm. This constitutes the AERONET-derived DOD assuming that the contribution of fine dust particles (particles with radii less than the inflection point in the volume size distribution) is small. Likewise, through this consideration any potential “contamination” from small-size particles of anthropogenic or natural origin (e.g., biomass burning), which is likely far away from the sources, is tempered or avoided.

3. Methods

3.1. Derivation of dust optical depth on MODIS swaths

The core concept of our approach is to derive DOD on MODIS L2 retrievals, provided at fine spatial resolution, via the synergy with the MERRA-2 products. More specifically, the MERRA-2 dust fraction (MDF) to total AOD_{550nm} (Eq. 1) is multiplied with the MODIS AOD_{550nm} in order to calculate DOD_{550nm} at swath-level (Eq. 2).

$$MDF = \frac{AOD_{DUST,MERRA-2}}{AOD_{TOTAL,MERRA-2}} \quad (\text{Eq. 1})$$

$$DOD_{MODIS} = AOD_{MODIS} * MDF \quad (\text{Eq. 2})$$

To achieve that, the datasets are collocated temporally and spatially. MERRA-2 outputs are provided at coarse spatial resolution ($0.5^\circ \times 0.625^\circ$) in contrast to MODIS-Aqua observations (10 km

Deleted: In contrast to the MODIS-AERONET AOD comparison, the corresponding evaluation for

Deleted: it is required

Deleted: define

Deleted: ,

Deleted: as much as possible based on columnar data,

Deleted: combining

Deleted: alpha

Deleted: ,

Formatted: English (United States)

x 10 km). MODIS swaths are composed by 203 x 135 retrievals and for each one of them we compute the distance from the MERRA-2 grid points, considering the closest hourly time step to MODIS overpass time. Then, the MDF is used to calculate the DOD from the AOD on MODIS swath native grid. Our approach avoids on purpose the inclusion of additional optical properties providing information on aerosol size (α) available from MODIS and absorptivity (Aerosol Index; [Torres et al., 1998](#)) from OMI that are characterized by inherent limitations. Previous evaluation studies (Levy et al., 2013; [Sayer et al., 2013](#)) have shown that size parameters acquired by MODIS are highly uncertain, particularly over land and at low AOD conditions. In addition, since early 2008, the OMI sensor has lost half of its swath due to a “row-anomaly” issue (Torres et al., 2018) thus “hampering” the MODIS-OMI collocation when it is attempted at fine spatial resolution.

Deleted: MERRA-2 dust portion

3.2 Uncertainty estimation

As expressed in Eq. 2, the MIDAS DOD results from the product of MODIS AOD and MDF. The uncertainty of the DOD product ($\Delta(DOD)$) accounts for the corresponding uncertainties of the AOD and MDF, which are calculated using AERONET and LIVAS, respectively, as a reference. The mathematical expression of the $\Delta(DOD)$, given in Eq. 3, as follows, results from the implementation of the product rule on Eq. 2.

$$\Delta(DOD) = \Delta(AOD) * MDF + AOD * \Delta(MDF) \quad (\text{Eq. 3})$$

The term $\Delta(AOD)$ defines the expected error (EE) confidence envelope in which ~68% of the MODIS-AERONET AOD differences are expected to fall within. This term varies depending on the applied MODIS aerosol retrieval algorithm.

For each of the two DT retrieval algorithms, we use the corresponding linear equations expressing $\Delta(AOD)$ with respect to AERONET AOD over ocean (Levy et al., 2013; Eq. 4) and land (Levy et al., 2010; Eq. 5). For the DB AOD land retrievals (Eq. 6), we use the formula for prognostic uncertainty estimates given in Sayer et al. (2013) but with updated coefficients a and b for C061 data varying between vegetated and arid surface types (https://atmosphere-imager.gsfc.nasa.gov/sites/default/files/ModAtmo/modis_deep_blue_c61_changes2.pdf). More specifically, over vegetated land, a and b are equal to 0.079 and 0.67, respectively, while the corresponding values over barren soils are equal to 0.12 and 0.61. The land cover classes have been extracted from the International Geosphere-Biosphere Programme (IGBP) database available via the MCD12C1 data (<https://lpdaac.usgs.gov/products/mcd12c1v006/>). For the merged (DB+DT) land AOD, the uncertainty is estimated via the square root of the quadrature sum of the DT-Land and DB-Land uncertainties divided by two (Eq. 7).

Deleted: the

Formatted: English (United States)

Deleted: from MERRA-2

Deleted: the

Deleted: CALIOP

Formatted: English (United States)

Formatted: English (United States)

Formatted: English (United States)

Formatted: English (United States)

Formatted: No Spacing, Indent: First line: 0.63 cm

Deleted: The term $\Delta(AOD)$ defines in Eq. 3, representing the expected error (EE) confidence envelope in which ~68% of the MODIS-AERONET AOD differences are expected to fall within. This term varies depending on the MODIS aerosol retrieval algorithm applied. MODIS provides AODs above oceans, dark vegetated land areas as well as over surfaces with high reflectivity (excluding snow- and ice-covered regions) based on retrieval techniques relying on different assumptions whereas over transition zones between arid and vegetated continental parts, DT and DB AODs are merged (Sayer et al., 2014). ¶

Formatted: English (United States)

Deleted: documented in the literature, for DT-Ocean

Deleted: .

Deleted: DT-Land

Deleted: .

Deleted: and DB-Land (Sayer et al., 2013;

Deleted: AODs

Deleted: structure

Deleted: the

Deleted: a and b

Field Code Changed

Deleted: error

Deleted: calculated

Deleted: assuming an independency between these two retrievals

$$\Delta(AOD_{DT-Ocean}) = \pm(0.10 * AOD + 0.04) \quad (\text{Eq. 4})$$

$$\Delta(AOD_{DT-Land}) = \pm(0.15 * AOD + 0.05) \quad (\text{Eq. 5})$$

$$\Delta(AOD_{DB-Land}) = \pm \left(\frac{a+b*AOD}{AMF} \right) \quad (\text{Eq. 6})$$

$$\Delta(AOD_{DTDB-Land}) = \pm \sqrt{\frac{[\Delta(AOD_{DT-Land})]^2 + [\Delta(AOD_{DB-Land})]^2}{2}} \quad (\text{Eq. 7})$$

Before proceeding with the calculation of the $\Delta(DOD)$, few key aspects must be highlighted for the sake of clarity. In equations 4 and 5, the AOD uncertainty is defined as a diagnostic error since it is calculated utilizing AERONET as reference. Here, we are using the same equations replacing AERONET AODs with those given by MODIS. This relies on the fact (results not shown here) that their averages from a global perspective are almost unbiased; however, at regional level, small negative or positive offsets (lower than 0.05 in absolute terms) are recorded in the vast majority of AERONET sites, thus supporting our argument. For the ocean AOD uncertainty, the defined EE margins (Levy et al., 2013) have been modified in order to sustain symmetry by keeping the upper bound (i.e., thus including more than 68% of expected MODIS-AERONET pairs within the EE). Sayer et al. (2013) estimated the uncertainty of DB AOD by taking into account the geometric air mass factor (AMF) resulting from the sum of the reciprocal cosines of the solar and viewing zenith angles (Eq. 6).

The LIVAS dust fraction is our reference for estimating the MDF uncertainty. The analysis is performed at $1^\circ \times 1^\circ$ spatial resolution considering only grid cells in which both MERRA-2 and LIVAS DODs are higher than or equal to 0.02. According to this criterion, more than 450000 LIVAS-MERRA-2 collocated pairs have been found that are sorted (ascending order) based on MDF (ranging from 0 to 1) and then are grouped in equal size bins containing 20000 data for each sub-sample. For every group, we computed the median MDF (x axis) as well as the 68th percentile of the absolute MERRA-2 - LIVAS dust fraction (y axis) and then we found the best polynomial fit (Eq. 8).

$$\Delta(MDF) = \pm(2.282 * MDF^4 - 6.222 * MDF^3 + 4.700 * MDF^2 - 0.969 * MDF + 0.199) \quad (\text{Eq. 8})$$

Depending on the selected MODIS algorithm, the appropriate combination between AOD (Eqs. 4, 5, 6 and 7) and MDF (Eq. 8) uncertainties is applied to calculate the $\Delta(DOD)$ (Eq. 3) on each daily measurement (i.e., DOD) at each grid cell. These pixel-level DOD uncertainties are averaged over the entire study period as well as for each season and the obtained findings will be discussed along with the global spatial patterns (Section 4.5) of dust optical depth in order to provide a measure of the reliability of the derived MIDAS DOD product.

Formatted: English (United States)

Formatted

Formatted

Formatted

Formatted

Formatted: English (United States)

Deleted: ¶

$\Delta(\quad) \quad (\text{Eq. 4})$ ¶

$\Delta(\quad) \quad (\text{Eq. 5})$ ¶

$\Delta(\quad) - (\text{Eq. 6})$ ¶

$\Delta(\quad) \sqrt{(\quad)(\quad)}$ ¶

¶

Deleted: CALIOP ...IVAS DOD-to-AOD ratio

Deleted: limits

Deleted: of the MERRA-2 dust fraction (MDF)... The analysis is performed at $1^\circ \times 1^\circ$ spatial resolution considering only grid cells in which both MERRA-2 and CALIOP LIVAS DODs are higher than or equal than...o 0.02. According to this criterion, more than 450000 CALIOP

Formatted: English (United States)

Deleted: which

Deleted: MERRA-2 ...DF (ranging from 0 to 1) and then are grouped in equal size bins containing 20000 data for each sub-sample. For every group, we computed the median MDF (x axis) as well as the 68th percentile of the absolute MERRA-2 - CALIOP

Formatted: English (United States)

Formatted

Deleted: ,

Deleted: and

Deleted: , throughout the study period... These pixel-level DOD uncertainties are averaged over the entire study period as well as for each season and When averaging each grid cell at each considered timescale the uncertainty is obtained by propagating each individual measurement uncertainty, i.e., taking the square root of the sum of the quadratic $\Delta(DOD)$ divided by the number of available measurements. We also estimate the uncertainty of the average due to sampling using the standard error (i.e., the standard deviation divided by the square root of the number of measurements). These two uncertainty quantities are in turn combined into a total uncertainty that is calculated as the square root of their quadratic sum. T

Deleted: in parallel

Formatted: English (United States)

4. Results

On the following sections, a series of analyses including the evaluation of MDF with respect to LIVAS (Section 4.1), the evaluation of MIDAS DOD versus AERONET observations (Section 4.2) as well as an intercomparison among MIDAS, LIVAS and MERRA-2 DODs (Section 4.3), is presented. All the aforementioned steps are performed in order to justify the validity of the applied methodology and to understand its limitations. In the last section (4.4), the global annual and seasonal DOD patterns are presented as a demonstration of the MIDAS dataset, and the obtained spatiotemporal features are briefly discussed. The detailed climatological study is provided in a companion paper.

4.1. Evaluation of MERRA-2 dust fraction versus LIVAS

The evaluation of the MDF is a critical step of our analysis since it is used as the scaling factor of the MODIS AOD for the derivation of the MIDAS DOD. For this reason, the corresponding columnar parameter provided by LIVAS (see Section 2.3) is used as reference. It must be highlighted that the only existing evaluation studies of MERRA-2 aerosol products have been performed either for specific aerosol species or limited time periods (e.g., Buchard et al., 2017; Veselovskii et al., 2018) or for the total load (e.g., Mukkavilli et al., 2019; Sun et al., 2019) in specific regions, showing the ability of MERRA-2 in reproducing the integrated aerosol fields. Nevertheless, the speciation of the suspended particles, which is to a large extent determined by the model physics assumptions (Gelaro et al., 2017), has not been thoroughly evaluated. Therefore, the present analysis complements and expands further the existing works providing insight about the performance of MERRA-2 in terms of discriminating among aerosol types (particularly for dust) and subsequently estimating their contribution to the total atmospheric load.

Figure 1 depicts the geographical distributions of the dust-to-total AOD ratio, based on MERRA-2 (i) and LIVAS (ii), averaged over the timeframe (2007-2015) of the LIVAS dataset. The corresponding maps of mean bias, fractional bias (FB), fractional gross error (FGE) and correlation coefficient (R) are given in Figure 2. For consistency, we regredded the MERRA-2 data to $1^\circ \times 1^\circ$ spatial resolution and selected the closest output to the CALIOP overpass time only during daytime hours when aerosol retrievals obtained by passive sensors at visible wavelengths are assimilated. At a first glance, the spatial patterns are very similar, particularly in areas where the presence of dust is predominant. Across the “dust belt” (Prospero et al., 2002), the most evident deviations (MDF underestimation by ~0.1 or 10%) are recorded in the borders of Afghanistan and Pakistan (Dasht-e

- Deleted:** an intercomparison between MERRA-2 and MODIS AODs (Section 4.1),
- Deleted:** CALIOP
- Deleted:** 2
- Deleted:** an
- Deleted:** 3
- Deleted:** CALIOP
- Deleted:** 4
- Deleted:** necessary
- Deleted:** 5
- Deleted:** since a
- Deleted:** it
- Deleted:** is the scientific topic of the
- Formatted:** English (United States)
- Deleted:** ¶
¶
¶
¶
¶
- Deleted:** portion
- Deleted:** CALIOP retrievals
- Deleted:** MERRA-2 dust portion (i.e., MDF)
- Deleted:** computed from the quality assured and updated CALIOP profiles
- Deleted:**
- Deleted:** will c
- Deleted:** current
- Deleted:** 2
- Deleted:** CALIOP
- Deleted:** ,
- Deleted:** (i.e.
- Deleted:** period
- Deleted:** 2007 – 2015)
- Deleted:** 3
- Deleted:** . Both datasets provide nighttime observations; however, the analysis has been restricted to sunlight hours only when
- Deleted:** of MERRA-2 dust portion b

Margo and Kharan Deserts) as well as in the Taklamakan Desert (Fig. 2-i). However, the FB (Fig. 2-ii) and FGE (Fig. 2-iii) metrics (Yu et al., 2006), which are less affected by outliers compared to the bias, are close to zero (ideal score) in most of the aforementioned regions, thus indicating a very good performance of MERRA-2. In terms of temporal covariation (Fig. 2-iv), moderate R values (0.5-0.6) are obtained in land areas where the presence of dust is predominant, with the exception of the western parts of Sahara where the correlation levels are slightly higher than zero. Due to the complex and highly variable nature of the emission processes and therefore the poorer behavior of the model, the correlation tends to be smaller over the main dust sources throughout the year (right column in Figure S2). In downwind regions of the N. Hemisphere, particularly over the main transport pathways (i.e., Atlantic Ocean, Mediterranean, Arabian Sea, E. Asia), correlation substantially increases (up to 0.9). In addition, FB and FGE metrics reveal a good performance by MERRA-2; which, however, downgrade for increasing distances from the sources due to the weaker dust contribution to the total aerosol load. An exception is observed for the mean bias along the tropical Atlantic Ocean where the MDF is overestimated by up to 10% in the eastern parts in contrast to longitudes westward of 45° W where zero biases or slight underestimations (~5%, Caribbean Sea) are obtained.

A discrepancy between the LIVAS and MERRA-2 dust portion is found in the Mojave, Sonoran, Chihuahuan desert areas extending between southwestern US and northern Mexico. As shown in Figure 1, the dust contribution given by LIVAS in those areas is more widespread and stronger in contrast to MERRA-2, which simulates less dust amount over the sources (Mojave Desert) and the surrounding regions (maximized during DJF and MAM; Fig. S2). According to the evaluation metrics in those areas (Figure 2), the MDF underestimation ranges between 20% to 50%, negative FB (down to -1) and high FGE values (locally exceeding 1) are evident while the correlation levels are low, particularly over Mexico. In the S. Hemisphere, the deficiency of MERRA-2 is pronounced along the western coasts of S. America as well as in the Patagonian and Monte Deserts, particularly during JJA and SON (Fig. S2), both situated in Argentina. Similar results are found in S. Africa while in Australia a contrast between its western/eastern and central parts with slight MDF underestimations and overestimations, up to 20% in absolute terms, respectively, are recorded (Figure 2-i). Nevertheless, the agreement between MERRA-2 and LIVAS in temporal terms is supported by the moderate-to-high R values over the “hotspot” regions (Figure 2-iv). Outside of the main dust-affected regions, an obvious discrepancy is found in the eastern Canada and northeastern Russia where MDF yields very low values (< 20%) in contrast to LIVAS reaching values of dust fraction up to 50%. Due to their geographical position, the occurrence of dust loads might not be frequent there, however, their contribution to the total load can be significant under low AOD conditions, which are mainly recorded in the region. This might indicate a poor representation by MERRA-2. However, potential cloud contaminations in the lidar signals, affecting LIVAS reliability, must also be taken into account.

Deleted: 3

Deleted: from

Deleted: 3

Deleted: 3

Deleted: maps

Deleted: not so much

Deleted: as

Deleted: it is evident that the calculated values in most of the aforementioned regions

Deleted: 3

Deleted: ~

Deleted: computed

Deleted: while in

Deleted: This is further supported by the

Deleted: reduction

Deleted: of

Deleted: MERRA-2 dust portion

Deleted: its

Deleted: computed

Formatted: English (United States)

Deleted: CALIOP

Deleted: 2

Deleted: based on spaceborne retrievals

Deleted: 3

Deleted: of MERRA-2 dust contribution to the total aerosol load

Deleted: outhern

Deleted: outh

Deleted: MERRA-2

Deleted: 3

Deleted: CALIOP

Deleted: 3

Deleted: MERRA-2 dust contribution

Deleted: CALIOP

Deleted: but

Deleted: s

Deleted: ;

Deleted: h

Deleted: it must also be taken into account a

Deleted: that can

Formatted: English (United States)

The obtained discrepancies are mainly driven by the partial representation of dust sources in MERRA-2 resulting in potentially underestimated dust emission and subsequently to lower dust contribution to the total burden. Dust is originated either from natural (arid lands, salt lakes, glacial lakes) or from anthropogenic sources (Ginoux et al., 2012). Nevertheless, dust sources in MERRA-2 are based on Ginoux et al. (2001) accounting mostly for natural dust emission areas. This could partly explain the higher LIVAS dust contribution levels that are also evident on the seasonal distributions where the inter-annual variability of dust fraction is illustrated (Figure S2). Interestingly, most of the MDF underestimations (i.e. bluish colors in Figure 2-i) are recorded in mountainous areas. Depending on the homogeneity of the atmospheric scene over regions characterized by complex topography, variations in the optical paths of subsequent CALIPSO L2 profiles considered in the LIVAS product may result in unrealistic DOD and AOD values. Previous evaluation studies (e.g., Omar et al., 2013) have shown that CALIOP underestimates AOD with respect to ground-based AERONET retrievals, particularly over desert areas (Amiridis et al., 2015), which was attributed primarily to the incorrect assumption of the lidar ratio (LR) (Wandinger et al., 2010) and secondarily to the inability of the lidar to detect thin aerosol layers (particularly during daytime conditions due to the low signal-to-noise ratio). The former factor is related to aerosol type and for Saharan dust particles the necessary increase of LR (from 40 to 58 sr) improved substantially the level of agreement with AERONET and MODIS (Amiridis et al., 2013). Similar adjustments (increments) to the raw LR values, which are highly variable (Müller et al., 2007; Baars et al., 2016), considered in the CALIOP retrieval algorithm have been applied in the LIVAS product over other source areas of mineral particles (see Section 2.3; Figure S1). An additional factor that must be taken into account is the number of MERRA-2 – LIVAS pairs that are used for the metrics calculation. The corresponding global geographical distribution (Figure S3-i), calculated over the period 2007–2015, shows that in areas where the model-satellite agreement is good (Figure 2) the number of common samples is high (>100) in contrast to regions with a low number of common samples (<50) where the computed metrics are degraded.

In order to complete the evaluation of the MDF versus LIVAS, the dependency of the level of agreement on the spatial representativeness within the $1^\circ \times 1^\circ$ LIVAS grid-cell has also been investigated. Figure S3-ii displays the long-term averaged geographical distribution of the number of CALIOP L2 profiles (up to 24) aggregated for the derivation of the LIVAS $1^\circ \times 1^\circ$ grid-cell. According to the global map, the maximum number is recorded in the latitudinal band extending from 45° S to 45° N while the “impact” of extended clouds around the equator is apparent. Outside this zone, the number of profiles used is mainly less than 14 and decreases towards the poles due to the enhanced cloudiness. The same evaluation metrics presented in Figure 2 have been computed also at planetary scale for individual classes of CALIOP L2 number of profiles (Figure S4) aggregated for the derivation of the LIVAS $1^\circ \times 1^\circ$ grid cells. Overall, about 3.4 million pairs (x tick named “ALL” in

Deleted: areas

Deleted: In many areas dust

Deleted: CALIOP

Deleted: being

Deleted: also

Deleted: (Figure S2) in which

Deleted: positive CALIOP-MERRA-2 differences

Deleted: 3

Deleted: characterized by complex terrain

Deleted: Due to the variable geomorphology, the enhanced surface returns contaminate the CALIOP signal close to the ground leading to higher columnar AODs and lower contribution by dust loads suspended aloft. In addition, d

Deleted: aerosol

Deleted: L3

Deleted: to

Deleted: S

Deleted: S

Deleted: versus

Deleted: Similar adjustments (increments) onto the raw LRS values, which are highly variable (Müller et al., 2007; Baars et al., 2016), considered in the CALIOP retrieval algorithm, and which are highly variable (Müller et al., 2007; Baars et al., 2016), have been applied in the LIVAS product overin other source areas of mineral particles (see Section 2.3; Figure S1).

Deleted: ,

Deleted: CALIOP

Deleted: which is

Deleted: derivation

Deleted: 2

Deleted: representative

Deleted: 3

Formatted: English (United States)

Deleted: MERRA-2 dust portion

Deleted: CALIOP

Deleted: CALIOP

Deleted: 2

Deleted: 3

Deleted: of CALIOP profiles are

Deleted: of

Deleted: cloud coverage

Deleted: 3

Deleted: also

Deleted: S3

Figure S4-a) have been found over the period 2007-2015 and are almost equally distributed for bins spanning from 8 to 20 while the number of collocated data is higher in the lowermost (≤ 7) and uppermost (≥ 21) tails of the distribution. The FB (Figure S4-c), FGE (Figure S4-d) and correlation (Figure S4-e) results reveal that the consistency between MDF and LIVAS gradually improves for higher grid-cell representativeness. At global scale, MERRA-2 overestimates the dust fraction by up to 1.5% with respect to LIVAS (Figure S4-b, “ALL” sample). Among the bin classes, the MDF-LIVAS differences are mostly positive and lower than ~3% and decrease further when at least 12 CALIOP profiles are aggregated for the derivation of the LIVAS grid cell.

4.2. Evaluation of MIDAS DOD versus AERONET

In the present section, we provide an evaluation of the MIDAS DOD against the corresponding AERONET product (Section 2.4). An illustration of the MODIS-AERONET collocation method (an example from aerosol optical depth without applying the criteria for DOD) is shown in Figure S5. The obtained results at global and station level are presented.

in Figures 3 and 4, respectively. As expected, the number of coincident spaceborne and ground-based DODs collected at 436 AERONET stations (red circles in Figure 3-i) is low (10478 pairs) due to the limited amount of almucantar retrievals and the implementation of filters for the determination of DOD in AERONET data. According to the global scatterplot metrics (Figure 3-ii), a very good performance of the MIDAS DOD is revealed since both datasets are well correlated ($R=0.89$) with MIDAS only slightly overestimating DOD compared to AERONET (0.004 or 2.7%). Only AERONET AODs associated with α lower/equal than/0.75 are kept for the evaluation procedure. While this threshold is higher compared to previous applied cut-off levels (e.g. Dey et al., 2004; Tafuro et al., 2006; Reid et al., 2008; Kim et al., 2011; Gkikas et al., 2016), our global scatterplot metrics are very similar when reducing α from 0.75 to 0.25 (results not shown here).

The evaluation analysis was also performed for each station individually. Figure 4 depicts only sites with at least 30 coincident MIDAS-AERONET observations, thus making meaningful the comparison at station level. This criterion is satisfied in 86 stations, which overall comprise 7% (or 8095) of the total population of coincident DODs, and are mostly located over dust sources as well as in areas affected by dust transport. Figure 4-i shows the station-by-station variability of the number of common MIDAS/AERONET observations ranging from 100 to 457 (Banizoumbou, Niger) across N. Africa and the Middle East whereas in the remaining sites is mainly lower than 70. Between the two datasets, very high R values (up to 0.98) are found in N. Africa, the Middle East, outflow regions (Cape Verde, Canary Islands, Mediterranean) and at distant areas (Caribbean Sea) affected by long-

Deleted: 3

Deleted: Based on

Deleted: 3...-c), FGE (Figure S3...-d) and correlation (Figure S3

Deleted: it is revealed

Deleted: MERRA-2...DF and CALIOP ...IVAS gradually improves for higher CALIOP g...rid-cell representativeness. In quantitative terms, FB decreases from ~1.2 to ~0.2, FGE decreases from ~1.6 to ~ 0.9 and R increases from ~0.5 to ~0.8 while the corresponding overall results (i.e., first red bar) are equal to ~0.7, ~1.3 and ~0.7, respectively. ...t global scale, MERRA-2 overestimates the dust portion ...raction by up to 1.5% with respect to CALIOP ...IVAS (Figure S3

Deleted: while

Deleted: . Among the bin classes, the maximum overestimation (~2.8%) is recorded when four CALIOP profiles are averaged for the derivation of the $1^{\circ} \times 1^{\circ}$ cell, while the positive MERRA-2-CALIOP differences become lower than 0.1 when ...t least 12 CALIOP profiles are considered...re aggregated for the derivation of the LIVAS grid cell. Regarding the bias sign, the only exception is observed for cases where 22 or 23 CALIOP profiles are used resulting in slight MERRA-2 underestimations.

Formatted: English (United States)

Deleted: Based on the findings of the Sections 4.1 and 4.2, the MERRA-2 related outputs (AOD, MDF) used in this method, after their quantitative evaluation with MODIS and CALIPSO products, showed reasonable results comparing

Deleted: observations

Deleted: assessment of MODIS L2 AOD and the

Deleted: in order . The validation of the MODIS quality

Deleted: 4... The obtained results at global and station lev

Deleted: The corresponding analysis for DOD is presented

Deleted: the ...oincident spaceborne and ground-based

Deleted: 37...36 AERONET stations (red circles in Figure

Deleted: ,

Deleted: are drastically reduced down to...s low (7299

Deleted: the ...lmucantar retrievals and the implementatio

Deleted: from...n AERONET data (Section 2.4)...

Deleted: it

Deleted: . B...both datasets are well correlated

Deleted: It is reminded that only...nly the ...ERONET

Deleted: . The defined upper threshold on α values

Deleted: which is ... While thisa...threshold is higher

Formatted: English (United States)

Deleted: individually ...or each station individually. Figu

Deleted: common

Deleted: MODIS

Deleted: /

Deleted: meaningful... This criterion is satisfied in 61...61

Deleted: MIDAS-AERONET...coincident DODs, and are

Deleted: , from short to long range... Figure 5...-i shows

range transport. Across the Sahel, maximum RMSE levels (up to 0.26) are recorded (Figure 4-iii) due to the intense loads and strong variability of the Saharan dust plumes. Regarding biases, positive deviations of up to 0.08 are computed in most AERONET sites in the area while the largest negative offsets (down to -0.14) are recorded at the stations of Ilorin and Djougou (near to the coasts of the Gulf of Guinea) in agreement with Wei et al. (2019b). Several reasons may explain the obtained MIDAS-AERONET differences over the above-mentioned stations taking into account that the MDF is generally well reproduced. The first one is related to the MODIS retrieval algorithm itself and more specifically to the applied aerosol models, surface reflectance and cloud screening procedures (Sayer et al., 2013). The second factor is the omission of fine DOD in AERONET data, which would likely reduce the positive biases. However, its contribution to the total dust AOD is difficult and probably impossible to be quantified accurately. Similar tendencies are found for RMSE and bias in the Middle East where the satellite and ground-based DODs are in general well-correlated. In the Mediterranean, the temporal covariation between the two datasets is quite consistent ($R>0.8$) with the MIDAS DOD being slightly underestimated probably due to the MDF underestimation (mainly recorded in JJA; Fig. S2).

In Asia, few stations are available with sufficient number of MIDAS-AERONET matchups in which the slight positive and the negative DOD biases (Figure 4-iv) are generally consistent with those of AOD (results not shown here). This indicates that the MODIS AOD offsets are “transferred” to MIDAS DOD, which is also affected by the MDF underestimation (Figure 2-i). In the southwestern United States, the evaluation scores at 12 AERONET sites show a moderate performance of the derived DOD ($R: 0.28-0.94$, bias: $-0.034-0.003$, RMSE: $0.02-0.04$) attributed to the deficiency of MERRA-2 to reproduce adequately the contribution of dust particles to the total aerosol load in optical terms. Finally, our assessment analysis in the Southern Hemisphere for stations located in Argentina, Namibia and Australia, reveals MIDAS-AERONET deviations, spanning from -0.03 (Cordoba-CETT) to 0.02 (Gobabeb), and correlations ranging from 0.14 (Fowlers_Gap) to 0.96 (Canberra).

4.3. Intercomparison of MIDAS, MERRA-2 and LIVAS DOD products

Following the evaluation of MIDAS DOD against AERONET, the MIDAS, MERRA-2 and LIVAS DOD products are investigated in parallel. For this purpose, the MERRA-2 and MIDAS data have been regressed to $1^\circ \times 1^\circ$ grid cells between 2007 and 2015 to match the spatial resolution and availability of LIVAS. Then, the three datasets have been collocated spatially and temporally. The intercomparison has been performed only during daytime conditions and the obtained findings are presented through geographical distributions (Section 4.3.1) and average monthly timeseries of

Deleted: Over the stations located a

Deleted: the

Deleted: 43... are recorded (Figure 5...-iii) due to the intense loads and strong variability of the Saharan dust plumes...Regarding biases, . The maximum ...ositve biases

Deleted: (

Deleted: 133

Deleted:)

Deleted:

Deleted: of

Deleted:

Deleted: maximum...argest negative offsets (down to -0.14) worldwide ...re recorded at the stations of Ilorin and Djougou (near to the coasts of the Gulf of Guinea) being in accordance with the results of

Deleted: indicate that the derived MIDAS DOD is overestimated... Several reasons may explain the predominance ...btained of positive

Deleted: taken

Deleted: MERRA-2 dust portion...DF is generally adequately ...ell reproduced with respect to CALIOP

Deleted: with

Deleted: However, for AOD (results not shown here), small negative biases are observed in agreement with the findings by Sayer et al. (2013) who utilized DB products only.

Deleted: absence

Deleted: o

Deleted: have ...ikely reduced...the obtained positive differences...ositve biases but

Deleted: However, its contribution to the total dust AOD it is difficult and, probably impossible to be quantified...Similar tendencies, but at a lesser degree, are found

Deleted: the ...MSE and bias scores

Deleted: of the MERRA-2 dust portion

Formatted: English (United States)

Deleted: MODIS

Deleted: collocations ...atchups in which the slight positive and the negative (down to -0.08)

Deleted: recorded ...nsistent with those of both for DOD (Figure 5-iv) and ...OD (results not shown here). This agreement ...ndicates that the MODIS AOD underestimation offsets is ...re “transferred” also ...o MIDAS DOD, which is also affected by the and locally can be further enhanced

Deleted: ,

Deleted: indicate ...evels slight MODIS...IDAS-

Deleted: CALIOP

Deleted: three ...OD products derived from MIDAS,

Deleted: in order to match CALIOP's LIVAS spatial

Deleted: by selecting the coincident pixel for which the

Deleted: intra-annual

regional, hemispherical and planetary averages (Section 4.3.2). Finally, it must be clarified that our focus in this part of the analysis is the intercomparison among the DOD products and not to interpret their spatiotemporal features. The latter will be discussed thoroughly in a companion paper analyzing the MIDAS fine resolution DOD dataset.

4.3.1. *Geographical distributions*

The annual geographical distributions of LIVAS, MERRA-2 and MIDAS DODs are depicted in Figures 5-i, 5-ii and 5-iii, respectively, while the corresponding global seasonal maps are provided in Figure S6. Among the three datasets, both for annual and seasonal geographical distributions, it is apparent a very good agreement in spatial terms in contrast to the magnitude of the simulated (MERRA-2) and retrieved (MIDAS, LIVAS) DODs. The most evident differences of MERRA-2 (Figure 5-ii) and MIDAS (Figure 5-iii), with respect to LIVAS (Figure 5-i), are encountered across N. Africa forming clear patterns with positive and negative deviations over the Sahara and the Sahel, respectively. In particular, MERRA-2 DOD positive offsets mostly range from 0.04 to 0.20 while those of MIDAS-LIVAS are lower; placing our DOD product between active remote sensing retrievals and reanalysis dataset. Previous studies relying on satellite (Yu et al., 2010; Kittaka et al., 2011; Ma et al., 2013) and ground-based (Schuster et al., 2012; Omar et al., 2013) observations have reported that CALIOP underestimates AOD over the Sahara. Konsta et al. (2018), who utilized higher and more realistic dust lidar ratio (55 sr; adopted also for the region in the current study) compared to the aforementioned works (40 sr), reported similar tendencies of lower magnitude against MODIS. Therefore, additional factors might contribute to the lower lidar-derived DODs over the arid regions in N. Africa. For example, it has been observed that CALIOP can misclassify as clouds very intense dust layers which on the other hand can attenuate significantly or totally the emitted laser beam (Yu et al., 2010; Konsta et al., 2018). All these aspects, most likely met over dust sources, act towards reducing DOD (resulting from the vertical integration of the extinction coefficient profiles) and might explain the “missing” hotspot by LIVAS in/around the Bodélé Depression in contrast to single-view, multi-angle and geostationary passive satellite sensors (e.g., Banks and Bridley, 2013; Wei et al., 2019a). Across the Sahel, LIVAS provides higher DODs (mainly up to 0.2) against both simulated and satellite products. These differences might be attributed to the misrepresentation of dust sources in MERRA-2 along this zone where vegetation cover has a prominent seasonal cycle (Kergoat et al., 2017). An inaccurate representation of vegetation also impacts the surface reflectance which in turn can introduce critical errors in the MODIS retrieval algorithm. Wei et al. (2019b) showed that MODIS underestimates AOD with respect to AERONET in that region, which is in agreement with the fact

- Deleted:** the
- Deleted:** 4
- Deleted:** of
- Deleted:** different
- Deleted:** which
- Deleted:** DODs from the

Deleted: CALIOP
Deleted: 6
Deleted:
Deleted: 6
Deleted: 6
Deleted: CALIOP
Deleted: deviations
Deleted: 6
Deleted: 6
Deleted: CALIOP
Deleted: 6
Deleted: biases
Deleted: declinations
Deleted: overestimations
Deleted: the
Deleted: CALIOP
Deleted: deviations

Deleted: A common feature is the location where the maximum “overestimations” are observed. These areas are identified in Algeria, Niger and Chad featuring substantially high dust concentrations.

Deleted: relied

Deleted: noted

Deleted: , with respect

Deleted: other

Deleted: of

Deleted: also

Deleted: ed

Deleted: and may

Deleted:

Deleted: ing

Deleted: on

Deleted: CALIPSO

Deleted: CALIOP

Deleted: both

Deleted: Sayer

Deleted: 3

Deleted: overestimates

~~that~~ the maximum MIDAS-AERONET negative DOD ~~differences are found at Ilorin and Djougou sites~~ (Figure 4-iv).

Over the eastern Tropical Atlantic Ocean, the difference between LIVAS and MIDAS is negligible whereas MERRA-2 ~~gives lower DODs~~ by up to 0.08. In the Middle East, MERRA-2 and MIDAS DODs are higher than ~~in LIVAS~~ over the Tigris-Euphrates basin while an opposite tendency ~~for MERRA-2~~ is found in the interior parts of Saudi Arabia. Lower DODs are also ~~given by LIVAS~~ over the arid/semi-arid regions ~~eastwards of the Caspian Sea, including also the Aral Sea~~. This area of the planet is one of the most challenging for spaceborne passive observations due to the terrain complexity prohibiting the accurate characterization of the surface reflectance and type, resulting in unrealistically high MODIS AODs (Klingmüller et al., 2016; see interactive comment posted by Andrew Sayer) that may also affect MERRA-2 via assimilation. ~~The largest negative MIDAS-LIVAS differences (exceeding 0.2) worldwide are recorded in the Taklamakan Desert whereas the corresponding results between MERRA-2 and LIVAS are somewhat lower. This might be attributed to an inappropriate selection (overestimation) of the lidar ratio taking into account that CALIOP mainly underestimates AOD over the region, dust contribution to the total AOD exceeds 70% (Proestakis et al., 2018), throughout the year, and MDF shows robust consistency (Figure 2).~~ Eastwards of the Asian continent, the situation is reversed and the LIVAS DODs are lower by up to 0.2 when compared to MERRA-2 and MIDAS indicating a weaker trans-Pacific transport, predominant during boreal spring (second row in Figure S6), being in agreement with the findings of Yu et al. (2010) and Ma et al. (2013). In the S. Hemisphere, negative MERRA-2-LIVAS and MIDAS-LIVAS differences are computed in Patagonia, ~~attributed to the underperformance of MDF, which are not however spatially coherent. On the contrary, in the desert areas of the inland parts of Australia, there is a clear signal of positive MERRA-2-LIVAS deviations, not seen between MIDAS and LIVAS, most likely attributed to the overestimation of aerosol (dust) optical depth by MERRA-2 as it has been recently presented by Mukkavilli et al. (2019). On a global and long-term perspective, based on ~440000 collocated data, MERRA-2 agrees slightly better with LIVAS than MIDAS as it is revealed by the correlation (R=0.74 vs. 0.71) and bias (8.2% vs. 13.3%) metrics.~~

4.3.2. Planetary, hemispherical and regional intra-annual variability

We compared the monthly variability of the planetary (Figure 6-i) and hemispherical (Figures 6-ii, 6-iii) averages of LIVAS (black curve), MERRA-2 (red curve) and MIDAS (blue curve) DODs. We note that for each considered timescale, the averaging has been ~~made~~ following the upper branch shown in Figure 5 of Levy et al. (2009), ~~where each grid cell is first temporally averaged and the resulting field is spatially averaged. In the N. Hemisphere, the annual cycle of DOD is reproduced by the three datasets with maximum levels in June (0.118 for LIVAS/MERRA-2 and ~0.126 for MIDAS)~~

Deleted: while

Deleted: bias ...ifferences (-0.154) is recorded at Ilorin...re found at Ilorin and Djougou sites (Figure 5)

Formatted: English (United States)

Deleted: CALIOP ...IVAS and MIDAS is negligible whereas MERRA-2 underestimates

Deleted: those retrieved obtained by

Deleted: CALIOP ...IVAS over the Tigris-Euphrates basin while an opposite tendency , particularly for MIDAS,...or MERRA-2 is found in the interior parts of Saudi Arabia. Lower DODs are also observed ...iven by CALIOP ...IVAS over the arid/semi-arid regions, including the Aral Sea,..eastwards of the Caspian Sea, including also the Aral Sea. This area of the planet is one of the most challenging for spaceborne passive observations from space...due to the terrain complexity prohibiting the accurate characterization of the surface reflectance and type, . Such conditions impose artifacts to the retrieval algorithm ...resulting in unrealistically high MODIS AODs (Klingmüller et al., 2016; see interactive comment posted by Andrew Sayer) that may also affect MERRA-2 via assimilation. Along the mountainous western parts of Iran, CALIPSO DOD is substantially higher than those derived with our methodology while against MERRA-2 the obtained positive or negative differences are close to zero. The largest negative MIDAS-CALIOP ...IVAS differences (exceeding 0.2) worldwide , not only in Asia but all over the world, ...re recorded in the Taklamakan Desert whereas the corresponding results between MERRA-2 and CALIOP

Deleted: .

Deleted: 3...). Eastwards of the Asian continent, the situation is reversed and the CALIOP ...IVAS DODs are lower by up to 0.2 when compared to MERRA-2 and MIDAS indicating a weaker trans-Pacific transport, predominant during boreal spring (second row in Figure S6), being in agreement with the findings of Yu et al. (2010) and Ma et al. (2013). In the S. Hemisphere, negative MERRA-2-CALIOP LIVAS and MIDAS-CALIOP ...IVAS differences are computed in Patagonia, attributed to the underperformance of MDF, which are not however spatially coherent. On the contrary, in the desert areas of the inland parts of Australia, there is a clear signal of positive MERRA-2-CALIOP LIVAS deviations, not seen between MIDAS and CALIOP...IVAS, most likely attributed to the overestimati

Formatted: English (United States)

Formatted: English (United States)

Deleted: At a next step of the intercomparison,...e compared the intra-annual

Deleted: 7...-i) and hemispherical (Figures 7...-ii, 7...-iii) monthly ...verages of CALIOP

Deleted: , it were comparedis investigated....It is clarified that at...e note that for each considered timescale, the calculations

Deleted: presented here

Deleted: ve

Deleted: performed...ade , at each considered timescale,

Deleted: comprising first a temporal averaging and then a spatial averaging

Deleted: taking into the weight of the grid cell surface area to the total domain area with available data.

Deleted: commonly

and minimum ones in Nov-Dec (0.034-0.040). Nevertheless, the most evident deviations in terms of magnitude are recorded during the high-dust seasons with MIDAS giving slightly higher DODs than MERRA-2 and even higher than LIVAS, particularly during boreal spring. On an annual basis (Table 1), the averaged MERRA-2 and MIDAS DODs for the Northern Hemisphere are equal to 0.056 and 0.060, respectively, and higher than the LIVAS climatological value (0.051). In the S. Hemisphere (Figure 6-iii), DODs range at very low levels (up to ~0.011), attributed to the low amounts of mineral particles emitted from spatially restricted desert areas, and the limited dust transport over oceanic regions. Despite the low annual levels (0.008; Table 1), there is an intra-annual cycle pattern not entirely commonly reproduced by the three datasets. In particular, MIDAS and MERRA-2 DODs are maximized in February, while the highest levels for LIVAS are recorded in September. For all DOD products, the minimum values are found in May, which are slightly lower than those observed during April-July (austral winter). At global scale (Figure 6-i), the seasonal patterns of DODs are mainly driven by those of the N. Hemisphere, particularly for LIVAS and at a lesser degree for MIDAS and MERRA-2. More specifically, there are two peaks (~0.055, March and June) for MIDAS, flat maximum levels (~0.05) between March and June for MERRA-2 while there is a primary (~0.05) and a secondary (~0.04) maximum in June and March, respectively, in LIVAS. Even though there are month-by-month differences, the LIVAS (0.029), MERRA-2 (0.031) and MIDAS (0.033) global annual DODs are relatively close indicating a sufficient level of agreement among the three datasets (Table 1). The obtained value for MIDAS is 10% higher and within the uncertainty estimate of the global DOD average (0.030±0.005) reported by Ridley et al. (2016).

The consistency among the three DOD datasets, in terms of magnitude and temporal covariation, is highly dependent on the region of interest. Figure 7 shows the defined sub-domains considered in this study. Figure S7 depicts the corresponding intra-annual DOD timeseries, while Table 1 lists the computed annual averages as well as their minimum/maximum values between 2007 and 2015. The best agreement among MIDAS, LIVAS and MERRA-2 is found along the Tropical Atlantic Ocean. In the nearby outflow regions (i.e., ETA), considerably high DODs (> 0.1) are found between January-August, being maximum in June, as indicated by the three datasets, with slight underestimations in MERRA-2 (Fig. S7-k). Over the western Tropical Atlantic Ocean, the sharp increase of DOD from May to June indicates the arrival of considerable amounts of Saharan particles, which are sustained at high levels in summer and diminish during autumn and winter (Fig. S7-q). This seasonal fluctuation is almost identically reproduced by the three products. Nevertheless, when the dust activity is well established in the area (i.e., boreal summer), LIVAS shows higher values than MERRA-2 and MIDAS.

Across N. Africa, and particularly in the Bodélé (Fig. S7-a) and W. Sahara (Fig. S7-h), the LIVAS DODs are substantially lower when compared to MIDAS and MERRA-2. In the Bodélé, this is

Deleted: most evident deviations among the three products occur from March to June when the dust activity is more pronounced (Figure 7-ii). During the high-dust seasons, the DOD peaks are recorded in June, being identical (0.117) for MERRA-2 and MIDAS with CALIOP giving lower levels (0.114). Both the MIDAS/MERRA-2 “temporal consistency” and the CALIOP “underestimation” are mostly valid during boreal spring and summer with few exceptions, highlighted when focus is given on the temporal covariation. Within the course of the year, CALIOP and MERRA-2 DODs gradually increase from January to June while decrease during the second half of the annual cycle. While the trends in MIDAS DOD are similar overall, there is a local minimum observed in May (0.083) resulting in deviations of -0.009 and -0.021 compared to CALIOP and MERRA-2, respectively.

Deleted:,

Deleted: northern ...thern hemisphere

Deleted:,

Deleted: the same ...0.055...) and higher by up to 10% than the corresponding CALIOP mean (0.050)... In the S. Hemisphere (Figure 7-iii), DODs range at very low levels (up to ~0.011...), attributed to the low amounts of mineral particles emitted from spatially restricted desert areas,...and the limited dust transport over oceanic regions. Despite these...low annual values...evels (0.008; Table 1) , ...here is an intra-annual cycle pattern , which, however, is ...ot entirely commonly reproduced by the three datasets by the three datasets in contrast to the annual means which are almost identical among them (0.007-0.008; Table 1)... In particular, MIDAS and MERRA-2 DODs are maximized in

Deleted: for

Deleted: CALIOP

Deleted: DODs

Deleted: CALIOP ...IVAS (0.029), MERRA-2 (0.031) and MIDAS (0.031)

Deleted: very ...atively close indicating a sufficient level of agreement among the three datasets (Table 1) being also

Deleted: DOD ...agnitude and temporal covariation, is highly dependent on the region of interest. Table 1 lists the

Deleted: in

Deleted: 8

Deleted: are ...epicted

Deleted: ir

Deleted: and

Deleted: in ...able 1 are ...isted... the computed annual averages as well as their minimum/maximum limits...values

Deleted: CALIOP

Deleted: it

Deleted: DODs ...s found along the Tropical Atlantic Ocean, which is affected by Saharan dust transport

Deleted: the spaceborne (MIDAS, CALIOP/LIVAS) and reanalysis (MERRA-2)...he three products. Nevertheless,

Deleted: CALIOP

Deleted: levels compared to those...hows higher values than MERRA-2 and MIDAS, which are quite similar

Formatted: English (United States)

Deleted: 8...-a) and W. Sahara (Fig. S8...-h), the CALIO

evident for the entire year and in W. Sahara it can be clearly seen between March and June, Similar findings are drawn either for other source areas, such as Central Asia (Fig. S7-c), or outflow regions, such as the Mediterranean (Fig. S7-m), In SUS (Fig. S7-e), the seasonal variation of DODs is in a very good agreement between MERRA-2 and MIDAS but a positive offset is seen for the reanalysis data. On the contrary, LIVAS does not reproduce the secondary maximum in July while it gives very high DODs in Nov-Dec, which are not reliable. Over the Taklamakan (Fig. S7-f), the LIVAS DODs are higher than the corresponding MIDAS and MERRA-2 regional averages in the high-dust months (i.e., April-May) and in July. On the contrary, in the Gobi Desert residing eastwards, the LIVAS-MIDAS agreement is very good while MERRA-2 DODs are less variable, within the course of the year, (Fig. S7-b). Among the three DOD products, a very good temporal agreement it is found in the Thar Desert (Fig. S7-g), but there are deviations regarding the peak of July which is higher in LIVAS (0.88) than in MIDAS (0.75) and MERRA-2 (0.48), respectively. Over downwind continental areas of E. Asia (Fig. S7-i), only few exceptions break down the consistency between MIDAS and LIVAS, whereas MERRA-2 is able to reproduce the annual cycle but underestimates the intensity of dust loads. In southern Middle East (Fig. S7-n), the reanalysis and the spaceborne lidar DODs are very well correlated within the course of the year and lower than MIDAS during February-May. In the northern parts (Fig. S7-d), MIDAS gives substantially higher DODs against the well correlated and matched values of LIVAS and MERRA-2. Over the Northern Pacific, Asian dust is transported eastwards during spring affecting nearby (Fig. S7-p) and distant (Fig. S7-j) oceanic areas. The “signal” of this mechanism is clearly evident in MIDAS and MERRA-2 timeseries in contrast to LIVAS, which exhibits substantially lower DOD maxima. Moreover, these maxima appear in the western North Pacific Ocean earlier (March) with respect to the other two datasets (April). Based on MERRA-2 and MIDAS, in the sub-Sahel (Fig. S7-o), a primary and a secondary maximum are recorded in March and October, in agreement with ground-based visibility records (N'Tchayi Mbourou et al., 1997). LIVAS reproduces both peaks, but with a weaker intensity in March compared to MIDAS and MERRA-2. However, throughout the year, the maximum LIVAS DOD is observed in June (a local maximum is also recorded in MIDAS), which might be attributed to the strong convection activity favoring the occurrence of haboobs. Saharan dust aerosols, under the impact of the northeasterly harmattan winds, are carried over the Gulf of Guinea (Fig. S7-l) during boreal winter, although DODs among the three datasets reveal a noticeable variability in terms of intensity.

4.4. MIDAS DOD global climatology

The annual and seasonal DOD patterns, representative for the period 2003 – 2017, are illustrated in Figures 8 and 9, respectively. Among the desert areas of the planet, the most intense dust loads

Deleted: during the high-dust boreal summer season

Deleted: Similar findings are drawn either for other source areas, such as Central Asia (Fig. S8-c), the northern Middle East (Fig. S8-d), the southwest United States (Fig. S8-e) or outflow regions, such as the Mediterranean (Fig. S8-m).

Deleted: Over the Taklamakan (Fig. S8-f) and Gobi (Fig. S8-b) Deserts, the CALIOP DODs are higher than the corresponding MIDAS and MERRA-2 regional averages in April-May.

Deleted: 8

Deleted: MIDAS

Deleted: 1

Deleted: 172

Deleted: CALIOP

Deleted: 0.978

Deleted: 484

Deleted: downwind

Deleted: 8

Deleted: CALIOP

Deleted: and

Deleted: In southern Middle East (Fig. S8-n), the reanalysis and the spaceborne lidar DODs are very well correlated and reveal minor differences within the course of the year.

Deleted: MIDAS captures satisfactorily the monthly variability of DOD, despite the local minimum in May, but fails to reproduce the magnitude of the recorded maximum in June.

Deleted: 8

Deleted: 8

Deleted:

Deleted: on

Deleted: CALIOP

Deleted: y

Deleted: in the western North Pacific Ocean

Deleted: ,

Deleted: 8

Deleted: CALIOP

Deleted: However, throughout the year, the maximum CALIOP DOD is observed in June (a local maximum is also recorded in MIDAS), which might be unrealistic since it is not expected the accumulation of dust particles during summer months, when the precipitation heights in the area are maximized.

Deleted: 8

Formatted: English (United States)

Deleted: ,

Deleted: averaged over

Deleted: 7

Deleted: 6

(DODs up to ~1.2; Fig. 8) are observed in the Bodélé Depression located in the northern Lake Chad Basin (Washington et al., 2003). Over the region, these high DODs are sustained throughout the year (Fig. 9) while due to the prevailing meteorological conditions, during MAM (Fig. 9-ii) and JJA (Fig. 9-iii), mineral particles are transported westwards, along the Sahel, contributing to the locally emitted anthropogenic dust (Ginoux et al., 2012). Substantial high climatological DODs (up to 0.6; Fig. 8) are recorded in the western sector of Sahara, in contrast to the eastern parts, attributed to the accumulation of dust aerosols primarily in JJA (Fig. 9-iii) and secondarily in MAM (Fig. 9-ii), under the impact of the Saharan Heat Low (Schepanski et al., 2017). Saharan dust is subjected to short-range transport affecting frequently the nearby maritime areas of the Gulf of Guinea (Ben-Ami et al., 2009), the Mediterranean Sea (Gkikas et al., 2015) as well the Red Sea (Banks et al., 2017). Nevertheless, the strongest signal of Saharan dust transport appears over the Tropical Atlantic Ocean with massive loads of mineral particles, confined within the Saharan Air Layer (SAL; Kanitz et al., 2014), reaching the Caribbean Sea (Prospero, 1999), under the impact of the trade winds. The characteristics of the transatlantic dust transport reveal a remarkable intra-annual variation (Fig. 9) as it concerns plumes' latitudinal position, longitudinal extension and intensity, being maximum during boreal summer (Fig. 9-iii).

Dust activity over the Middle East is more pronounced in a "zone" extending from the alluvial plain of the Tigris-Euphrates River to the southern parts of the Arabian Peninsula (Fig. 8), through the eastern flat-lands of Saudi Arabia (Hamidi et al., 2013). Mineral particles emitted from these sources affect also the Persian Gulf (Giannakopoulou and Toumi, 2011) and the Red Sea (Banks et al., 2017); however, the major transport pattern is recorded across the northern Arabian Sea in JJA (Fig. 9-iii), when dust plumes can reach the western coasts of India (Ramaswamy et al., 2018). In the Asian continent, the Taklamakan Desert (Ge et al., 2014), situated in the Tarim basin (NW China), is one of the strongest dust source of the planet yielding DODs up to 1 during spring (Fig. 9-ii). These intensities are substantially higher than those recorded in the Gobi Desert, located eastwards in the same latitudinal band, due to the different composition of the erodible soils (Sun et al., 2013). Midlatitude cyclones, propagating eastwards during springtime (Fig. 9-ii), mobilize dust emission from both sources inducing uplifting and subsequently advection of mineral particles towards the continental E. Asia (Yu et al., 2019) as well as over the north Pacific Ocean (Yu et al., 2008) and exceptionally over the United States (Husar et al., 2001). Other hotspots of dust activity in Asia are recorded in the central parts (Li and Sokolik, 2018) and in the Sistan Basin (Alizadeh Choobari et al., 2013). Dust aerosols originating from agricultural activities along the Indus River basin (Ginoux et al., 2012) and natural processes in the Thar Desert (Proestakis et al., 2018) result in the accumulation of mineral particles in the Pakistan-India borders while under favorable meteorological conditions these loads are carried towards the Indo-Gangetic plain mainly during the pre-monsoon season (Dey

Deleted: hosted

Deleted: across the Sahara Desert and particularly

Deleted: of

Deleted: 7

Deleted: consists

Deleted: situated

Deleted: ,

Deleted: ,

Deleted: .

et al., 2004). In North America, dust production becomes more evident in the southwestern United States and northwest Mexico in regional terms and during spring within the course of the year (Fig. 9-ii). However, DODs are mostly lower than 0.2, with few local exceedances, indicating relatively weak dust emission from the natural (Mojave and Sonoran Deserts; Hand et al., 2017) and anthropogenic (Chihuahuan Desert and Southern Great Plains; Hand et al., 2016) dust sources of the region. Between the two hemispheres, there is a clear contrast in DODs, being substantially lower in the S. Hemisphere, attributed to the weaker processes triggering dust emission from the spatially restricted deserts located in S. Africa (Bryant et al., 2007), S. America (Gassó and Torres, 2019) and in the interior parts of Australia (Prospero et al., 2002).

In addition to the global climatological DOD pattern in Figure 8-i, the average of the daily DOD uncertainties provided within the dataset (not to be confused with the uncertainty of the average DOD), and the temporal availability of the MIDAS dataset are shown in Figs. 8-ii and -iii, respectively. More than 70% of daily satellite retrievals with respect to the full period are included in the calculation of the mean DODs (Fig. 8-i) over the cloud-free desert areas. Over dust-affected downwind regions the corresponding percentages range from 30 to 60% (Fig. 8-iii). As expected from Eqs. 4 to 7, daily DOD uncertainties (Fig. 8-ii), scale with DOD and reach up to 0.4 on annual average and 0.5 averaged over MAM and JJA (Figure S8) in the regions with strongest DODs.

5. Summary and conclusions

In the current study, we presented the MIDAS (ModIs Dust AeroSol) dust optical depth (DOD) dataset, developed via the synergistic implementation of MODIS-Aqua AOD and dust fraction extracted from collocated MERRA-2 reanalysis outputs. The derived fine resolution ($0.1^\circ \times 0.1^\circ$) global dataset between 2003 and 2017, provides DOD both over continental and oceanic areas, in contrast to similar available satellite products restricted over land surfaces (Ginoux et al., 2012), thus making feasible a thorough and consistent description of dust loads not only over the sources but also over downwind regions. Reanalysis datasets, spanning through decades and available at high temporal frequency, can fulfill such tasks; however, their coarser spatial resolution imposes a restriction when investigating mineral loads' features at finer spatial scales. Our developed DOD product aims at complementing existing observational gaps and can be exploited in a variety of studies (e.g., climatology, trends, evaluation of atmospheric-dust models, radiative effects and data assimilation).

The core concept of the applied methodology relies on the utilization of MODIS AOD and MERRA-2 dust fraction (MDF) for the derivation of DOD on MODIS swaths. The validity of MDF has been justified through its evaluation, against reference values obtained by the LIVAS database.

Deleted: Apart from
Deleted: the corresponding distributions of the long-term
Deleted: d
Deleted: total
Deleted: y
Deleted: (taking into account the propagation of each individual DOD uncertainty to the average grid cell value as well as the sampling uncertainty expressed by the standard error)
Deleted: , thus allowing to assess the accuracy of the derived product as well as its representativeness throughout the study period (2007-2016)
Deleted: .
Deleted: .
Deleted: are participating
Deleted: while
Deleted: o
Deleted: Regarding the total averaged
Deleted: uncertainty
Deleted: .
Deleted: the annual spatial pattern is similar with those of DOD with
Deleted: indicates maxi
Deleted: maximum absolute levels (up lower than
Deleted: to 0.1
Deleted: . O) in the sub-Saharan and in the Gulf of Guinea whereas similar values are found in the Taklamakan Desert and lower in the Tropical Atlantic.
Deleted: On a seasonal basis (Figure S89), the spatial agreement between the two patterns is valid following dust activity and the DOD uncertainty do not exceed 0.5 during MAM and JJA.
Deleted: spatial features of DOD uncertainties are driven
Deleted: combining
Deleted: DOD-to-AOD ratio
Deleted: , valid for
Deleted: a 15-year period decade (
Deleted: 7
Deleted: -
Deleted: 6
Deleted: ,
Deleted: where transport, from short- to long-range, is
Deleted: related to dust
Deleted: and
Deleted: estimation of dust
Deleted: assessment of the associated impacts as well as o
Deleted: DOD-to-AOD ratio
Deleted: Nevertheless, two prior steps have been done
Deleted: The second prior step comprises the evaluation o
Deleted: the columnar integration of quality assured dust

Over dust-abundant areas extending across the “dust belt”, MERRA-2 reproduces adequately the magnitude of dust portion as indicated by the calculated primary statistics (bias, FB, FGE) with the maximum underestimations (up to 10%) being observed in Asian deserts. The agreement between MDF and LIVAS is reduced in the main dust regions of N. America and in the S. Hemisphere.

Regarding the temporal covariation of the observed and simulated dust portions, over the period 2007–2015, moderate R values (up to 0.5) are computed above the sources, attributed to the high spatiotemporal variability of the emission processes. On the contrary, the correlation increases substantially (up to 0.9) over maritime downwind regions (Tropical Atlantic Ocean, north Pacific Ocean, Arabian Sea, Mediterranean Sea) where the main dust transport pathways are recorded. Apart from the geographical dependency of the level of agreement between MDF and LIVAS dust fraction, we also investigated the impact of the spatial representativeness of the CALIOP observations. Through this analysis, we revealed that for an increasing number of CALIOP L2 profiles (ranging from 1 to 23), that are aggregated for the derivation of the $1^\circ \times 1^\circ$ LIVAS grid cell, the computed metrics converge towards the ideal scores.

Finally, the obtained MIDAS DOD was evaluated against AERONET retrievals and compared with LIVAS and MERRA-2 DODs. AERONET observations were processed to minimize the contribution of other aerosol species making also the assumption that dust loads mainly consist of coarse particles (their radii is larger than the defined inflection point). Overall, the agreement between ~10500 MIDAS-AERONET pairs is very high ($R=0.89$), whereas the satellite DODs are higher by 2.7% with respect to the ground-based ones. At station level, the R values are mainly above 0.8 at most sites of the N. Hemisphere (except western US) while they are mostly lower than 0.5 in the S. Hemisphere. Moreover, positive MIDAS-AERONET deviations (up to 0.2) are mainly encountered in N. Africa and Middle East in contrast to negative values (down to -0.14) recorded at the remaining sites. Based on the annual and seasonal global DOD patterns, corresponding to the period 2007–2015, the locations with the maximum DODs are in a good agreement among the three datasets. Nevertheless, in many regions (e.g., Bodélé, sub-Saharan, north Pacific Ocean) there are deviations on the intensity of dust loads, attributed to the inherent weaknesses of DOD derivation techniques based on different approaches. Despite the regional dependency of deviations among the three datasets, the collocated global long-term averaged DOD is very similar (0.029 for LIVAS, 0.031 for MERRA-2 and 0.033 for MIDAS) and close to that reported (0.030) in Ridley et al. (2016). In the S. Hemisphere, the corresponding levels are equal to 0.008 for the three datasets, whereas in the N. Hemisphere, LIVAS DODs (0.051) are lower with respect to MIDAS (0.060) and MERRA-2 (0.056).

As a demonstration of the MIDAS dataset, a brief discussion about dust load regime at global scale is made by analyzing the annual and seasonal DOD patterns. The most pronounced dust activity recorded in the Bodélé Depression (DODs up to ~1.2), across the Sahel (DODs up to 0.8), in western

Deleted: MERRA-2
Deleted: CALIOP
Deleted: maritime
Deleted: MERRA-2
Deleted: CALIOP DOD-to-AOD ratios
Deleted: 3
Deleted: ir
Formatted: English (United States)
Deleted: CALIOP
Deleted: E
Deleted: and
Deleted: assuming
Deleted: are
Deleted: 7300
Deleted: resides
Deleted: =
Deleted: 882
Deleted: lower
Deleted: -5
Deleted: don't exceed
Deleted: 13
Deleted: 3
Deleted: 15
Deleted: 4
Deleted: averaged over
Deleted: based
Deleted: relied
Deleted: biases
Deleted: s
Deleted: are
Deleted: CALIOP
Deleted: very
Deleted: those
Deleted: by
Deleted: (0.007-
Deleted:)
Deleted: slightly differ for the three datasets
Deleted: CALIOP
Deleted: 0
Deleted: by 10%
Deleted: hemispherical averages
Deleted: 5
Formatted: English (United States)
Deleted: s'
Deleted: of the northern Lake Chad Basin

parts of the Sahara Desert (DODs up to 0.6), in the eastern parts of the Arabian Peninsula (DODs up to ~1), along the Indus river basin (DODs up to 0.8) and in the Taklamakan Desert (DODs up to ~1). On the contrary, the weaker emission mechanisms triggering dust mobilization over the spatially limited sources of Patagonia, South Africa and interior arid areas of Australia do not favor the accumulation of mineral particles at large amounts (DODs up to 0.4 at local hotspots), even during high-dust seasons. Over oceans, the main pathways of long-range dust transport are observed along the tropical Atlantic and the northern Pacific, revealing a remarkable variation, within the course of the year, in terms of intensity, latitudinal position and range. Finally, the Mediterranean and the Arabian Sea are affected by advected dust plumes originating from N. Africa and Middle East, respectively. Based on the performed uncertainty analysis, the MIDAS DOD product is highly reliable over dust rich regions and becomes more uncertain in areas where the existence of dust loads is not frequent.

The exploitation of the MIDAS DOD product will be expanded in other studies in preparation or schedule. At present, focus is given on: (i) the DOD climatology over dust sources and downwind regions, (ii) the implementation of the MIDAS dataset in the DA scheme of the MONARCH model (Di Tomaso et al., 2017), (iii) the estimation of dust radiative effects and the associated impacts on solar energy production, in North Africa and Middle East, upgrading the work of Kosmopoulos et al. (2018) and (iv) the analysis of global and regional trends of dust loads.

Acknowledgments

The DUST-GLASS project has received funding from the European Union's Horizon 2020 Research and Innovation programme under the Marie Skłodowska-Curie grant agreement No. 749461. The authors acknowledge support from the EU COST Action CA16202 "International Network to Encourage the Use of Monitoring and Forecasting Dust Products (inDust). We would like to thank the principal investigators maintaining the AERONET sites used in the present work. We thank the NASA CALIPSO team and NASA/LaRC/ASDC for making available the CALIPSO products which are used to build the LIVAS products and ESA which funded the LIVAS project (contract no. 4000104106/11/NL/FF/fk). We are grateful to the AERIS/ICARE Data and Services Center for providing access to the CALIPSO data used and their computational center (<http://www.icare.univ-lille1.fr/>, last access: 8 August 2019). Vassilis Amiridis acknowledges support by the European Research Council (grant no. 725698, D-TECT). Eleni Marinou acknowledges support by the Deutscher Akademischer Austauschdienst (grant no. 57370121). Carlos Pérez García-Pando acknowledges support by the European Research Council (grant no. 773051, FRAGMENT), the AXA Research Fund, and the Spanish Ministry of Science, Innovation and Universities (RYC-2015-18690 and CGL2017-88911-R). The authors acknowledge support by the DustClim Project as part of

Deleted: , within the course of the year,

Deleted: (less than 0.1 and 20% in absolute and relative terms, respectively)

Deleted: (>60%)

Deleted: This contradiction is interpreted by the stronger "signal" of dust loads and the larger data availability thus converging towards lower measurement and sampling uncertainties.

Deleted: scheduled and under

Deleted: preparation

Deleted: s

Deleted: NMMB-

Deleted: and

Formatted: English (United States)

Deleted: and

ERA4CS, an ERA-NET initiated by JPI Climate, and funded by FORMAS (SE), DLR (DE), BMWFW (AT), IFD (DK), MINECO (ES), ANR (FR) with co-funding by the European Union (Grant 690462). PRACE is acknowledged for awarding access to MareNostrum Supercomputer in the Barcelona Supercomputing Center. We acknowledge support of this work by the project “PANhellenic infrastructure for Atmospheric Composition and climatE change” (MIS 5021516) which is implemented under the Action “Reinforcement of the Research and Innovation Infrastructure”, funded by the Operational Programme "Competitiveness, Entrepreneurship and Innovation" (NSRF 2014-2020) and co-financed by Greece and the European Union (European Regional Development Fund). NOA members acknowledge support by the Stavros Niarchos Foundation (SNF). The authors would like to thank Dr. Andrew Mark Sayer for his valuable and constructive comments. The authors would like also to thank Thanasis Georgiou for developing the ftp server where the MIDAS dataset is stored.

Formatted: English (United States)

Data availability

The MIDAS dataset is available at <https://zenodo.org/record/4244106>

Author contribution

AG was responsible for the design of the study and the whole analysis having support from SK and CP. EP processed the CALIPSO data and had an advisory role in the relevant parts of the study. VA, ET, EM and NH provided feedback on the analysis conduction as well as AT, who contributed also to the part of the manuscript related to AERONET data. All authors contributed to the manuscript editing. AG prepared the replies to the two anonymous Reviewers having feedback from SK, CP and ET.

Competing interests

The authors declare that they have no conflict of interest.

References

Ackerman, S. A.: Remote sensing aerosols using satellite infrared observations, J. Geophys. Res., 102, 17069–17079, <https://doi.org/10.1029/96JD03066>, 1997.

Deleted: Data availability

The MIDAS dataset is available at
<https://doi.org/10.5281/zenodo.3719222>

Formatted: English (United States)

Alizadeh Choobari, O., Zawar-Reza, P., and Sturman, A.: Low level jet intensification by mineral dust aerosols, *Ann. Geophys.*, 31, 625–632, <https://doi.org/10.5194/angeo-31-625-2013>, 2013.

Amiridis, V., Wandinger, U., Marinou, E., Giannakaki, E., Tsekeli, A., Basart, S., Kazadzis, S., Gkikas, A., Taylor, M., Baldasano, J., and Ansmann, A.: Optimizing CALIPSO Saharan dust retrievals, *Atmos. Chem. Phys.*, 13, 12089–12106, <https://doi.org/10.5194/acp-13-12089-2013>, 2013.

Amiridis, V., Marinou, E., Tsekeli, A., Wandinger, U., Schwarz, A., Giannakaki, E., Mamouri, R., Kokkalis, P., Binietoglou, I., Solomos, S., Herekakis, T., Kazadzis, S., Gerasopoulos, E., Proestakis, E., Kottas, M., Balis, D., Papayannnis, A., Kontoes, C., Kourtidis, K., Papagiannopoulos, N., Mona, L., Pappalardo, G., Le Rille, O., and Ansmann, A.: LIVAS: a 3-D multi-wavelength aerosol/cloud database based on CALIPSO and EARLINET, *Atmos. Chem. Phys.*, 15, 7127–7153, <https://doi.org/10.5194/acp-15-7127-2015>, 2015.

Anderson, T. L., Wu, Y., Chu, D. A., Schmid, B., Redemann, J., and Dubovik, O.: Testing the MODIS satellite retrieval of aerosol fine-mode fraction, *J. Geophys. Res.*, 110, D18204, doi:10.1029/2005JD005978, 2005.

Baars, H., Kanitz, T., Engelmann, R., Althausen, D., Heese, B., Komppula, M., Preissler, J., Tesche, M., Ansmann, A., Wandinger, U., Lim, J.-H., Ahn, J. Y., Stachlewska, I. S., Amiridis, V., Marinou, E., Seifert, P., Hofer, J., Skupin, A., Schneider, F., Bohlmann, S., Foth, A., Bley, S., Pfuller, A., Giannakaki, E., Lihavainen, H., Viisanen, Y., Hooda, R. K., Pereira, S. N., Bortoli, D., Wagner, F., Mattis, I., Janicka, L., Markowicz, K. M., Achtert, P., Artaxo, P., Pauliquevis, T., Souza, R. A. F., Sharma, V. P., van Zyl, P. G., Beukes, J. P., Sun, J., Rohwer, E. G., Deng, R., Mamouri, R.-E. and Zamorano, F.: An overview of the first decade of Polly(NET): an emerging network of automated Raman-polarization lidars for continuous aerosol profiling, *Atmos. Chem. Phys.*, 16(8), 5111–5137, doi:10.5194/acp-16-5111-2016, 2016.

Banks, J. R. and Brindley, H. E.: Evaluation of MSG-SEVIRI mineral dust retrieval products over Africa and the Middle East, *Remote Sensing of Environment*, 128, 58–73, doi:10.1016/j.rse.2012.07.017, 2013.

Banks, J. R., Brindley, H. E., Stenckhoff, G., and Schepanski, K.: Satellite retrievals of dust aerosol over the Red Sea and the Persian Gulf (2005–2015), *Atmos. Chem. Phys.*, 17, 3987–4003, <https://doi.org/10.5194/acp-17-3987-2017>, 2017.

Basart, S., Pérez, C., Cuevas, E., Baldasano, J. M., and Gobbi, G. P.: Aerosol characterization in Northern Africa, Northeastern Atlantic, Mediterranean Basin and Middle East from direct-sun AERONET observations, *Atmos. Chem. Phys.*, 9, 8265–8282, <https://doi.org/10.5194/acp-9-8265-2009>, 2009.

Basart, S., Pérez, C., Nickovic, S., Cuevas, E., and Baldasano, J. M.: Development and evaluation of the BSC-DREAM8b dust regional model over Northern Africa, the Mediterranean and the Middle East, *Tellus B*, 64, 18539, doi:10.3402/tellusb.v64i0.18539, 2012.

Ben-Ami, Y., Koren, I., and Altaratz, O.: Patterns of North African dust transport over the Atlantic: winter vs. summer, based on CALIPSO first year data, *Atmos. Chem. Phys.*, 9, 7867–7875, <https://doi.org/10.5194/acp-9-7867-2009>, 2009.

Benedetti, A., Morcrette, J.-J., Boucher, O., Dethof, A., Engelen, R. J., Fisher, M., Flentje, H., Huneeus, N., Jones, L., Kaiser, J. W., Kinne, S., Mangold, A., Razinger, M., Simmons, A. J., Suttie, M., and the GEMS-AER team: Aerosol analysis and forecast in the European Centre for Medium-Range Weather Forecasts Integrated Forecast System: 2. Data assimilation, *J. Geophys. Res.*, 114, D13205, doi:10.1029/2008JD011115, 2009.

Bryant, R. G., Bigg, G. R., Mahowald, N. M., Eckardt, F. D., and Ross S. G.: Dust emission response to climate in southern Africa, *J. Geophys. Res.*, 112, D09207, doi:10.1029/2005JD007025, 2007.

Buchard, V., da Silva, A. M., Colarco, P. R., Darmenov, A., Randles, C. A., Govindaraju, R., Torres, O., Campbell, J., and Spurr, R.: Using the OMI aerosol index and absorption aerosol optical depth to evaluate the NASA MERRA Aerosol Reanalysis, *Atmos. Chem. Phys.*, 15, 5743–5760, <https://doi.org/10.5194/acp15-5743-2015>, 2015.

Buchard, V., Randles, C.A., da Silva, A.M., Darmenov, A., Colarco, P.R., Govindaraju, R., Ferrare, R., Hair, J., Beyersdorf, A.J., Ziemb, L.D. and Yu, H.: The MERRA-2 aerosol reanalysis, 1980 onward. Part II: Evaluation and case studies. *Journal of Climate*, 30, 6851–6872. <https://doi.org/10.1175/JCLI-D-16-0613>, 2017.

Bullard, J. E., Baddock, M., Bradwell, T., Crusius, J., Darlington, E., Gaiero, D., Gassó, S., Gisladottir, G., Hodgkins, R., McCulloch, R., McKenna-Neuman, C., Mockford, T., Stewart, H., and,

Thorsteinsson, T.: High-latitude dust in the Earth system, *Rev. Geophys.*, 54, 447–485, <https://doi.org/10.1002/2016RG000518>, 2016.

Burton, S. P., Hair, J. W., Kahnert, M., Ferrare, R. A., Hostetler, C. A., Cook, A. L., Harper, D. B., Berkoff, T. A., Seaman, S. T., Collins, J. E., Fenn, M. A. and Rogers, R. R.: Observations of the spectral dependence of linear particle depolarization ratio of aerosols using NASA Langley airborne High Spectral Resolution Lidar, *Atmos. Chem. Phys.*, 15(23), 13453–13473, doi:10.5194/acp-15-13453-2015, 2015.

Capelle, V., Chédin, A., Pondrom, M., Crevoisier, C., Armante, R., Crépeau, L. and Scott, N. A.: Infrared dust aerosol optical depth retrieved daily from IASI and comparison with AERONET over the period 2007–2016, *Remote Sensing of Environment*, 206, 15–32, doi.org/10.1016/j.rse.2017.12.008, 2018

Chen, S., Huang, J., Kang, L., Wang, H., Ma, X., He, Y., Yuan, T., Yang, B., Huang, Z., and Zhang, G.: Emission, transport, and radiative effects of mineral dust from the Taklimakan and Gobi deserts: comparison of measurements and model results, *Atmos. Chem. Phys.*, 17, 2401–2421, <https://doi.org/10.5194/acp-17-2401-2017>, 2017.

Chin, M., Ginoux, P., Kinne, S., Torres, O., Holben, B. N., Duncan, D. N., Martin, R. V., Logan, J. A., Higurashi, H., and Nakajima, T.: Tropospheric aerosol optical thickness from the GOCART model and comparisons with satellite and Sun photometer measurements, *J. Atmos. Sci.*, 59, 451–483, [https://doi.org/10.1175/1520-0469\(2002\)059<0451:TAOTFT>2.0.CO;2](https://doi.org/10.1175/1520-0469(2002)059<0451:TAOTFT>2.0.CO;2), 2002.

Clarisso, L., Clerbaux, C., Franco, B., Hadji-Lazaro, J., Whitburn, S., Kopp, A. K., et al.: A decadal data set of global atmospheric dust retrieved from IASI satellite measurements, *Journal of Geophysical Research: Atmospheres*, 124, <https://doi.org/10.1029/2018JD029701>, 2019.

Colarco, P., da Silva, A., Chin, M., and Diehl, T.: Online simulations of global aerosol distributions in the NASA GEOS-4 model and comparisons to satellite and ground-based aerosol optical depth, *J. Geophys. Res.*, 115, D14207, <https://doi.org/10.1029/2009JD012820>, 2010.

Colarco, P. R., Nowotnick, E. P., Randles, C. A., Yi, B., Yang, P., Kim, K.-M., Smith, J. A., and Bardeen, C. G.: Impact of radiatively interactive dust aerosols in the NASA GEOS-5 climate model: Sensitivity to dust particle shape and refractive index, *J. Geophys. Res.-Atmos.*, 119, 753–786, <https://doi.org/10.1002/2013JD020046>, 2014.

Field Code Changed

Formatted: English (United States)

Dey, S., Tripathi, S. N., Singh, R. P., and Holben, B. N.: Influence of dust storms on the aerosol optical properties over the Indo-Gangetic basin, *J. Geophys. Res.-Atmos.*, 109, 1–10, doi:10.1029/2004jd004924, 2004.

Di Tomaso, E., Schutgens, N. A. J., Jorba, O., and Pérez García-Pando, C.: Assimilation of MODIS Dark Target and Deep Blue observations in the dust aerosol component of NMMB-MONARCH version 1.0, *Geosci. Model Dev.*, 10, 1107–1129, <https://doi.org/10.5194/gmd-10-1107-2017>, 2017.

Diehl, T., Heil, A., Chin, M., Pan, X., Streets, D., Schultz, M., and Kinne, S.: Anthropogenic, biomass burning, and volcanic emissions of black carbon, organic carbon, and SO₂ from 1980 to 2010 for hindcast model experiments, *Atmos. Chem. Phys. Discuss.*, 12, 24895–24954, <https://doi.org/10.5194/acpd-12-24895-2012>, 2012.

Du, Y., Xu, X., Chu, M., Guo, Y., and Wang, J.: Air particulate matter and cardiovascular disease: the epidemiological, biomedical and clinical evidence, *J. Thorac. Dis.*, 8, E8, <https://doi.org/10.3978/j.issn.2072-1439.2015.11.37>, 2016.

Dubovik, O. and King, M. D.: A flexible inversion algorithm for retrieval of aerosol optical properties from Sun and sky radiance measurements, *J. Geophys. Res.*, 105, 20673–20696, <https://doi.org/10.1029/2000JD900282>, 2000.

Dubovik, O., Sinyuk, A., Lapyonok, T., Holben, B. N., Mishchenko, M., Yang, P., Eck, T. F., Volten, H., Munoz, O., Veihelmann, B., and Van der Zande, W. J.: Application of spheroid models to account for aerosol particle nonsphericity in remote sensing of desert dust, *J. Geophys. Res.-Atmos.*, 111, D11208, <https://doi.org/10.1029/2005JD006619>, 2006.

Ekström, M., McTainsh, G. H. and Chappell, A.: Australian dust storms: temporal trends and relationships with synoptic pressure distributions (1960–99), *Int. J. Climatol.*, 24, 1581–1599, doi:10.1002/joc.1072, 2004.

Engelstaedter, S., Tegen, I., and Washington, R.: North African dust emissions and transport, *Earth-Sci. Rev.*, 79, 73–100, <https://doi.org/10.1016/j.earscirev.2006.06.004>, 2006.

Fiedler, S., Schepanski, K., Heinold, B., Knippertz, P., and Tegen, I.: Climatology of nocturnal low-level jets over North Africa and implications for modeling mineral dust emission, *J. Geophys. Res.-Atmos.*, 118, 6100–6121, 2013.

Flaounas, E., Kotroni, V., Lagouvardos, K., Kazadzis, S., Gkikas, A., and Hatzianastassiou, N.: Cyclone contribution to dust transport over the Mediterranean region, *Atmos. Sci. Lett.*, 16, 473–478, doi:10.1002/asl.584, 2015.

Fotiadi, A., Hatzianastassiou, N., Drakakis, E., Matsoukas, C., Pavlakis, K. G., Hatzidimitriou, D., Gerasopoulos, E., Mihalopoulos, N., and Vardavas, I.: Aerosol physical and optical properties in the Eastern Mediterranean Basin, Crete, from Aerosol Robotic Network data, *Atmos. Chem. Phys.*, 6, 5399–5413, <https://doi.org/10.5194/acp-6-5399-2006>, 2006.

Freudenthaler, V., Esselborn, M., Wiegner, M., Heese, B., Tesche, M., Ansmann, A., Mueller, D., Althausen, D., Wirth, M., Fix, A., Ehret, G., Knippertz, P., Toledano, C., Gasteiger, J., Garhammer, M. and Seefeldner, A.: Depolarization ratio profiling at several wavelengths in pure Saharan dust during SAMUM 2006, *Tellus Ser. B-Chem. Phys. Meteorol.*, 61(1), 165–179, doi:10.1111/j.1600-0889.2008.00396.x, 2009.

Gassó, S., & Torres, O.: Temporal characterization of dust activity in the Central Patagonia desert (years 1964–2017), *Journal of Geophysical Research: Atmospheres*, 124, 3417– 3434, <https://doi.org/10.1029/2018JD030209>.

Ge, J. M., Huang, J. P., Xu, C. P., Qi, Y. L., and Liu, H. Y.: Characteristics of Taklimakan dust emission and distribution: a satellite and reanalysis field perspective, *J. Geophys. Res.-Atmos.*, 119, 11772–11783, <https://doi.org/10.1002/2014JD022280>, 2014.

Gelaro, R., McCarty, W., Suárez, M. J., Todling, R., Molod, A., Takacs, L., Randles, C. A., Darmenov, A., Bosilovich, M. G., Reichle, R., Wargan, K., Coy, L., Cullather, R., Draper, C., Akella, S., Buchard, V., Conaty, A., da Silva, A. M., Gu, W., Kim, G., Koster, R., Lucchesi, R., Merkova, D., Nielsen, J. E., Partyka, G., Pawson, S., Putman, W., Riendecker, M., Schubert, S. D., Sienkiewicz, M., and Zhao, B.: The Modern-Era Retrospective Analysis for Research and Applications, Version 2 (MERRA-2), *J. Climate*, 30, 5419–5454, <https://doi.org/10.1175/JCLI-D-16-0758.1>, 2017.

Georgoulias, A. K., Alexandri, G., Kourtidis, K. A., Lelieveld, J., Zanis, P., Pöschl, U., Levy, R., Amiridis, V., Marinou, E., and Tsikerdekis, A.: Spatiotemporal variability and contribution of different aerosol types to the aerosol optical depth over the Eastern Mediterranean, *Atmos. Chem. Phys.*, 16, 13853–13884, doi:10.5194/acp-16-13853-2016, 2016.

Georgoulias, A. K., Tsikerdekis, A., Amiridis, V., Marinou, E., Benedetti, A., Zanis, P., Alexandri, G., Mona, L., Kourtidis, K. A. and Lelieveld, J.: A 3-D evaluation of the MACC reanalysis dust product over Europe, northern Africa and Middle East using CALIOP/CALIPSO dust satellite observations, *Atmos. Chem. Phys.*, 18(12), 8601–8620, doi:10.5194/acp-18-8601-2018, 2018.

Giannakopoulou, E. M. and Toumi, R.: The Persian Gulf summertime low-level jet over sloping terrain, *Q. J. Roy. Meteor. Soc.*, 138, 145–157, doi:10.1002/qj.901, 2011.

Giles, D. M., Holben, B. N., Eck, T. F., Sinyuk, A., Smirnov, A., Slutsker, I., Dickerson, R. R., Thompson, A. M., and Schafer, J. S.: An analysis of AERONET aerosol absorption properties and classifications representative of aerosol source regions, *J. Geophys. Res.*, 117, D17203, <https://doi.org/10.1029/2012JD018127>, 2012.

[Giles, D. M., Sinyuk, A., Sorokin, M. G., Schafer, J. S., Smirnov, A., Slutsker, I., Eck, T. F., Holben, B. N., Lewis, J. R., Campbell, J. R., Welton, E. J., Korkin, S. V., and Lyapustin, A. I.: Advancements in the Aerosol Robotic Network \(AERONET\) Version 3 database – automated near-real-time quality control algorithm with improved cloud screening for Sun photometer aerosol optical depth \(AOD\) measurements, Atmos. Meas. Tech., 12, 169–209, https://doi.org/10.5194/amt-12-169-2019, 2019.](#)

Ginoux, P., Chin, M., Tegen, I., Prospero, J. M., Holben, B., Dubovik, O., and Lin, S. J.: Sources and distributions of dust aerosols simulated with the GOCART model, *J. Geophys. Res.-Atmos.*, 106, 20255–20273, <https://doi.org/10.1029/2000jd000053>, 2001.

Ginoux, P., Prospero, J. M., Torres, O., and Chin, M.: Longterm simulation of global dust distribution with the GOCART model: correlation with North Atlantic Oscillation, *Environ. Modell. Softw.*, 19, 113–128, [https://doi.org/10.1016/S1364- 8152\(03\)00114-2](https://doi.org/10.1016/S1364- 8152(03)00114-2), 2004.

Ginoux, P., Prospero, J. M., Gill, T. E., Hsu, N. C., and Zhao, M.: Global-scale attribution of anthropogenic and natural dust sources and their emission rates based on MODIS Deep Blue aerosol products, *Rev. Geophys.*, 50, RG3005, <https://doi.org/10.1029/2012RG000388>, 2012.

Gkikas, A., Hatzianastassiou, N., Mihalopoulos, N., Katsoulis, V., Kazadzis, S., Pey, J., Querol, X., and Torres, O.: The regime of intense desert dust episodes in the Mediterranean based on contemporary satellite observations and ground measurements, *Atmos. Chem. Phys.*, 13, 12135-12154, <https://doi.org/10.5194/acp-13-12135-2013>, 2013.

Gkikas, A., Houssos, E. E., Lolis, C. J., Bartzokas, A., Mihalopoulos, N., and Hatzianastassiou, N.: Atmospheric circulation evolution related to desert-dust episodes over the Mediterranean, *Q. J. Roy. Meteor. Soc.*, 141, 1634–1645, doi:10.1002/qj.2466, 2015.

Gkikas, A., Basart, S., Hatzianastassiou, N., Marinou, E., Amiridis, V., Kazadzis, S., Pey, J., Querol, X., Jorba, O., Gassó, S., and Baldasano, J. M.: Mediterranean intense desert dust outbreaks and their vertical structure based on remote sensing data, *Atmos. Chem. Phys.*, 16, 8609-8642, <https://doi.org/10.5194/acp-16-8609-2016>, 2016.

Gkikas, A., Obiso, V., Pérez García-Pando, C., Jorba, O., Hatzianastassiou, N., Vendrell, L., Basart, S., Solomos, S., Gassó, S., and Baldasano, J. M.: Direct radiative effects during intense Mediterranean desert dust outbreaks, *Atmos. Chem. Phys.*, 18, 8757-8787, <https://doi.org/10.5194/acp-18-8757-2018>, 2018.

Gkikas, A., Giannaros, T.M., Kotroni, V., Lagouvardos, K.: Assessing the radiative impacts of an extreme desert dust outbreak and the potential improvements on short-term weather forecasts: The case of February 2015, *Atmos. Res.*, 226, 152-170, <https://doi.org/10.1016/j.atmosres.2019.04.020>, 2019.

Gong, S. L.: A parameterization of sea-salt aerosol source function for sub- and super-micron particles, *Global Biogeochem. Cy.*, 17, 1097, <https://doi.org/10.1029/2003GB002079>, 2003.

Hamidi, M., Kavianpour, M. R., and Shao, Y.: Synoptic analysis of dust storms in the Middle East, *Asia-Pac. J. Atmos. Sci.*, 49, 279–286, 2013.

Hand, J. L., White, W. H., Gebhart, K. A., Hyslop, N. P., Gill, T. E., and Schichtel, B. A.: Earlier onset of the spring fine dust season in the southwestern United States, *Geophys. Res. Lett.*, 43, 4001–4009, <https://doi.org/10.1002/2016gl068519>, 2016.

Hand, J. L., Gill, T. E., and Schichtel, B. A.: Spatial and seasonal variability in fine mineral dust and coarse aerosol mass at re-mote sites across the United States, *J. Geophys. Res.-Atmos.*, 122, 3080–3097, <https://doi.org/10.1002/2016jd026290>, 2017.

Haustein, K., Pérez, C., Baldasano, J. M., Jorba, O., Basart, S., Miller, R. L., Janjic, Z., Black, T., Nickovic, S., Todd, M. C., Washington, R., Müller, D., Tesche, M., Weinzierl, B., Esselborn, M., and Schladitz, A.: Atmospheric dust modeling from meso to global scales with the online NMMB/BSC-Dust model – Part 2: Experimental campaigns in Northern Africa, *Atmos. Chem. Phys.*, 12, 2933–2958, <https://doi.org/10.5194/acp-12-2933-2012>, 2012.

Haywood, J. and Boucher, O.: Estimates of the direct and indirect radiative forcing due to tropospheric aerosols: A review, *Rev. Geophys.*, 38, 513–543, <https://doi.org/10.1029/1999RG000078>, 2000.

Hess, M., Koepke, P., and Schult, I.: Optical Properties of Aerosols and Clouds: The Software Package OPAC, *B. Am. Meteorol. Soc.*, 79, 831–844, [https://doi.org/10.1175/1520-0477\(1998\)0792.0.CO;2](https://doi.org/10.1175/1520-0477(1998)0792.0.CO;2), 1998.

Holben, B. N., Eck, T. F., Slutsker, I., Tanre, D., Buis, J. P., Setzer, A., Vermote, E., Reagan, J. A., Kaufman, Y., Nakajima, T., Lavenue, F., Jankowiak, I., and Smirnov, A.: AERONET – A federated instrument network and data archive for aerosol characterization, *Remote Sens. Environ.*, 66, 1–16, [https://doi.org/10.1016/S0034-4257\(98\)00031-5](https://doi.org/10.1016/S0034-4257(98)00031-5), 1998.

Hsu, N. C., Tsay, S. C., King, M. D., and Herman, J. R.: Aerosol Properties Over Bright-Reflecting Source Regions, *IEEE T. Geosci. Remote*, 42, 557–569, doi:10.1109/TGRS.2004.824067, 2004.

Hubanks, P. A., Platnick, S., King, M., and Ridgway, R.: MODIS Atmosphere L3 Gridded Product Algorithm Theoretical Basis Document (ATBD) & Users Guide, ATBD Reference Number: L3_ATBD_C6_2018_04_11, 2018.

Hunt, W. H., Winker, D. M., Vaughan, M. A., Powell, K. A., Lucker, P. L. and Weimer, C.: CALIPSO Lidar Description and Performance Assessment, *J. Atmos. Oceanic Technol.*, 26(7), 1214–1228, doi:10.1175/2009JTECHA1223.1, 2009.

Hussain, A., Mir, H., Afzal, M.: Analysis of dust storms frequency over Pakistan during (1961–2000), *Pakistan J. Meteorol.*, 2(3): 49–68, 2005.

Husar, R. B., Tratt, D. M., Schichtel, D. M., Falke, S. R., Li, F., Jaffe, D., Gassó, S., Gill, T., Laulainen, N. S., Lu, F., Reheis, M. C., Chun, Y., Westphal, D., Holben, B. N., Gueymard, C., McKendry, I., Kuring, N., Feldman, G. C., McClain, C., Frouin, R. J., Merrill, J., DuBois, D., Vignola, F., Murayama, T., Nickovic, S., Wilson, W. E., Sassen, K., Sugimoto, N., and Malm, W. C.: Asian dust events of April 1998, *J. Geophys. Res.*, 106, 18317–18330, <https://doi.org/10.1029/2000JD900788>, 2001.

Hyer, E. J., Reid, J. S., and Zhang, J.: An over-land aerosol optical depth data set for data assimilation by filtering, correction, and aggregation of MODIS Collection 5 optical depth retrievals, *Atmos. Meas. Tech.*, 4, 379–408, <https://doi.org/10.5194/amt-4-379-2011>, 2011.

Inness, A., Baier, F., Benedetti, A., Bouarar, I., Chabriat, S., Clark, H., Clerbaux, C., Coheur, P., Engelen, R. J., Errera, Q., Flemming, J., George, M., Granier, C., Hadji-Lazaro, J., Huijnen, V., Hurtmans, D., Jones, L., Kaiser, J. W., Kapsomenakis, J., Lefever, K., Leitão, J., Razinger, M., Richter, A., Schultz, M. G., Simmons, A. J., Suttie, M., Stein, O., Thépaut, J.-N., Thouret, V., Vrekoussis, M., Zerefos, C., and the MACC team: The MACC reanalysis: an 8 yr data set of atmospheric composition, *Atmos. Chem. Phys.*, 13, 4073–4109, <https://doi.org/10.5194/acp13-4073-2013>, 2013.

Inness, A., Ades, M., Agustí-Panareda, A., Barré, J., Benedictow, A., Blechschmidt, A.-M., Dominguez, J. J., Engelen, R., Eskes, H., Flemming, J., Huijnen, V., Jones, L., Kipling, Z., Massart, S., Parrington, M., Peuch, V.-H., Razinger, M., Remy, S., Schulz, M., and Suttie, M.: The CAMS reanalysis of atmospheric composition, *Atmos. Chem. Phys.*, 19, 3515–3556, <https://doi.org/10.5194/acp-19-3515-2019>, 2019.

Jickells, T. D., An, Z. S., Andersen, K. K., Baker, A. R., Bergametti, G., Brooks, N., Cao, J. J., Boyd, P. W., Duce, R. A., Hunter, K. A., Kawahata, H., Kubilay, N., laRoche, J., Liss, P. S., Mahowald, N., Prospero, J. M., Ridgwell, A. J., Tegen, I., and Torres, R.: Global iron connections between desert dust, ocean biogeochemistry, and climate, *Science*, 308, 67–71, 2005.

Kanakidou, M., Mihalopoulos, N., Kindap, T., Im, U., Vrekoussis, M., Gerasopoulos, E., Dermitzaki, E., Unal, A., Kocak, M., Markakis, K., Melas, D., Kouvarakis, G., Youssef, A. F., Richter, A.,

Hatzianastassiou, N., Hilboll, A., Ebojie, F., Wittrock, F., von Savigny, C., Burrows, J. P., Ladstaetter-Weissenmayer, A., and Moubasher, H.: Megacities as hot spots of air pollution in the East Mediterranean, *Atmos. Environ.*, 45, 1223–1235, <https://doi.org/10.1016/j.atmosenv.2010.11.048>, 2011.

Kanatani, K.T., Ito, I., Al-Delaimy, W.K., Adachi, Y., Mathews, W.C., Ramsdell, J.W.: Toyama Asian Desert Dust and Asthma Study Group Members. Desert dust exposure is associated with increased risk of asthma hospitalization in children, *Am. J. Respir. Crit. Care Med.* 182 (12), 1475e1481. <https://doi.org/10.1164/rccm.201002-0296OC>, 2010.

Kanitz, T., Engelmann, R., Heinold, B., Baars, H., Skupin, A., and Ansmann, A.: Tracking the Saharan Air Layer with shipborne lidar across the tropical Atlantic, *Geophys. Res. Lett.*, 41, 1044–1050, doi:10.1002/2013GL058780, 2014.

Kaufman, Y. J., Koren, I., Remer, L. A., Tanré, D., Ginoux, P., and Fan, S.: Dust transport and deposition observed from the Terra-Moderate Resolution Imaging Spectroradiometer (MODIS) spacecraft over the Atlantic Ocean, *J. Geophys. Res.-Atmos.*, 110, 1–16, <https://doi.org/10.1029/2003JD004436>, 2005.

Kergoat, L., Guichard, F., Pierre, C., and Vassal, C.: Influence of dry-season vegetation variability on Sahelian dust during 2002–2015, *Geophys. Res. Lett.*, 44, 5231–5239, <https://doi.org/10.1002/2016GL072317>, 2017.

Kim, D., Chin, M., Yu, H., Eck, T. F., Sinyuk, A., Smirnov, A., and Holben, B. N.: Dust optical properties over North Africa and Arabian Peninsula derived from the AERONET dataset, *Atmos. Chem. Phys.*, 11, 10733–10741, <https://doi.org/10.5194/acp-11-10733-2011>, 2011.

Kittaka, C., Winker, D. M., Vaughan, M. A., Omar, A., and Remer, L. A.: Intercomparison of column aerosol optical depths from CALIPSO and MODIS-Aqua, *Atmos. Meas. Tech.*, 4, 131– 141, <https://doi.org/10.5194/amt-4-131-2011>, 2011.

Klingmüller, K., Pozzer, A., Metzger, S., Stenchikov, G. L., and Lelieveld, J.: Aerosol optical depth trend over the Middle East, *Atmos. Chem. Phys.*, 16, 5063–5073, <https://doi.org/10.5194/acp-16-5063-2016>, 2016.

Klose, M. and Shao, Y.: Stochastic parameterization of dust emission and application to convective atmospheric conditions, *Atmos. Chem. Phys.*, 12, 7309-7320, <https://doi.org/10.5194/acp-12-7309-2012>, 2012.

Knippertz, P., Deutscher, C., Kandler, K., Müller, T., Schulz, O., and Schütz, L.: Dust mobilization due to density currents in the Atlas region: Observations from the Saharan Mineral Dust Experiment 2006 field campaign, *J. Geophys. Res.-Atmos.*, 112, 1–14, <https://doi.org/10.1029/2007JD008774>, 2007.

Koch, J. and Renno, N. O.: The role of convective plumes and vortices on the global aerosol budget, *Geophys. Res. Lett.*, 32, L18806, doi:10.1029/2005GL023420, 2005.

Konsta, D., Binietoglou, I., Gkikas, A., Solomos, S., Marinou, E., Proestakis, E., Basart, S., Pérez García-Pando, C., El-Askary, H., Amiridis, V.: Evaluation of the BSC-DREAM8b regional dust model using the 3D LIVAS-CALIPSO, *Atmos. Environ.*, 195, 46-62, <https://doi.org/10.1016/j.atmosenv.2018.09.047>, 2018.

Kosmopoulos, P. G., Kazadzis, S., Taylor, M., Athanasopoulou, E., Speyer, O., Raptis, P. I., Marinou, E., Proestakis, E., Solomos, S., Gerasopoulos, E., Amiridis, V., Bais, A. and Kontoes, C.: Dust impact on surface solar irradiance assessed with model simulations, satellite observations and ground-based measurements, *Atmos. Meas. Tech.*, 10(7), doi:10.5194/amt-10-2435-2017, 2017.

Kosmopoulos, P.G., Kazadzis, S., El-Askary, H., Taylor, M., Gkikas, A., Proestakis, E., Kontoes, C., El-Khayat, M.M.: Earth-Observation-Based Estimation and Forecasting of Particulate Matter Impact on Solar Energy in Egypt, *Remote Sens.*, 10, 1870, 2018.

Lambert, F., Kug, J.-S., Park, R. J., Mahowald, N., Winckler, G., Abe-Ouchi, A., O’ishi, R., Takemura, T., and Lee, J.-H.: The role of mineral-dust aerosols in polar temperature amplification, *Nat. Clim. Change*, 3, 487–491, <https://doi.org/10.1038/nclimate1785>, 2013.

Levy, R. C., Remer, L. A., and Dubovik, O.: Global aerosol optical properties and application to Moderate Resolution Imaging Spectroradiometer aerosol retrieval over land, *J. Geophys. Res.-Atmos.*, 112, D13210, doi:10.1029/2006JD007815, 2007a.

Levy, R. C., Remer, L. A., Mattoo, S., Vermote, E. F., and Kaufman, Y. J.: Second-generation operational algorithm: Retrieval of aerosol properties over land from inversion of Moderate Resolution Imaging Spectroradiometer spectral reflectance, *J. Geophys. Res.-Atmos.*, 112, D13211, doi:10.1029/2006JD007811, 2007b.

Levy, R. C., Leptoukh, G. G., Kahn, R., Zubko, V., Gopalan, A., and Remer, L. A.: A critical look at deriving monthly aerosol optical depth from satellite data, *IEEE Transactions on Geoscience and Remote Sensing*, 47, 2942–2956, <https://doi.org/10.1109/TGRS.2009.2013842>, 25 2009.

Levy, R. C., Remer, L. A., Kleidman, R. G., Mattoo, S., Ichoku, C., Kahn, R., and Eck, T. F.: Global evaluation of the Collection 5 MODIS dark-target aerosol products over land, *Atmos. Chem. Phys.*, 10, 10399–10420, doi:10.5194/acp-10-10399-2010, 2010.

Levy, R. C., Mattoo, S., Munchak, L. A., Remer, L. A., Sayer, A. M., Patadia, F., and Hsu, N. C.: The Collection 6 MODIS aerosol products over land and ocean, *Atmos. Meas. Tech.*, 6, 2989–3034, <https://doi.org/10.5194/amt-6-2989-2013>, 2013.

Li, W., El-Askary, H., Qurban, M. A., Proestakis E., Garay M. J., Kalashnikova, O. V., Amiridis, V., Gkikas, A., Marinou, E., Piechota, T. and ManiKandan, K. P.: An Assessment of Atmospheric and Meteorological Factors Regulating Red Sea Phytoplankton Growth, *Remote Sens.*, 10(5), 673; doi:10.3390/rs10050673, 2018.

Li, L., and Sokolik, I.: Analysis of Dust Aerosol Retrievals Using Satellite Data in Central Asia, *Atmosphere*, 9, 288, 2018.

Liu, D., Wang, Z., Liu, Z., Winker, D., and Trepte, C.: A height resolved global view of dust aerosols from the first year CALIPSO lidar measurements, *J. Geophys. Res.-Atmos.*, 113, D16214, <https://doi.org/10.1029/2007JD009776>, 2008.

Liu, D., Taylor, J. W., Crosier, J., Marsden, N., Bower, K. N., Lloyd, G., Ryder, C. L., Brooke, J. K., Cotton, R., Marenco, F., Blyth, A., Cui, Z., Estelles, V., Gallagher, M., Coe, H., and Choularton, T. W.: Aircraft and ground measurements of dust aerosols over the west African coast in summer 2015 during ICE-D and AER-D, *Atmos. Chem. Phys.*, 18, 3817–3838, <https://doi.org/10.5194/acp-18-3817-2018>, 2018.

Lynch, P., Reid, J. S., Westphal, D. L., Zhang, J., Hogan, T. F., Hyer, E. J., Curtis, C. A., Hegg, D. A., Shi, Y., Campbell, J. R., Rubin, J. I., Sessions, W. R., Turk, F. J., and Walker, A. L.: An 11-year global gridded aerosol optical thickness reanalysis (v1.0) for atmospheric and climate sciences, *Geosci. Model Dev.*, 9, 1489–1522, <https://doi.org/10.5194/gmd-9-1489-2016>, 2016.

Ma, X., Bartlett, K., Harmon, K., and Yu, F.: Comparison of AOD between CALIPSO and MODIS: significant differences over major dust and biomass burning regions, *Atmos. Meas. Tech.*, 6, 2391–2401, <https://doi.org/10.5194/amt-6-2391-2013>, 2013.

Mamouri, R. E. and Ansmann, A.: Fine and coarse dust separation with polarization lidar, *Atmos. Meas. Tech.*, 7, 3717–3735, <https://doi.org/10.5194/amt-7-3717-2014>, 2014.

Mamouri, R.-E. and Ansmann, A.: Potential of polarization/Raman lidar to separate fine dust, coarse dust, maritime, and anthropogenic aerosol profiles, *Atmos. Meas. Tech.*, 10(9), 3403–3427, doi:10.5194/amt-10-3403-2017, 2017.

Marinou, E., Amiridis, V., Binietoglou, I., Tsikerdekis, A., Solomos, S., Proestakis, E., Konsta, D., Papagiannopoulos, N., Tsekeri, A., Vlastou, G., Zanis, P., Balis, D., Wandinger, U., and Ansmann, A.: Three-dimensional evolution of Saharan dust transport towards Europe based on a 9-year EARLINET-optimized CALIPSO dataset, *Atmos. Chem. Phys.*, 17, 5893–5919, <https://doi.org/10.5194/acp-17-5893-2017>, 2017.

McCarty, W., Coy, L., Gelaro, R., Huang, A., Merkova, D., Smith, E. B., Sienkiewicz, M., and Wargan, K.: MERRA-2 input observations: Summary and initial assessment. Technical Report Series on Global Modeling and Data Assimilation, Vol. 46, NASA Tech. Rep. NASA/TM–2016–104606, 61 pp., 2016. [Available online at <https://gmao.gsfc.nasa.gov/pubs/docs/McCarty885.pdf>.]

Meng, Z. K., Yang, P., Kattawar, G. W., Bi, L., Liou, K. N., and Laszlo, I.: Single-scattering properties of tri-axial ellipsoidal mineral dust aerosols: A database for application to radiative transfer calculations, *J. Aerosol Sci.*, 41, 501–512, <https://doi.org/10.1016/j.jaerosci.2010.02.008>, 2010.

Middleton, N. J. and Goudie, A. S.: Saharan dust: sources and trajectories, *T. I. Brit. Geogr.*, 26, 165–181, doi:10.1111/1475-5661.00013, 2001.

Molod, A., Takacs, L., Suarez, M., and Bacmeister, J.: Development of the GEOS-5 atmospheric general circulation model: evolution from MERRA to MERRA2, *Geosci. Model Dev.*, 8, 1339–1356, <https://doi.org/10.5194/gmd-8-1339-2015>, 2015.

Mukkavilli, S.K., Prasad, A.A., Taylor, R.A., Huang, J., Troccoli, A., Kay, M.J.: Assessment of atmospheric aerosols from two reanalysis products over Australia, *Atmos. Res.*, 215, 149–164, 2019.

Müller, D., Ansmann, A., Mattis, I., Tesche, M., Wandinger, U., Althausen, D., and Pisani, G.: Aerosol-type-dependent lidar ratios observed with Raman lidar, *J. Geophys. Res.-Atmos.*, 112, <https://doi.org/10.1029/2006JD008292>, 2007.

Nabat, P., Somot, S., Mallet, M., Michou, M., Sevault, F., Driouech, F., Meloni, D., di Sarra, A., Di Biagio, C., Formenti, P., Sicard, M., Léon, J.-F., and Bouin, M.-N.: Dust aerosol radiative effects during summer 2012 simulated with a coupled regional aerosol–atmosphere–ocean model over the Mediterranean, *Atmos. Chem. Phys.*, 15, 3303–3326, <https://doi.org/10.5194/acp-15-3303-2015>, 2015.

N'Tchayi Mbourou, G., Berrand, J. J., and Nicholson, S. E.: The diurnal and seasonal cycles of wind-borne dust over Africa north of the equator, *J. Appl. Meteorol.*, 36, 868–882, 1997.

Okin, G. S., Mahowald, N., Chadwick, O. A., and Artaxo, P.: Impact of desert dust on the biogeochemistry of phosphorus in terrestrial ecosystems, *Global Biogeochem. Cy.*, 18, GB2005, <https://doi.org/10.1029/2003GB002145>, 2004.

Omar, A. H., Winker, D. M., Vaughan, M. A., Hu, Y., Trepte, C. R., Ferrare, R. A., Lee, K. P., Hostetler, C. A., Kittaka, C., Rogers, R. R., and Kuehn, R. E.: The CALIPSO Automated Aerosol Classification and Lidar Ratio Selection Algorithm, *J. Atmos. Ocean. Tech.*, 26, 1994–2014, <https://doi.org/10.1175/2009JTECHA1231.1>, 2009.

Omar, A. H., Winker, D. M., Tackett, J. L., Giles, D. M., Kar, J., Liu, Z., Vaughan, M. A., Powell, K. A., and Trepte, C. R., CALIOP and AERONET aerosol optical depth comparisons: One size fits none, *J. Geophys. Res.-Atmos.*, 118, 4748–4766, <https://doi.org/10.1002/jgrd.50330>, 2013.

O'Neill, N. T., Eck, T. F., Smirnov, A., Holben, B. N., and Thulasiraman, S.: Spectral discrimination of coarse and fine mode optical depth, *J. Geophys. Res.*, 108, 4559–4573, <https://doi.org/10.1029/2002JD002975>, 2003.

Pease, P. P., Tchakerian, V. P., and Tindale, N. W.: Aerosols over the Arabian Sea: geochemistry and source areas for Aeolian desert dust, *J. Arid Environ.*, 39, 477–496, <https://doi.org/10.1006/jare.1997.0368>, 1998.

Pérez, C., Nickovic, S., Pejanovic, G., Baldasano, J. M., and Özsoy, E.: Interactive dust-radiation modeling: A step to improve weather forecasts, *J. Geophys. Res.*, 111, 1–17, 2006.

Pérez, C., Haustein, K., Janjic, Z., Jorba, O., Huneeus, N., Baldasano, J. M., Black, T., Basart, S., Nickovic, S., Miller, R. L., Perlitz, J. P., Schulz, M., and Thomson, M.: Atmospheric dust modeling from meso to global scales with the online NMMB/BSC-Dust model – Part 1: Model description, annual simulations and evaluation, *Atmos. Chem. Phys.*, 11, 13001–13027, <https://doi.org/10.5194/acp-11-13001-2011>, 2011.

Pérez García-Pando, C., Stanton, M. C., Diggle, P. J., Trzaska, S., Miller, R. L., Perlitz, J. P., Baldasano, J. M., Cuevas, E., Ceccato, P., Yaka, P., and Thomson, M. C.: Soil Dust Aerosols and Wind as Predictors of Seasonal Meningitis Incidence in Niger, *Environ. Health Perspect.*, 122, 679–686, doi:10.1289/ehp.1306640, 2014.

Peyridieu, S., Chédin, A., Capelle, V., Tsamalis, C., Pierangelo, C., Armante, R., Crevoisier, C., Crépeau, L., Siméon, M., Ducos, F., and Scott, N. A.: Characterisation of dust aerosols in the infrared from IASI and comparison with PARASOL, MODIS, MISR, CALIOP, and AERONET observations, *Atmos. Chem. Phys.*, 13, 6065–6082, <https://doi.org/10.5194/acp-13-6065-2013>, 2013.

Proestakis, E., Amiridis, V., Marinou, E., Georgoulas, A. K., Solomos, S., Kazadzis, S., Chimot, J., Che, H., Alexandri, G., Binietoglou, I., Daskalopoulou, V., Kourtidis, K. A., de Leeuw, G., and van der A, R. J.: Nine-year spatial and temporal evolution of desert dust aerosols over South and East Asia as revealed by CALIOP, *Atmos. Chem. Phys.*, 18, 1337–1362, <https://doi.org/10.5194/acp-18-1337-2018>, 2018.

Prospero, J. M.: Long-range transport of mineral dust in the global atmosphere: Impact of African dust on the environment of the southeastern United States, *P. Natl. Acad. Sci. USA*, 96, 3396–3403, 1999.

Prospero, J. M., Ginoux, P., Torres, O., Nicholson, S. E., and Gill, T. E.: Environmental characterization of global sources of atmospheric soil dust identified with the Nimbus 7 Total Ozone Mapping Spectrometer (TOMS) absorbing aerosol product, *Rev. Geophys.*, 40, 2-1–2-31, 2002.

Prospero, J. M. and Mayol-Bracero, O. L.: Understanding the transport and impact of African dust on the Caribbean Basin, *B. Am. Meteorol. Soc.*, 94, 1329–1335, 2013.

Querol, X., Tobías, A., Pérez, N., Karanasiou, A., Amato, F., Stafoggia, M., Pérez García-Pando, C., Ginoux, P., Forastiere, F., Gumy, S., P., Alastuey, A.: Monitoring the impact of desert dust outbreaks for air quality for health studies, *Environment International*, 130, 104867, 2019. <https://doi.org/10.1016/j.envint.2019.05.061>.

Deleted: ¶

Ramaswamy, V.P., Muraleedharan, M., Prakash Babu, C.: Mid-troposphere transport of Middle-East dust over the Arabian Sea and its effect on rainwater composition and sensitive ecosystems over India. *Scientific Reports* 7, 13676, <https://doi.org/10.1038/s41598-017-13652-1>, 2018.

Rashki, A., Kaskaoutis, D.G., Francois, P., Kosmopoulos, P.G., Legrand, M.: Dust-storm dynamics over Sistan region, Iran: seasonality, transport characteristics and affected areas, *Aeol. Res.*, 16, 35–48, 2015.

Reid, J. S., Reid, E. A., Walker, A., Piketh, S., Cliff, S., Al Mandoos, A., Tsay, S.-C., and Eck, T. F.: Dynamics of southwest Asian dust particle size characteristics with implications for global dust research, *J. Geophys. Res.*, 113, D14212, <https://doi.org/10.1029/2007JD009752>, 2008.

Remer, L. A., Tanre, D., Kaufman, Y. J., Ichoku, C., Mattoo, S., Levy, R., Chu, D. A., Holben, B., Dubovik, O., Smirnov, A., Martins, J. V., Li, R. R., and Ahmad, Z.: Validation of MODIS aerosol retrieval over ocean, *Geophys. Res. Lett.*, 29, MOD3.1–MOD3.4, doi:10.1029/2001GL013204, 2002.

Remer, L. A., Kaufman, Y. J., Tanre, D., Mattoo, S., Chu, D. A., Martins, J. V., Li, R. R., Ichoku, C., Levy, R. C., Kleidman, R. G., Eck, T. F., Vermote, E., and Holben, B. N.: The MODIS aerosol algorithm, products, and validation, *J. Atmos. Sci.*, 62, 947–973, doi:10.1175/JAS3385.1, 2005.

Remer, L. A., Kleidman, R. G., Levy, R. C., Kaufman, Y. J., Tanré, D., Mattoo, S., Martins, J. V., Ichoku, C., Koren, I., Yu, H. and Holben, B. N.: Global aerosol climatology from the MODIS satellite sensors, *J. Geophys. Res.-Atmos.*, 113, D14S07, doi:10.1029/2007JD009661, 2008.

Ridley, D. A., Heald, C. L., Kok, J. F., and Zhao, C.: An observationally constrained estimate of global dust aerosol optical depth, *Atmos. Chem. Phys.*, 16, 15097–15117, <https://doi.org/10.5194/acp-16-15097-2016>, 2016.

Rienecker, M. M., Suarez, M. J., Todling, R., Bacmeister, J., Takacs, L., Liu, H. C., Gu, W., Sienkiewicz, M., Koster, R. D., Gelaro, R., Stajner, I., and Nielsen, J. E.: The GEOS-5 Data Assimilation System-Documentation of Versions 5.0.1, 5.1.0, and 5.2.0 Technical Report Series on Global Modeling and Data Assimilation, v27, 2008.

Rodríguez, S., Alastuey, A., and Querol, X.: A review of methods for long term in situ characterization of aerosol dust, *Aeolian Res.*, 6, 55–74, doi:10.1016/j.aeolia.2012.07.004, 2012.

Sayer, A. M., Hsu, N. C., Bettenhausen, C., and Jeong, M.-J.: Validation and uncertainty estimates for MODIS Collection 6 “Deep Blue” aerosol data, *J. Geophys. Res.*, 118, 7864–7873, <https://doi.org/10.1002/jgrd.50600>, 2013.

Sayer, A. M., Munchak, L. A., Hsu, N. C., Levy, R. C., Bettenhausen, C., and Jeong, M.-J.: MODIS Collection 6 aerosol products: comparison between aqua’s e-deep blue, dark target, and “merged” data sets, and usage recommendations, *J. Geophys. Res.-Atmos.*, 119, 13965–13989, doi:10.1002/2014JD022453, 2014.

Schepanski, K., Tegen, I., Laurent, B., Heinold, B., and Macke, A.: A new Saharan dust source activation frequency map derived from MSG-SEVIRI IR-channels, *Geophys. Res. Lett.*, 34, L18803, <https://doi.org/10.1029/2007GL030168>, 2007.

Schepanski, K., Tegen, I., and Macke, A.: Comparison of satellite based observations of Saharan dust source areas, *Remote Sensing of Environment*, 123, 90–97, <http://www.sciencedirect.com/science/article/pii/S0034425712001381>, 2012.

Schepanski, K., Heinold, B., and Tegen, I.: Harmattan, Saharan heat low, and West African monsoon circulation: modulations on the Saharan dust outflow towards the North Atlantic, *Atmos. Chem. Phys.*, 17, 10223-10243, <https://doi.org/10.5194/acp-17-10223-2017>, 2017.

Schepanski, K.: Transport of Mineral Dust and Its Impact on Climate, *Geosciences*, 8, <https://doi.org/10.3390/geosciences8050151>, 2018.

Schuster, G. L., Vaughan, M., MacDonnell, D., Su, W., Winker, D., Dubovik, O., Lapyonok, T., and Trepte, C.: Comparison of CALIPSO aerosol optical depth retrievals to AERONET measurements, and a climatology for the lidar ratio of dust, *Atmos. Chem. Phys.*, 12, 7431-7452, <https://doi.org/10.5194/acp-12-7431-2012>, 2012.

Shi, Y., Zhang, J., Reid, J. S., Holben, B., Hyer, E. J., and Curtis, C.: An analysis of the collection 5 MODIS over-ocean aerosol optical depth product for its implication in aerosol assimilation, *Atmos. Chem. Phys.*, 11, 557-565, <https://doi.org/10.5194/acp-11-557-2011>, 2011.

Sinyuk, A., Holben, B. N., Eck, T. F., Giles, D. M., Slutsker, I., Korkin, S., Schafer, J. S., Smirnov, A., Sorokin, M., and Lyapustin, A.: The AERONET Version 3 aerosol retrieval algorithm, associated uncertainties and comparisons to Version 2, *Atmos. Meas. Tech.*, 13, 3375–3411, <https://doi.org/10.5194/amt-13-3375-2020>, 2020.

Sokolik, I. N. and Toon, O. B.: Direct radiative forcing by anthropogenic airborne mineral aerosols, *Nature*, 381, 681–683, <https://doi.org/10.1038/381681a0>, 1996.

Solomos, S., Kalivitis, N., Mihalopoulos, N., Amiridis, V., Kouvarakis, G., Gkikas, A., Binietoglou, I., Tsekeli, A., Kazadzis, S., Kottas, M., Pradhan, Y., Proestakis, E., Nastas, P. T. and Marenco, F.: From Tropospheric Folding to Khamsin and Foehn Winds: How Atmospheric Dynamics Advanced a Record-Breaking Dust Episode in Crete, *Atmosphere*, 9(7), 240, doi:10.3390/atmos9070240, 2018.

Stefanski, R. and Sivakumar, M. V. K.: Impacts of sand and dust storms on agriculture and potential agricultural applications of a SDSWS, *IOP Conf. Ser.: Earth Environ. Sci.*, 7, 012016, doi: 10.1088/1755-1307/7/1/012016, 2009.

Stephens, G. L., Vane, D. G., Boain, R. J., Mace, G. G., Sassen, K., Wang, Z. E., Illingworth, A. J., O'Connor, E. J., Rossow, W. B., Durden, S. L., Miller, S. D., Austin, R. T., Benedetti, A. and Mitrescu, C.: The cloudsat mission and the a-train - A new dimension of space-based observations of clouds and precipitation, *Bull. Amer. Meteorol. Soc.*, 83(12), 1771–1790, doi:10.1175/BAMS-83-12-1771, 2002.

Su, L. and Toon, O. B.: Saharan and Asian dust: similarities and differences determined by CALIPSO, AERONET, and a coupled climate-aerosol microphysical model, *Atmos. Chem. Phys.*, 11, 3263-3280, <https://doi.org/10.5194/acp-11-3263-2011>, 2011.

Sun, Y., Chen, H., Tada, R., Weiss, D., Lin, M., Toyoda, S., Yan, Y., and Isozaki, Y.: ESR signal intensity and crystallinity of quartz from Gobi and sandy deserts in East Asia and implication for tracing Asian dust provenance, *Geochem. Geophys. Geosy.*, 14, 2615–2627, <https://doi.org/10.1002/ggge.20162>, 2013.

Sun, E., Xu, X., Che, H., Tang, Z., Gui, K., An, L., Lu, C., and Shi, G.: Variation in MERRA-2 aerosol optical depth and absorption aerosol optical depth over China from 1980 to 2017, *J. Atmos. Sol.-Terr. Phys.*, 186, 8–19, <https://doi.org/10.1016/j.jastp.2019.01.019>, 2019.

Tackett, J. L., Winker, D. M., Getzewich, B. J., Vaughan, M. A., Young, S. A. and Kar, J.: CALIPSO lidar level 3 aerosol profile product: version 3 algorithm design, *Atmos. Meas. Tech.*, 11(7), 4129–4152, doi:10.5194/amt-11-4129-2018, 2018.

Tafuro, A. M., Barnaba, F., De Tomasi, F., Perrone, M. R., and Gobbi, G. P.: Saharan dust particle properties over the central Mediterranean, *Atmos. Res.*, 81, 67–93, 2006.

Tesche, M., Ansmann, A., Müller, D., Althausen, D., Engelmann, R., Freudenthaler, V., and Grob, S.: Vertically Resolved Separation of Dust and Smoke over Cape Verde Using Multiwavelength Raman and Polarization Lidars during Saharan Mineral Dust Experiment 2008, *J. Geophys. Res.*, 114, D13202, doi:10.1029/2009JD011862, 2009.

Textor, C., Schulz, M., Guibert, S., Kinne, S., Balkanski, Y., Bauer, S., Berntsen, T., Berglen, T., Boucher, O., Chin, M., Dentener, F., Diehl, T., Easter, R., Feichter, H., Fillmore, D., Ghan, S., Ginoux, P., Gong, S., Grini, A., Hendricks, J., Horowitz, L., Huang, P., Isaksen, I., Iversen, I., Kloster, S., Koch, D., Kirkevåg, A., Kristjansson, J. E., Krol, M., Lauer, A., Lamarque, J. F., Liu, X.,

Montanaro, V., Myhre, G., Penner, J., Pitari, G., Reddy, S., Seland, Ø., Stier, P., Takemura, T., and Tie, X.: Analysis and quantification of the diversities of aerosol life cycles within AeroCom, *Atmos. Chem. Phys.*, 6, 1777-1813, <https://doi.org/10.5194/acp-6-1777-2006>, 2006.

Toledano, C., Cachorro, V. E., Berjon, A., De Frutos, A. M., Sorribas, M., De la Morena, B. A., and Goloub, P.: Aerosol optical depth and Ångström exponent climatology at El Arenosillo AERONET site (Huelva, Spain), *Q. J. Roy. Meteor. Soc.*, 133, 795–807, 2007.

[Torres, O., Bhartia, P. K., Herman, J. R., Ahmad, Z., and Gleason, J.: Derivation of aerosol properties from satellite measurements of backscattered ultraviolet radiation: Theoretical basis, J. Geophys. Res., 103, 17099–17110, https://doi.org/10.1029/98JD00900, 1998.](#)

Torres, O., Bhartia, P. K., Jethva, H., and Ahn, C.: Impact of the ozone monitoring instrument row anomaly on the long-term record of aerosol products, *Atmos. Meas. Tech.*, 11, 2701-2715, <https://doi.org/10.5194/amt-11-2701-2018>, 2018.

Tsikerdekis, A., Zanis, P., Steiner, A. L., Solmon, F., Amiridis, V., Marinou, E., Katragkou, E., Karacostas, T., and Foret, G.: Impact of dust size parameterizations on aerosol burden and radiative forcing in RegCM4, *Atmos. Chem. Phys.*, 17, 769–791, <https://doi.org/10.5194/acp-17-769-2017>, 2017.

[Vandenbussche, S., Kochanova, S., Vandaele, A. C., Kumps, N., and De Mazière, M.: Retrieval of desert dust aerosol vertical profiles from IASI measurements in the TIR atmospheric window, Atmos. Meas. Tech., 6, 2577–2591, https://doi.org/10.5194/amt-6-2577-2013, 2013.](#)

[Vandenbussche, S., Callewaert, S., Schepanski, K., and De Mazière, M.: North African mineral dust sources: new insights from a combined analysis based on 3D dust aerosols distributions, surface winds and ancillary soil parameters, Atmos. Chem. Phys. Discuss., https://doi.org/10.5194/acp-2020-130, in review, 2020.](#)

Vaughan, M. A., Powell, K. A., Kuehn, R. E., Young, S. A., Winker, D. M., Hostetler, C. A., Hunt, W. H., Liu, Z., McGill, M. J. and Getzewich, B. J.: Fully Automated Detection of Cloud and Aerosol

Layers in the CALIPSO Lidar Measurements, *J. Atmos. Ocean. Technol.*, 26(10), 2034–2050, doi:10.1175/2009JTECHA1228.1, 2009.

Veselovskii, I., Goloub, P., Podvin, T., Tanre, D., da Silva, A., Colarco, P., Castellanos, P., Korenskiy, M., Hu, Q., Whiteman, D. N., Pérez-Ramírez, D., Augustin, P., Fourmentin, M., and Kolgotin, A.: Characterization of smoke and dust episode over West Africa: comparison of MERRA-2 modeling with multiwavelength Mie–Raman lidar observations, *Atmos. Meas. Tech.*, 11, 949–969, <https://doi.org/10.5194/amt-11-949-2018>, 2018.

Vickery, K. J., Eckardt, F. D., and Bryant, R. G.: A sub-basin scale dust plume source frequency inventory for southern Africa, 2005–2008, *Geophys. Res. Lett.*, 40, 5274–5279, doi:10.1002/grl.50968, 2013.

Voss, K. K., and Evan, A. T.: A new satellite-based global climatology of dust aerosol optical depth. *Journal of Applied Meteorology and Climatology*, doi:10.1175/jamc-d-19-0194.1, 2020.

Wandinger, U., Tesche, M., Seifert, P., Ansmann, A., Müller, D., and Althausen, D.: Size matters: Influence of multiple scattering on CALIPSO light-extinction profiling in desert dust, *Geophys. Res. Lett.*, 37, L10801, doi:10.1029/2010GL042815, 2010.

Washington, R., Todd, M., Middleton, N. J., and Goudie, A. S.: Dust-storm source areas determined by the total ozone monitoring spectrometer and surface observations, *Ann. Assoc. Am. Geogr.*, 93, 297–313, <https://doi.org/10.1111/1467-8306.9302003>, 2003.

Wei, J., Peng, Y., Mahmood, R., Sun, L., and Guo, J.: Intercomparison in spatial distributions and temporal trends derived from multi-source satellite aerosol products, *Atmos. Chem. Phys.*, 19, 7183–7207, <https://doi.org/10.5194/acp-19-7183-2019>, 2019a.

[Wei, J., Li, Z., Peng, Y., and Sun, L.: MODIS Collection 6.1 aerosol optical depth products over land and ocean: validation and comparison, Atmos. Environ., 201, 428–440, 2019b.](#)

Weinzierl, B., Sauer, D., Minikin, A., Reitebuch, O., Dahlkötter, F., Mayer, B., Emde, C., Tegen, I., Gasteiger, J., Petzold, A., Veira, A., Kueppers, U., and Schumann, U.: On the visibility of airborne volcanic ash and mineral dust from the pilot's perspective in flight, *Phys Chem Earth*, 45–46, 87–102, 10.1016/j.pce.2012.04.003, 2012.

Winker, D. M., Vaughan, M. A., Omar, A., Hu, Y., Powell, K. A., Liu, Z., Hunt, W. H. and Young, S. A.: Overview of the CALIPSO Mission and CALIOP Data Processing Algorithms, *J. Atmos. Oceanic Technol.*, 26(11), 2310–2323, doi:10.1175/2009JTECHA1281.1, 2009.

Winker, D. M., Pelon, J., Coakley, J. A., Ackerman, S. A., Charlson, R. J., Colarco, P. R., Flamant, P., Fu, Q., Hoff, R. M., Kittaka, C., Kubas, T. L., Le Treut, H., McCormick, M. P., Megie, G., Poole, L., Powell, K., Trepte, C., Vaughan, M. A. and Wielicki, B. A.: THE CALIPSO MISSION A Global 3D View of Aerosols and Clouds, *Bull. Amer. Meteorol. Soc.*, 91(9), 1211–1229, doi:10.1175/2010BAMS3009.1, 2010.

Wu, W. S., Purser, R. J., and Parrish, D. F.: Three-dimensional variational analysis with spatially inhomogeneous covariances, *Mon. Weather Rev.*, 130, 2905–2916, doi:10.1175/1520-0493(2002)1302.0.Co;2, 2002.

Yu, H., Remer, L. A., Chin, M., Bian, H., Kleidman, R. G., and Diehl, T.: A satellite-based assessment of transpacific transport of pollution aerosol, *J. Geophys. Res.-Atmos.*, 113, D14S12, <https://doi.org/10.1029/2007JD009349>, 2008.

Yu, H. B., Chin, M., Winker, D. M., Omar, A. H., Liu, Z. Y., Kittaka, C., and Diehl, T.: Global view of aerosol vertical distributions from CALIPSO lidar measurements and GOCART simulations: Regional and seasonal variations, *J. Geophys. Res.-Atmos.*, 115, D00H30, <https://doi.org/10.1029/2009jd013364>, 2010.

Yu, H. B., Chin, M., Yuan, T. L., Bian, H. S., Remer, L. A., Prospero, J. M., Omar, A., Winker, D., Yang, Y. K., Zhang, Y., Zhang, Z. B., and Zhao, C.: The fertilizing role of African dust in the Amazon rainforest: A first multiyear assessment based on data from Cloud-Aerosol Lidar and Infrared Pathfinder Satellite Observations, *Geophys. Res. Lett.*, 42, 1984–1991, <https://doi.org/10.1002/2015gl063040>, 2015.

Yu, S., Eder, B., Dennis, R., Chu, S. H., and Schwartz, S. E.: New unbiased symmetric metrics for evaluation of air quality models, *Atmos. Sci. Lett.*, 7, 26–34, 2006.

Yu, Y., Notaro, M., Liu, Z., Kalashnikova, O., Alkolibi, F., Fadda, E., and Bakhrjy, F.: Assessing temporal and spatial variations in atmospheric dust over Saudi Arabia through satellite, radiometric, and station data, *J. Geophys. Res.-Atmos.*, 118, 13253–13264, <https://doi.org/10.1002/2013JD020677>, 2013.

Yu, Y., Kalashnikova, O. V., Garay, M. J., and Notaro, M.: Climatology of Asian dust activation and transport potential based on MISR satellite observations and trajectory analysis, *Atmos. Chem. Phys.*, 19, 363–378, <https://doi.org/10.5194/acp-19-363-2019>, 2019.

Zender, C. S., Huisheng, B., and Newman, D.: Mineral Dust Entrainment and Deposition (DEAD) model: Description and 1990s dust climatology, *J. Geophys. Res.*, 108, 4416, <https://doi.org/10.1029/2002JD002775>, 2003.

Zender, C. S., Miller, R. L. L., and Tegen, I.: Quantifying mineral dust mass budgets: Terminology, constraints, and current estimates, *Eos, Transactions American Geophysical Union*, 85, 509–512, <https://doi.org/10.1029/2004EO480002>, 2011.

Zhang, J. and Reid, J. S.: MODIS aerosol product analysis for data assimilation: Assessment of over-ocean level 2 aerosol optical thickness retrievals, *J. Geophys. Res.-Atmos.*, 111, D22207, <https://doi.org/10.1029/2005JD006898>, 2006.

Table 1: Planetary (GLB), hemispherical (NHE and SHE) and regional DOD averages, representative for the period 2007–2015, based on collocated **LIVAS**, MERRA-2 and MIDAS $1^\circ \times 1^\circ$ data. Within the brackets are given the minimum and maximum **annual values**. The regional averages have been calculated following the upper branch (first temporal averaging and then spatial averaging) in Figure 5 of Levy et al. (2009). The full names of the acronyms for each sub-region are given in the caption of Figure 7.

REGION	LIVAS	MERRA-2	MIDAS
GLB	0.029 [0.028 – 0.035]	0.031 [0.028 – 0.036]	0.033 [0.031 – 0.040]
NHE	0.051 [0.050 – 0.064]	0.056 [0.050 – 0.067]	0.060 [0.056 – 0.074]
SHE	0.008 [0.007 – 0.008]	0.008 [0.007 – 0.008]	0.008 [0.007 – 0.008]
ETA	0.107 [0.085 – 0.175]	0.096 [0.079 – 0.143]	0.110 [0.089 – 0.167]
WTA	0.027 [0.022 – 0.034]	0.019 [0.016 – 0.024]	0.022 [0.018 – 0.029]
MED	0.074 [0.061 – 0.096]	0.089 [0.079 – 0.105]	0.097 [0.085 – 0.110]
GOG	0.164 [0.085 – 0.303]	0.275 [0.077 – 0.440]	0.326 [0.098 – 0.512]
WSA	0.271 [0.241 – 0.341]	0.339 [0.315 – 0.383]	0.325 [0.291 – 0.439]
SSA	0.287 [0.236 – 0.390]	0.260 [0.158 – 0.350]	0.249 [0.160 – 0.353]
BOD	0.302 [0.211 – 0.366]	0.510 [0.393 – 0.633]	0.612 [0.415 – 0.896]
NME	0.252 [0.121 – 0.305]	0.265 [0.148 – 0.295]	0.360 [0.201 – 0.397]
SME	0.236 [0.177 – 0.277]	0.220 [0.181 – 0.288]	0.257 [0.199 – 0.346]
CAS	0.077 [0.047 – 0.091]	0.140 [0.129 – 0.207]	0.146 [0.109 – 0.185]
THA	0.169 [0.115 – 0.197]	0.138 [0.113 – 0.150]	0.125 [0.080 – 0.155]
TAK	0.362 [0.284 – 0.429]	0.259 [0.236 – 0.322]	0.140 [0.099 – 0.290]
GOB	0.105 [0.076 – 0.140]	0.118 [0.105 – 0.138]	0.139 [0.066 – 0.141]
EAS	0.088 [0.053 – 0.127]	0.065 [0.048 – 0.080]	0.074 [0.055 – 0.089]
WNP	0.015 [0.012 – 0.020]	0.027 [0.021 – 0.030]	0.029 [0.023 – 0.032]
ENP	0.008 [0.006 – 0.010]	0.019 [0.016 – 0.020]	0.020 [0.017 – 0.023]
SUS	0.021 [0.011 – 0.031]	0.028 [0.019 – 0.038]	0.020 [0.013 – 0.025]

Deleted: 11

Field Code Changed

Deleted: ,

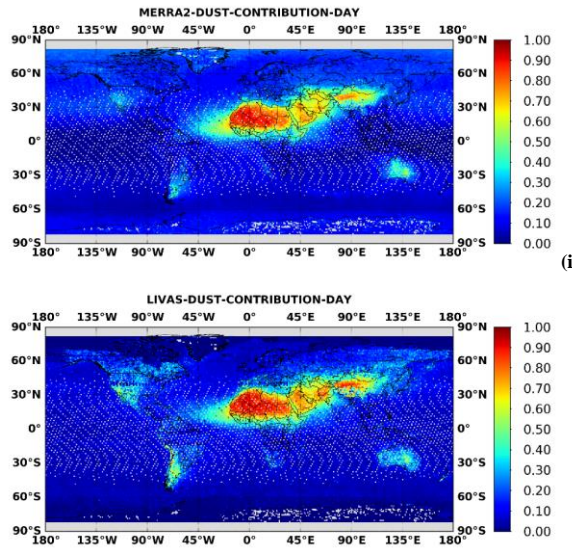
Formatted: English (United States), Do not check spelling or grammar

Deleted: CALIOP

Deleted: limits

Deleted: S

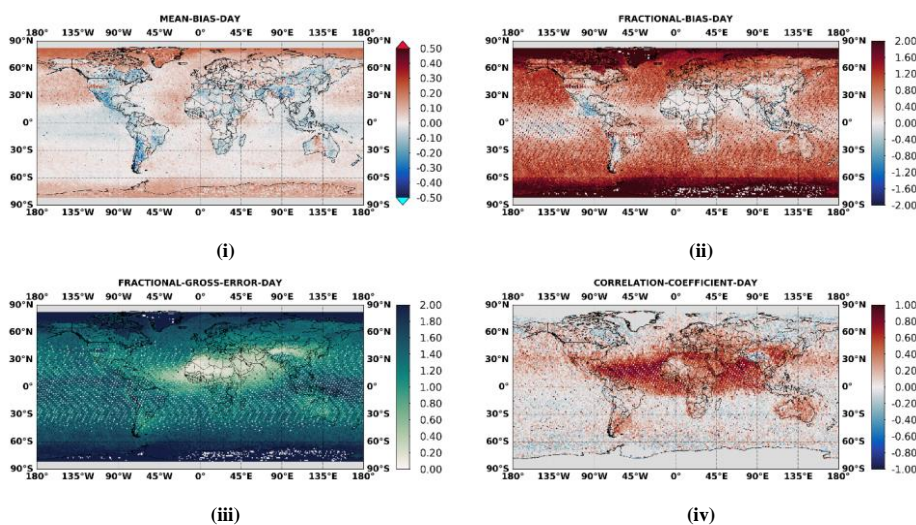
Formatted: English (United States)



(ii)

2 **Figure 1:** Annual geographical distributions of dust contribution to total aerosol optical depth at $1^\circ \times 1^\circ$ spatial resolution,
3 based on (i) MERRA-2 at 550 nm and (ii) LIVAS at 532 nm, during daytime conditions, over the period 2007-2015.

4



(iii)

(iv)

5 **Figure 2:** Annual geographical distributions illustrating the assessment of MDF versus LIVAS dust fraction, during
6 daytime conditions at $1^\circ \times 1^\circ$ spatial resolution, according to the primary skill metrics of: (i) mean bias, (ii) fractional
7 bias, (iii) fractional gross error and (iv) correlation coefficient, representative for the period 2007-2015.

8

9

Deleted: 11

Field Code Changed

Deleted: ,

Deleted: ,

Formatted: English (United States), Do not check spelling or grammar

Deleted: :

Deleted: products

Deleted: CALIOP

Deleted: retrievals

Deleted: ,

Formatted: English (United States)

Field Code Changed

Deleted: 22

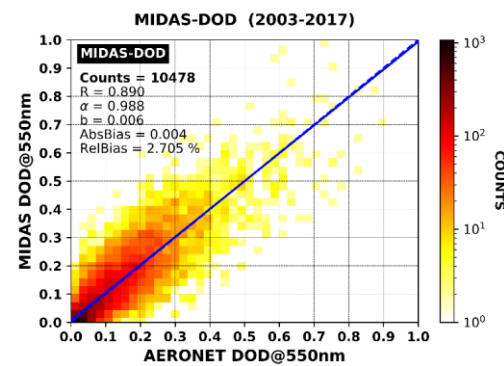
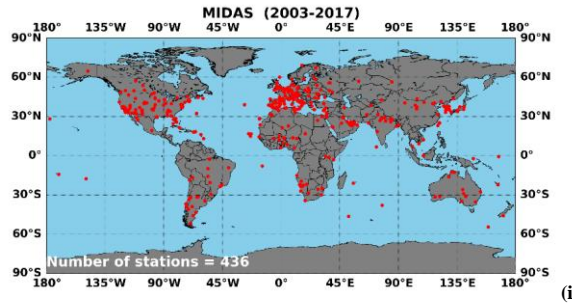
Formatted: English (United States), Do not check spelling or grammar

Deleted: MERRA-2 dust-to-total AOD ratio

Deleted: CALIOP

Deleted: retrievals

Formatted: English (United States)



22 **Figure 2:** (i) AERONET sites where at least one pair of ground-based and spaceborne retrievals has been recorded, according to the defined collocation criteria, during the period 2003 – 2017. (ii) Density scatterplot between **MIDAS** (y-axis) and AERONET (x-axis) dust optical depth at 550nm. The solid and dashed lines stand for the linear regression fit and equal line ($y=x$), respectively.

Deleted: 33

Formatted: English (United States), Do not check spelling or grammar

Deleted: ,

Field Code Changed

Deleted: ,

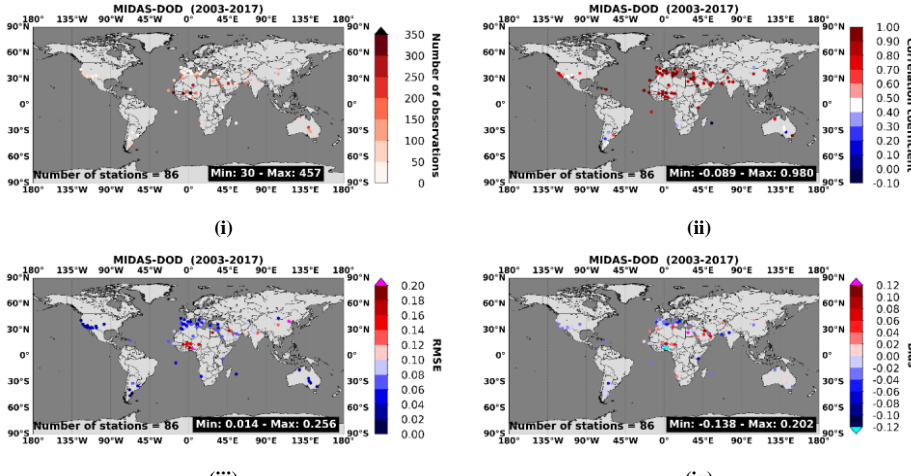
Deleted: 7

Deleted: 6

Deleted: MODIS

Deleted: LOC in the titles indicates that both land (L) and ocean (OC) MODIS retrievals are considered.

Formatted: English (United States)



45 **Figure 4:** Scatterplot metrics between MIDAS and AERONET DOD_{550nm}, at station level, during the period 2003 – 2017.
46 (i) Number of concurrent MIDAS-AERONET observations, (ii) correlation coefficient, (iii) root mean square error and
47 (iv) bias defined as spaceborne minus ground-based retrievals. The obtained scores are presented only for sites with at
48 least 30 MIDAS-AERONET matchups.

49 **Deleted: 44**

50 **Field Code Changed**

51 **Deleted: MODIS**

52 **Deleted: 7**

53 **Deleted: 6**

54 **Formatted: English (United States), Do not check**
55 **spelling or grammar**

56 **Deleted: MODIS**

57 **Deleted: MODIS**

58 **Formatted: English (United States)**

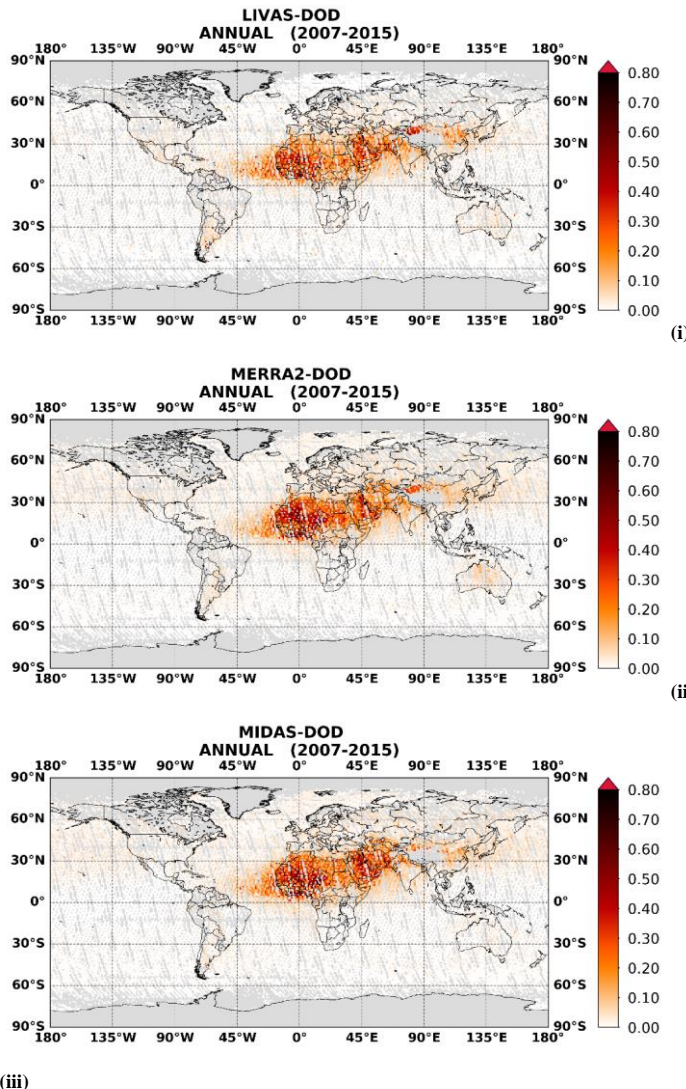


Figure 5: Long-term (2007 – 2015) average geographical collocated distributions at $1^\circ \times 1^\circ$ spatial resolution, during daytime for: (i) LIVAS DOD_{532nm}, (ii) MERRA-2 DOD_{550nm} and (iii) MIDAS DOD_{550nm}.

78 **Deleted:** 55

79 **Field Code Changed**

80 **Deleted:** ,

81 **Deleted:** ,

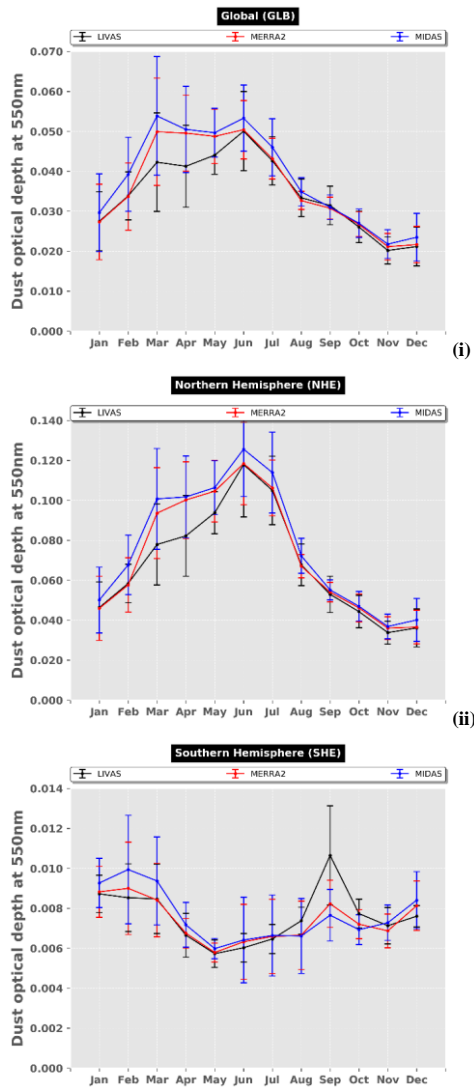
82 **Deleted:** of

83 **Formatted:** English (United States), Do not check
84 spelling or grammar

85 **Deleted:** CALIOP

86 **Deleted:** (MODIS)

87 **Formatted:** English (United States)



(iii)

94 **Figure 6:** Monthly variability of LIVAS (black curve), MERRA-2 (red curve) and MIDAS (blue curve) DODs, regionally
 95 averaged over: (i) the whole globe (GLB), (ii) the Northern Hemisphere (NHE) and (iii) the Southern Hemisphere (SHE).

96 The error bars correspond to the monthly interannual standard deviation computed during the period 2007 – 2015.

97

98

99

100

101

102

Deleted: 66

Field Code Changed

Deleted: Intra-annual

Deleted: CALIOP

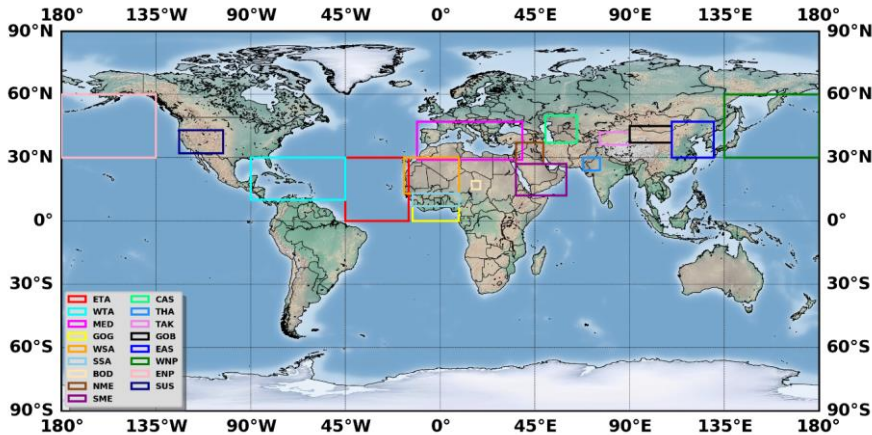
Deleted: MODIS

Formatted: English (United States), Do not check
spelling or grammar

Deleted: monthly

Deleted: from the interannual timeseries

Formatted: English (United States)



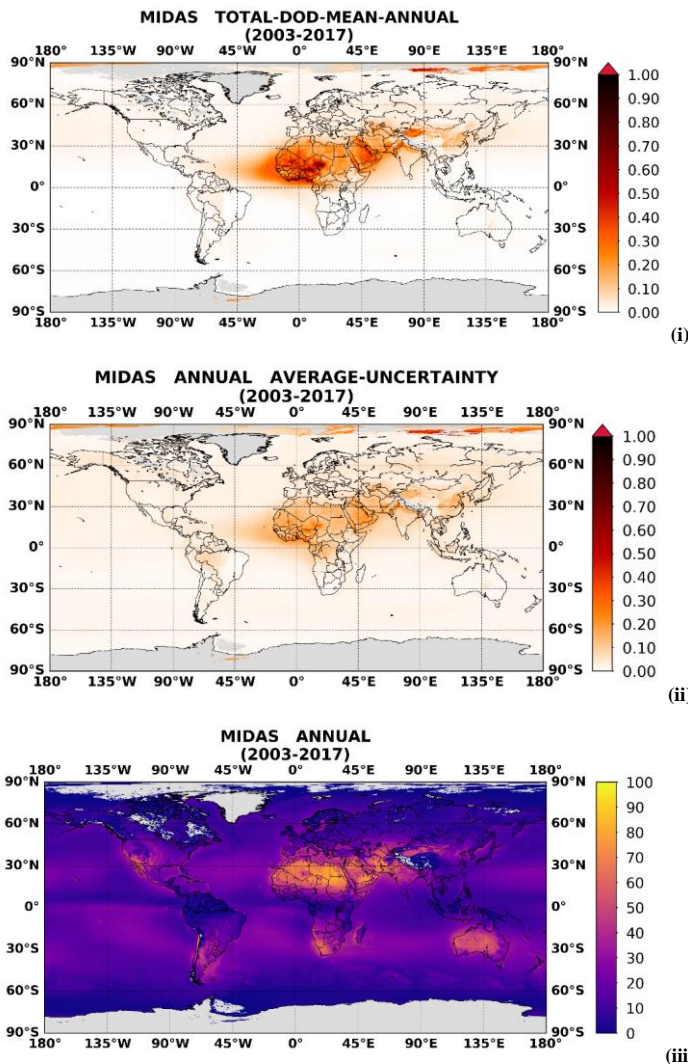
109
110 **Figure 7:** Regional domains of: East Tropical Atlantic (ETA), West Tropical Atlantic (WTB), Mediterranean (MED),
111 Gulf of Guinea (GOG), West Sahara (WSA), Sub-Saharan Africa (SSA), Bodélé Depression (BOD), North Middle East (NME),
112 South Middle East (SME), Central Asia (CAS), Thar Desert (THA), Taklamakan Desert (TAK), Gobi Desert (GOB),
113 East Asia (EAS), West North Pacific (WNP), East North Pacific (ENP) and Southwest United States (SUS).
114

Field Code Changed

Deleted: 77

Formatted: English (United States), Do not check
spelling or grammar

Formatted: English (United States)



129 **Figure 8:** Annual geographical distributions, at $0.1^\circ \times 0.1^\circ$ spatial resolution, of: (i) the climatological DODs, (ii) the
 130 ~~average of the daily DOD uncertainties~~ and (iii) the percentage availability of ~~MIDAS data~~ with respect to the entire study
 131 period spanning from 1 January 2003 to 31 December 2017. Grey color represent areas with absence of data.

Deleted: 88

Formatted: English (United States), Do not check spelling or grammar

Field Code Changed

Deleted: absolute

Deleted: d

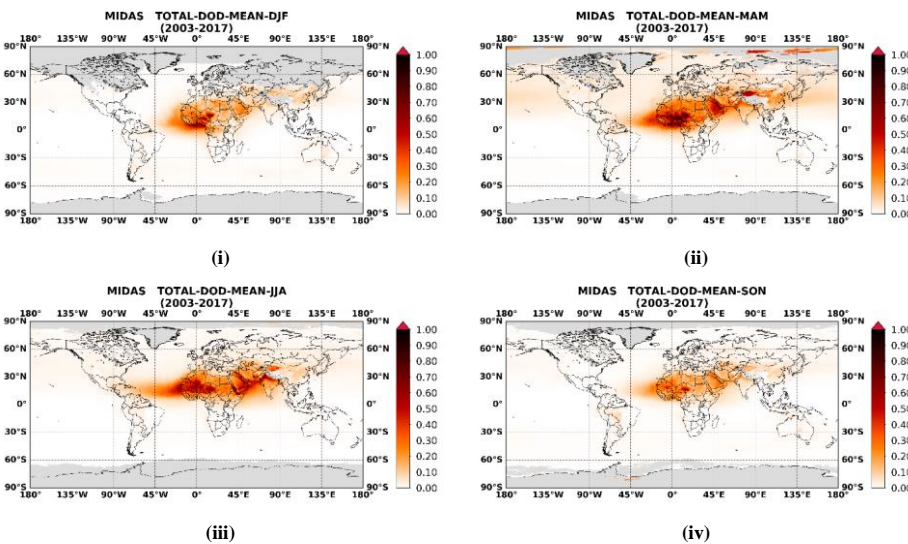
Deleted: uncertainty

Deleted: MODIS-Aqua retrievals

Deleted: 7

Deleted: 6

Formatted: English (United States)



146 **Figure 9:** As in Figure 8-i but for: (i) December-January-February (DJF), (ii) March-April-May (MAM), (iii) June-July-
 147 August (JJA) and (iv) September-October-November (SON).

148

Field Code Changed

Deleted: 99

Formatted: English (United States), Do not check spelling or grammar

Formatted: English (United States)